
SYLVA

SYLVA

Advancing Lignin Cellulose Biocomposites through Robotic Additive Manufacturing

Robotic Additive Manufacturing of Lignin-Cellulose Biocomposites:
Computational Slicing Strategies for Architectural Applications

MSc Graduation P5 Report
June 2025

Cansu Ersoy
5901340

Mentors
Dr. Serdar Asut
Architectural Engineering + Technology
Design Informatics

Dr. Rebecca Hartwell
Architectural Engineering + Technology
Structural Design & Mechanics

TU Delft Delft University of Technology

ACKNOWLEDGEMENTS

This thesis marks not just the culmination of an academic journey, but the weaving together of resilience, hope, and the strength borrowed from the people who never let me fall.

To my family, my unshakable foundation: especially my mother **Zülfüye Üzgül**, and my sister **Bengüsu Ersoy**—your belief in me, especially when I couldn't find it in myself, carried me farther than you'll ever know. Your strength became my own. Your support pushed me through. Thank you for your endless support.

To my dearest friends across the distance, **Elif Naz Yılmaz** and **Nil Özkan**—you've held space for me in ways words can't possibly describe. Your unwavering presence made the distance feel like nothing at all. You reminded me that I'm never alone, no matter how far I may be.

To the ones who stood right next to me through the long nights and chaotic days—**Berk Adsan**, **Evanthia Soumelidou**, and **Arian Babaei**—thank you for reminding me that I didn't have to fight this battle alone. Your kindness and companionship made this weight lighter.

To my partner **Leon Ravenhorst**, for standing by me through every sleepless night, for grinding materials by my side, for showing up in the lab, and holding my hand through every breakdown—thank you for believing in me without hesitation.

To my mentors, **Serdar Aşut** and **Rebecca Hartwell**, your guidance pulled me out of the deepest pits of self-doubt. When everything seemed to push back, you gave me direction, patience, and the push I needed to keep going.

To **Paul de Ruiter**, who didn't have to help, but chose to—thank you for generously giving your time, building a homemade extruder, and being an anchor through the unpredictable storms of fabrication.

To **Gerbert Smits** and the team at **10XL**, your openness, resources, and thoughtful feedback helped shape my work into something tangible and real. I couldn't have brought these prototypes to life without your generosity.

And finally, to **Sevil Sariyildiz**—though you are no longer with us, your impact is felt in every line of this work. Your belief in me as a woman, as a researcher, and as a human being gave me strength I didn't know I had. You reminded me to stand firm, and I will always carry your words with me. You are missed, and you are remembered.

This work exists not because I was strong—but because I was surrounded by people who lent me their strength. This is as much yours as it is mine.

ABSTRACT

The construction industry faces significant challenges related to environmental sustainability, including high carbon emissions and excessive reliance on non-renewable resources. Traditional construction materials often have substantial environmental footprints. Lignin-cellulose composites, derived from renewable resources such as wood waste, can offer a promising eco-friendly alternative. However, achieving the necessary mechanical properties, printability, and scalability for practical construction applications remains a critical challenge.

This research explores the potential of lignin-cellulose biocomposites as sustainable alternatives to traditional construction materials. The study focuses on developing bio-based polymers through lignin-cellulose composites combined with bio-based binders and plasticizers, aiming to create a material suitable for hot extrusion-based additive manufacturing. By utilizing robotic additive manufacturing and parametric design approaches, the research addresses the challenges and opportunities of using bio-based materials in construction, with a primary focus on creating modular partition walls.

The primary objective of this research is to develop and optimize three distinct lignin-cellulose composite ratios, each tailored to different mechanical strength requirements. These ratios correspond to three types of bricks, strategically implemented within the partition wall according to their structural demands. Mechanical properties, rheological behavior, and printability are evaluated through a combination of experimental methods and extrusion-based fabrication processes.

Further, this study develops and tests computational slicing workflows tailored for robotic hot extrusion. Through a comparative analysis of different slicing strategies and tools, the research seeks to improve the translation of complex architectural designs into feasible robotic printing paths, optimizing material distribution according to structural performance requirements.

By integrating material innovation with computational manufacturing techniques, this research aims to demonstrate how high lignin-cellulose biocomposites can serve as a sustainable and structurally viable alternative to conventional materials. The findings will contribute insights into the advancement of bio-based composites, robotic fabrication, and computational design strategies for sustainable construction.

INDEX

1. INTRODUCTION

1.1 Introduction

The construction industry is increasingly confronted with the need to reduce its environmental impact while addressing the demand for more sustainable, resilient building materials. Traditional materials like concrete and steel are energy-intensive and contribute significantly to carbon emissions, pushing the industry to explore alternative materials with less environmental footprint. With the changes in the field with technological and material advancement, the industry started looking into more advanced solutions in terms of rapid construction and sustainable alternatives. This includes more time and resources spent in research and material advancements in order to improve their stance in the construction game.

More and more bio-based alternatives are surfacing every day, as the companies and researchers are starting to catch up with the technological age. These materials are deemed necessary for the industry to move forward in the golden age of sustainable construction, while helping the companies reduce carbon footprint and environmental impact. While these are explored, advancements in the fabrication processes are also crucial to catch up with. Additive manufacturing and computational design have become the main characters lining up with these advancements, and the ease of customization of the end product and the optimization of the design to fit several needs is becoming more important.

As we move onto this innovative era, traditional construction methods may be limiting in terms of time efficiency and uniqueness. Customized and interchangeable elements for more flexible architectural products are starting to play a big role in the industry. Disassembly for future and flexible use is becoming an important factor in the design understanding of this technological generation.

In light of these, this research will be addressing how the bio-based alternatives can be manufactured to fit mechanical and design needs, and how computational design and additive manufacturing support these materials through prototyping, material science and design of customized elements that come together for an architectural product.

1.2 Problem Statement

The construction industry is under increasing pressure to transition toward sustainable materials, as traditional options such as concrete and steel are highly resource-intensive and among the largest contributors to global carbon emissions (Jiang et al., 2023). In this context, additive manufacturing (AM) has emerged as a compelling alternative, offering material efficiency, on-demand production, and the ability to create geometry-driven, performance-based components. These features make AM particularly suitable for advancing sustainability goals in architecture and construction.

However, despite the growing body of research on AM for small-scale polymer-based components, its application at the architectural scale—particularly with biobased materials—remains relatively underdeveloped. While biopolymers such as PLA and PHA have been successfully integrated into processes like Fused Deposition Modeling (FDM) and Direct Ink Writing (DIW), their adaptation to hot extrusion-based AM continues to face challenges. These challenges include limited mechanical strength, rheological instability, and thermal degradation under extrusion conditions (Jiang et al., 2023).

In particular, lignin and cellulose, two of the most abundant natural polymers, offer strong potential as renewable, biodegradable alternatives for sustainable construction materials (Wan et al., 2023). Yet, their complex thermal and flow characteristics limit their direct application in hot-extrusion processes. Lignin tends to be brittle and incompatible with many extrusion binders, while cellulose often degrades before reaching the desired melt state. Prior studies have highlighted these processing limitations, particularly for high-lignin content composites, indicating the need for further formulation and blending strategies (Ebers, 2021).

To date, research in this field has predominantly focused on material characterization or demonstration of small-scale prints, without fully integrating these findings into digital fabrication workflows suited for architectural components. Furthermore, many so-called "wood-based" filaments are merely composites of PLA and sawdust, which do not represent a fundamentally biopolymer-based solution (Gauss et al., 2021).

This gap is particularly evident in brick-based production systems, which present a practical testbed for scalable AM in architecture. Conventional bricks, though modular, lack the adaptability, performance customization, and sustainability required by today's construction paradigms. Embedding material intelligence into brick production through the use of mechanically optimized lignin–cellulose composites and computational design enables a new class of functionally graded, performance-driven components. However, this opportunity remains largely unexplored.

Accordingly, this research addresses two intersecting gaps:

1. The limited material processing knowledge around lignin–cellulose composites for pellet-based robotic extrusion;

2. The lack of computational strategies that couple material formulation with structural performance for architectural elements such as bricks.

Through a combined approach of material experimentation, mechanical testing, and customized slicing workflow development, this thesis proposes a structurally-informed brick design strategy. The aim is to translate material performance into fabrication logic, thereby advancing the integration of sustainable composites into scalable, modular construction systems via robotic additive manufacturing.

1.3 Research Question

The idea of creating a renewable, biobased feedstock tailored for advanced manufacturing processes presents exciting possibilities for the construction industry. Lignin and cellulose, abundant natural polymers derived from biomass, hold the potential to redefine how sustainable materials are integrated into modern design and production. But what are the limits and potentials of these polymers with hot extrusion? What will be the mechanical properties after the binding process? How will the biobased binders complement the polymers to work with heat? More specifically, can they be utilized to produce material-customized bricks with computational tools, and what technical and design considerations are critical to making this vision a reality? In this process, computational tools play a central role—linking material behavior to structural logic and enabling the parametric design, simulation, and toolpath generation required to fabricate performance-driven components.

With all of these questions in mind, the main objective and the refined question can be summed down to:

> *"What are the challenges and opportunities of **lignin-cellulose biocomposites** as feedstock for **hot extrusion-based robotic additive manufacturing,** and how can different **material ratios** be optimized to ensure mechanical performance, printability, and structural viability through **computational slicing strategies** for architectural applications?"*

The findings of this research will be important to finding out if the lignocellulosic composites have the necessary properties to be a feedstock for hot extrusion additive manufacturing to be optimized for use in architectural applications, by being used in the making of customized bricks. The end result will be concluded through the experiments and testing mentioned in this report.

1.4 Research Sub-Questions

In work of the main research question, some sub-questions are also necessary to refine and organize the research and experiment process. A set of these sub-questions have been derived and organized according to category, to support the main question.

In terms of "Material Research":

- What are the optimal ratios of lignin, cellulose and the biobased binder for achieving a balance between mechanical performance and printability in hot extrusion additive manufacturing?

In terms of "Fabrication":

- What challenges (e.g., material flow, temperature control, interlayer adhesion) arise when fabricating strength-graded modular bricks, and how can adjustments in process settings improve overall quality and structural stability?

In terms of "Mechanical Properties":

- How does the mechanical performance (compressive strength, flexural strength) of extrusion-printed lignin-cellulose composite bricks vary with different fiber-to-binder ratios?

How can simplified mechanical tests be used to effectively validate the structural viability of strength-graded bricks in partition wall construction?

In terms of "Prototyping":

- How can computational design be integrated with prototyping workflows to optimize infill patterns and geometry for specific architectural applications?

In terms of "End of Life Potential"

- How do lignin-cellulose composites compare to traditional materials in terms of end-of-life potentials, such as recyclability, reusability, and biodegradability?

In terms of "Computational Design"

- How can material formulation and computational design inform each other?
- Which computational slicing tools and workflows can be developed and adapted to optimize the placement of these strength-graded bricks based on structural performance requirements?

1.5 Design Assignment

Building on the findings from the material research, this design assignment investigates the application of lignin-cellulose biocomposites in the development of modular partition walls for contemporary office environments. The aim is to design customized bricks to optimized for robotic hot extrusion additive manufacturing,to form a partition wall responding to the evolving architectural demands for flexibility, material efficiency, and sustainability.

Through computational slicing strategies and strength-graded material formulations, the project elaborates on conventional masonry by introducing performance-driven design and digital fabrication methodologies. The final outcome will materialize as a modular partition wall system, demonstrating the structural, aesthetic, and environmental potential of biobased composites.

Applications in Office Spaces

The bricks are intended for partition walls that define office zones while maintaining openness. They enable space division for private work areas, meeting rooms, or collaborative spaces while also integrating conduits for cables and ventilation systems. Their reusable composition and modularity allow for reconfiguration as office needs evolve, making them valuable for dynamic workplaces focused on sustainability and adaptability.

Rationale for Additive Manufacturing

Additive manufacturing is central to this research for its capacity to fabricate highly customized bricks that respond to specific spatial and structural needs. Unlike traditional mass production, this method allows each brick to serve a unique role within a larger assembly. In this project, all bricks share a fixed parametric geometry but are differentiated by two layers of adaptability: material strength grading and rotational orientation. Through computational design, each brick is assigned a distinct fiber-to-binder ratio based on its structural placement, enabling zoned mechanical performance. Additionally, the geometry supports dual adaptability—bricks can be rotated horizontally or vertically depending on assembly logic, allowing spatial flexibility without altering the part file. Additive manufacturing enables this fine-tuned customization, embedding function and adaptability directly into the fabrication process while maintaining geometric consistency across the wall system.

Computational Design Process

The transition from material formulation to full-scale partition wall systems opens new opportunities for computational design and fabrication. In this research, the focus is not merely on tuning material properties in isolation, but on developing customized slicing workflows that translate mechanical performance data into fabrication logic. These workflows serve as the bridge between material behavior and toolpath generation—by

embedding structural simulation data (e.g., stress distribution, stiffness requirements) directly into the slicing process, extrusion parameters such as wall thickness, infill density, and deposition speed are adapted for each brick. This allows the robotic system to vary fiber-to-binder ratios and extrusion behavior in real-time, ensuring that each printed unit is structurally optimized according to its location and load demands within the wall system. Through the integration of parametric modeling, structural simulation with Karamba3D, and robotic toolpath generation in Grasshopper, the system enables automated material grading—tailoring each brick to its functional role while maintaining geometric consistency. This approach advances a more intelligent, feedback-driven fabrication process suited for hot extrusion-based additive manufacturing with biobased composites.

Structural and Mechanical Testing

Ensuring the mechanical performance of the modular bricks is critical for their application in partition walls. The tensile and flexural strength of the lignin-cellulose composites will be evaluated across three distinct material ratios, corresponding to different structural performance requirements. This testing phase will validate the structural viability of the bricks for use in office environments while emphasizing material efficiency and sustainability, within the structural restrictions of a self-standing partition wall structure.

Design and Prototyping

The design phase focuses on developing a brick-based wall system that aligns with the structural behavior and fabrication limits of lignin–cellulose composites. Instead of pursuing formal aesthetics, the design is driven by technical criteria: material performance, robotic printability, and assembly logic. The parametric brick geometry remains fixed but allows rotational placement (vertical or horizontal), enabling adaptive patterns across the wall. Prototyping aims to validate the computational design strategy under real fabrication conditions, iteratively refining the geometry, slicing parameters, and assembly methods to ensure compatibility with the different pellet extrusion systems and structural requirements. The resulting wall system is not only visually coherent but functionally responsive to material constraints and robotic workflow.

This assignment explores multiple configurations of customized bricks to balance structural optimization, material efficiency, and aesthetic appeal. Iterative design and testing produced prototypes and insights into the feasibility of these bricks for scalable, sustainable architectural applications. By addressing the challenges of modularity and adaptability, this project aims to redefine masonry for the needs of contemporary architecture.

1.6 Process & Methodology

There has been some experimentation on lignin and cellulose used as feedstock for additive manufacturing, as graduation projects in Building Technology. The resources published by Coelho and Bierarch (2021), have

been extremely helpful in the formatting of the experiment mixture of this research. These resources have paved the starting point of this research.

The research has been divided to several parts, with two main topics in mind: the material research, and the design configuration. Hereby, this suggests a combination of an experimental and design-based framework, as well as a lengthy research period.

- 0. Preparation
- 1. Literature Review
- 2. Material Development
- 3. Printability Trials
- 4. Mechanical Testing
- 5. Computational Tool Advancement
- 6. Design & Prototyping
- 7. Conclusions

The early phase of this thesis was as much about setting a technical foundation as it was about defining a direction that felt grounded and meaningful. Initial meetings with mentors and lab coordinators shaped not only the scope of the research but also the confidence to pursue a hybrid approach: one that links hands-on material experimentation with computational tool development. These discussions clarified early concerns—Would lignin and cellulose behave predictably under heat? Could biobased composites be extruded with robotic precision?—and they helped form a roadmap that felt both ambitious and achievable.

Material sourcing was guided by lessons from previous attempts with biopolymer blends. I prioritized samples that showed promise in prior extrusion contexts, while staying mindful of thermal behavior, binder compatibility, and mechanical potential. Rather than starting from scratch, I used this moment to bridge what I already knew with what I needed to prove. This made the formulation strategy more focused, reducing unnecessary trial-and-error and opening up space for refining slicing parameters earlier on.

The literature review became more than a background exercise—it was a diagnostic tool. Beyond surveying the typical scope of biopolymers in additive manufacturing, I searched specifically for where these materials fall short when used in hot extrusion systems. A recurring theme was evident: material development often stops at lab-scale proof-of-concept, rarely connecting to real-world fabrication logic. This helped clarify the niche of my thesis—addressing not only how biobased materials behave, but how they can be encoded into computational workflows that adapt to their behavior.

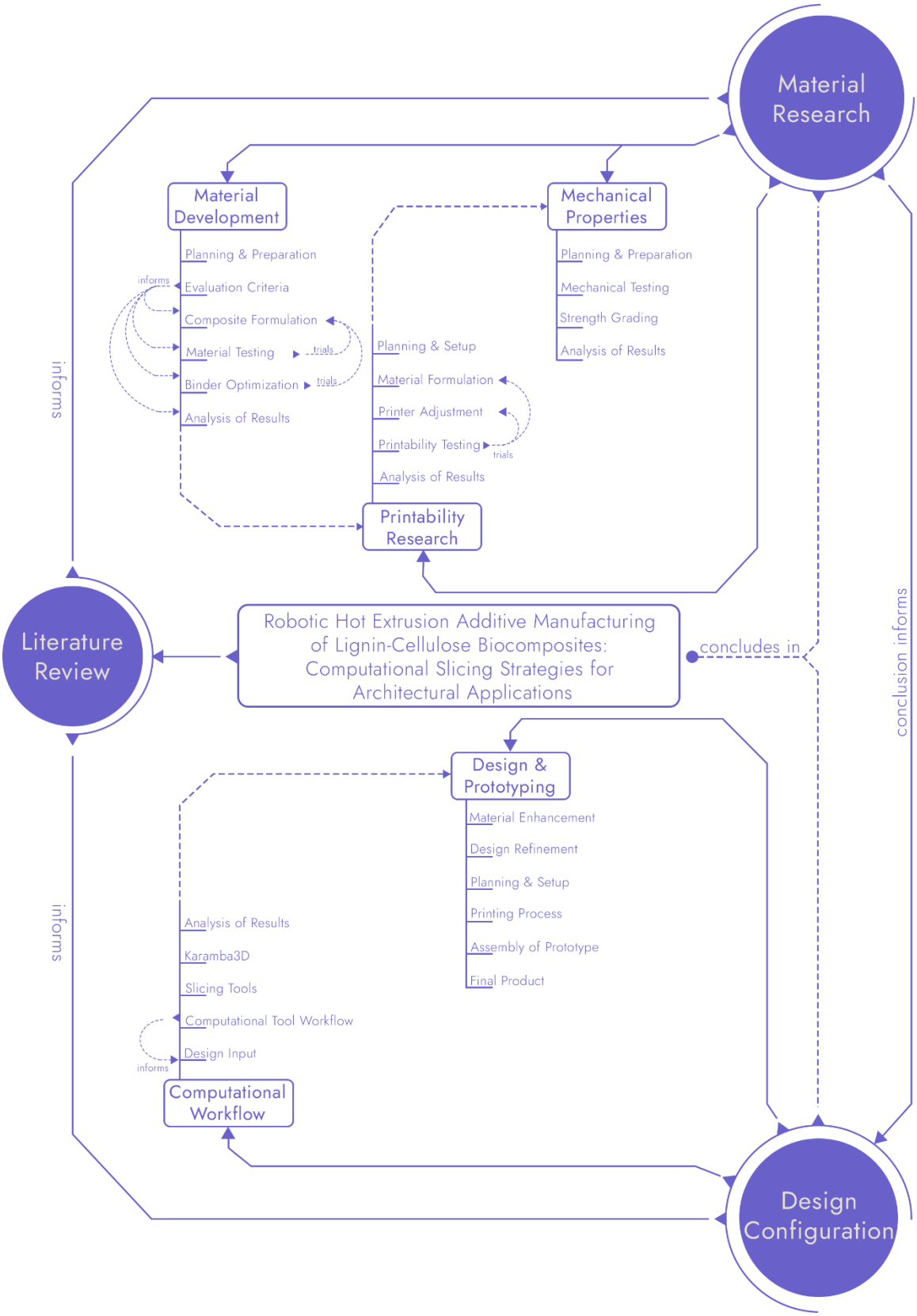

Figure 1 – Methodology Diagram

The review addresses several critical areas: the properties of lignin and cellulose, challenges in their application to additive manufacturing, innovations in bio-based binders and plasticizers, extrusion parameters, and modular construction strategies. Additionally, computational design approaches for modular construction are explored, with a focus on slicing strategies tailored to robotic extrusion.

In collaboration with faculty laboratories, material development was initiated at the Heritage and Architecture Lab and further advanced at the LAMA Lab. Given the fine particulate nature of lignin and cellulose, early handling and mixing were conducted under a fume hood to ensure both safety and precision. Initial printability assessments were carried out using a homemade pellet-based extruder setup at LAMA. These trials aimed to evaluate basic flow behavior, material homogeneity, and extrusion feasibility under heat. Observations such as surface finish, viscosity, and workability were systematically recorded, providing an early indication of how well the formulations could perform in larger-scale robotic setups

Parallel to material optimization, extrusion testing was conducted at the LAMA Lab using a robotic setup equipped with a CEAD pellet extruder. These trials focused on validating the printability of lignin–cellulose formulations under controlled parameters, including nozzle diameter, temperature settings, print speed, and deposition continuity. Scaled-down brick prototypes were produced to assess interlayer bonding, extrusion stability, and surface consistency.

While SAM|XL supported the extrusion workflow, its primary contribution was the approval and verification of the generated G-code, ensuring that the toolpaths matched safety and operation standards of the robotic system. Due to limited availability for physical prototyping, SAM|XL served more as a technical checkpoint than a production site.

In parallel, collaboration with 10XL provided practical insights into adapting the slicing logic for larger-scale robotic systems. Their industrial experience helped validate the feasibility of the customized G-code on pellet-based extrusion tools, contributing to the alignment between the computational slicing strategy and real-world robotic printing conditions.

This research integrates a computational slicing strategy using Grasshopper-based slicing tools. Slicers such as Droid, Termite, COMPAS, and Silkworm are analyzed and compared to develop optimized path-planning workflows for the robotic extrusion process. Customized slicing enables variation in print paths and toolpaths, responding directly to the mechanical requirements and material constraints of each brick type.

The mechanical properties of the optimized composites were evaluated through tensile, compressive, and flexural testing conducted at the Mechanical Engineering faculty. These tests were carried out in collaboration with Dr. Fred Veer, whose expertise guided the experimental setup and interpretation of results. Standardized protocols were followed to ensure accurate assessment of strength, stiffness, and failure behavior. The collected

data enabled the classification of three material ratios into distinct performance categories—high strength, medium strength, and low strength—each tailored to a specific brick type within the partition wall system. These results directly informed the structural logic behind the strength-graded design approach.

Finally, the design of the modular partition wall system integrates all findings. Using parametric brick design and computational slicing, the partition wall is assembled with different brick types positioned according to their structural performance requirements. The prototypes will be printed and assembled at the LAMA Lab and SAM|XL and evaluated for modularity, scalability, and performance in office environments.

This process aims to demonstrate the potential of lignin-cellulose composites combined with robotic additive manufacturing and computational slicing as a sustainable and technically feasible alternative to conventional construction techniques.

1.7 Framework & Time Plan

Here is the expected timeline:

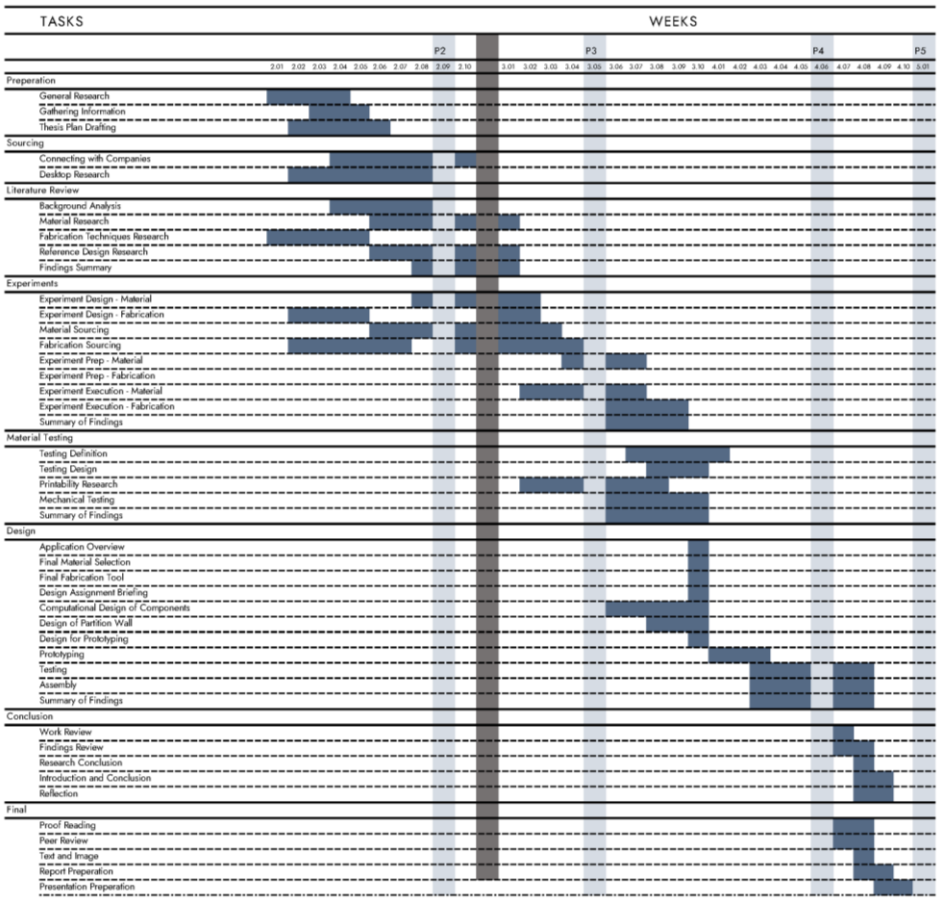

Figure 2 – Time Plan Diagram

1.8 Relevance

Socially, this work tackles the global urgency for sustainable construction in light of escalating climate change and resource depletion. Conventional materials like concrete and steel are significant contributors to carbon emissions and environmental degradation. By exploring bio-based alternatives such as lignin and cellulose, this research advocates for renewable, low-impact materials. Moreover, the use of computationally informed material formulations enables adaptive, resource-efficient construction strategies—especially relevant for rapidly urbanizing contexts that demand modular, lightweight, and easy-to-assemble solutions.

Professionally, the project bridges material science with digital design and robotic manufacturing. It leverages computational workflows and slicing strategies to enhance printability and structural performance of high lignin-cellulose composites. These methods introduce automation into material research, guiding architects and engineers toward designing functional and customizable building components. By optimizing fiber-to-binder ratios and aligning them with structural performance requirements, the research streamlines fabrication while lowering labor intensity and waste—paving the way for smarter, more sustainable architectural production.

Scientifically, the study contributes to advancing bio-based composite research and digital fabrication techniques. It addresses some of the key challenges in the hot extrusion of high lignin-cellulose materials, including viscosity control, mechanical robustness, and processing stability. The integration of computational tools (e.g., parametric modeling, structural performance analysis, and slicing algorithms) allows for data-driven testing and refinement, minimizing the need for excessive physical prototyping. The findings support the broader application of renewable polymers in construction, offering an alternative solution to replace fossil-based materials in additive manufacturing.

2. LITERATURE REVIEW

2.1 Overview of Additive Manufacturing

As mentioned by Gibson et al. (2021), additive manufacturing is based on a digital model created using computer-aided design (CAD) software, allowing for rapid modifications without the need for new moulds or tools. This is a flexibility that basically enables manufacturers to produce customized parts with low volumes efficiently, which has a particular benefit in industries where product specifications and requirements can change rapidly, such as the construction industry (Jiang et al., 2023).

Additive Manufacturing (AM), commonly simplified to "3D printing", had been evolving significantly as a rapid prototyping tool, to a versatile technology that has been utilized in many different industries, main ones including construction, aerospace and healthcare. Additive manufacturing allows the creating of complex geometries from direct digital models, and supports the fact customization and rapid iteration of all type of design. There is a great contrast between traditional manufacturing and additive manufacturing, that has a more layer-by-layer approach, as traditional manufacturing often requires extensive tooling, planning and extra time (Arias-Ferreiro et al., 2022).

Traditional manufacturing processes involve significant upfront costs and time for mould creation and setup. These methods require careful design consideration to optimize part geometry for manufacturability, assembly, and functionality. For high-volume production, traditional methods can be cost-effective; however, they are less adaptable to design changes once production has commenced (Nguyen et al., 2018).

Additive manufacturing (AM) offers remarkable design flexibility, enabling architects and engineers to produce intricate structures—such as lattice forms and topology-optimized components—that are nearly impossible to fabricate with traditional methods (Ngo et al., 2018; Alfaify et al., 2020). It is increasingly recognized as a key enabler for sustainable construction practices, as it reduces reliance on traditional, resource-intensive processes. By tailoring material usage to specific design and structural needs, it aligns with modern priorities of efficiency and environmental responsibility. Its application in architecture and construction has opened new avenues for integrating innovative materials into functional and aesthetically driven designs. Publications in the field emphasize that biodegradable composites are gaining traction for 3D printing in architecture, blending sustainability and functionality while enabling creative material expression (Semyari Roudbari, 2025).

The AM process typically involves several key steps, as described by Gibson et al. (2021):

- CAD Development: Creating a digital model of the desired object.
- STL Conversion: Converting the digital model into an STL file, which describes the external surfaces of the object and is used for slicing the model into layers.
- Transfer to AM Tool: Uploading the STL file to the printer and adjusting settings such as size and orientation.
- Machine Setup: Preparing the machine for fabrication, including material selection and parameter adjustments.
- Fabrication: The automated process of layer-by-layer fabrication.
- Post-Processing: Cleaning and finishing the printed part to achieve the desired quality and functionality.

2.1.1 Types of Additive Manufacturing

Additive manufacturing comes in various technologies and types, each with their own processes and areas of application.

Fused Deposition Modeling (FDM)

This is a widely used techniques of additive manufacturing, utilizing a heated nozzle, and is mainly known for extruding thermoplastic filaments through this nozzle. Its suitability for biobased materials has been observed with examples such as polylactic acid (PLA), especially due to its abundance and ease of use.

Stereolithography (SLA)

This method utilizes a laser to cure the liquid resin unto solid parts. This technique is ultimately known for the high precision it provides and for its advantage of producing complex geometries with smooth surface finished, unlike a layered look. It has been utilized in sectors where precision and detailing is pressing.

Selective Laser Sintering (SLS)

SLS uses a laser to fuse powdered materials such as plastics ort metals into solid structures. This method allows for the use of alpha bind variety of materials and is advantageous for producing functional prototypes and end-use parts.

Binder Jetting

This method involves the deposition of liquid binders onto a powder bed, then curing it into solid parts. It can be used with a various selection of materials, most common ones ceramics and metals, but it does consist the potential of including biobased materials for sustainable construction (Sigley et al., 2023).

Material Extrusion

This type includes techniques like FDM, as mentioned before, and it's essentially a continuous deposition of material through a nozzle. It is particularly biobased composites as it can use various feedstocks for direct usage (Özgüner & Özgüner, 2022).

Digital Light Processing (DLP)

Similar to SLA, DLP uses light to cure resin, but it employs a digital light projector to flash an entire layer at once, significantly speeding up the printing process. This technique can also be adapted for various materials, allowing for rapid prototyping of complex designs (Arias-Ferreiro et al., 2022).

Powder Bed Fusion (PBF)

This method involves using a heat source to fuse powdered materials together. It can accommodate a range of materials and has potential applications in creating biobased composites for various uses (Feng et al., 2022).

2.1.2 Use in Architecture

The application of additive manufacturing (AM) in architecture and the built environment is an emerging field that has gained attention due to advancements in digital design, material science, and robotic fabrication. AM enables complex, customized, and materially efficient components that are challenging to achieve with conventional methods. Its role in architecture extends across several key areas: structural systems, customizable building parts, large-scale fabrication, hybrid processes, and functionally graded materials (FGMs).

AM supports architectural creativity by translating digital forms directly into built elements, removing the geometric limitations of formwork and enabling new construction paradigms. Yang et al. (2018) demonstrated the potential of biomimetic additive manufacturing for creating thermally efficient, load-responsive structures inspired by natural gradients. These techniques facilitate the production of performance-driven elements such as panels with embedded insulation zones or acoustically tuned surface textures.

The potential for rapid customization is one of AM's most impactful contributions to architectural design. Raspall et al. (2020) outlined workflows that enable the direct translation of parametric models into fabrication-ready toolpaths, supporting minimal-waste, tailor-made designs tailored to project-specific requirements.

Recent developments also emphasize the shift toward decentralized, on-demand production. As noted by Pajonk et al. (2021), large-scale 3D printing systems can enable localized manufacturing with reduced material waste and increased material adaptability. These computationally integrated workflows empower architects to produce site-adaptive elements that respond to structural or environmental needs and align with circular economy goals.

Hybrid approaches are additionally gaining traction. Pajonk et al. (2021) explored hybrid fabrication workflows that integrate additive and subtractive techniques, expanding the formal, material, and structural possibilities in architecture. This reflects a broader trend in architectural AM: combining additive processes with conventional methods to expand material capabilities, formal control, and architectural expression.

In sum, AM is reshaping architectural workflows by bridging form generation with sustainable material application and robotic fabrication. As new tools emerge and materials evolve, its impact on architectural performance, material efficiency, and design freedom will only grow

2.2 Additive Manufacturing with Biobased Materials

2.2.1 General Information

The integration of biobased materials into additive manufacturing (AM) is an innovative approach that addresses the growing demand for sustainable production methods. Biobased materials, derived from renewable resources such as plants and agricultural waste, can offer an environmentally friendly alternative to traditional petroleum-based materials.

Polylactic acid (PLA) is one of the most widely used biobased polymers in AM due to its renewability, biocompatibility, and favourable mechanical properties (Voet et al., 2018). PLA is derived from renewable resources like corn starch or sugarcane, making it an attractive option for various applications, including packaging, consumer goods, and biomedical devices (Vazquez-Martel et al., 2021).

Chin et al. (2023) explored the use of lignin-derived (meth)acrylates to create bio derivable photo resins for vat photopolymerization, demonstrating the potential for producing robust thermoplastic parts with sustainable

materials (Chin et al., 2023). Additionally, the exploration of vegetable oils as feedstock for AM has gained attention. Vazquez-Martel et al. (2021) developed sustainable formulations for digital light processing (DLP) using various vegetable oils, which were modified to incorporate photopolymerizable groups, enabling their use in 3D printing (Vazquez-Martel et al., 2021). Foley et al. (2012) discussed the potential of microbially-produced polyhydroxyalkanoates (PHAs) as renewable surfactants, which could enhance the performance of biobased polymers in AM applications (Foley et al., 2012).

As research continues to advance in this field, the potential for developing innovative materials and processes that reduce environmental impact while maintaining high performance will likely expand.

2.2.2 Methods Used

Out of the seven standard AM techniques, five have been researched or applied using biobased composites as feedstock: material extrusion, powder bed fusion, photopolymerization, binder jetting, and sheet lamination. Choosing among these depends on intended applications, material attributes, and performance requirements. Among them, material extrusion—including FDM and direct ink writing (DIW)/liquid deposition modeling (LDM)—is the most widely adopted in biocomposite research.

Biobased polymers are gaining traction in FDM due to their renewability and biodegradability. Tailored PLA-based filaments reinforced with natural fibers—such as cellulose, flax, hemp, or coconut—deliver improved mechanical properties while retaining printability and cost-effectiveness (Vyavahare et al., 2020). Recent reviews detail how PLA–cellulose natural fiber composite filaments can be successfully printed via FDM, with particular attention to dimensional accuracy, strength, and ecological benefits

Studies on PLA–lignin blends further support the potential for printing more sustainable structural biocomposites using pellet or filament extrusion (Ebers et al., 2021).

DIW/LDM techniques extrude viscous pastes, gels, or clay slurries, often used in ceramic arts, bioprinting, and large-scale construction prototypes. Cellulose-based hydrogels and clay pastes offer excellent viscosity and form retention—essential for architectural-scale extrusion .

Within photopolymerization, modified cellulose resins in SLA have demonstrated enhanced mechanical and thermal properties in small-scale prototypes (Musazzi et al., 2018).

SLS research involving lignin and cellulose powders has shown promise in terms of part strength and sustainability, although consistent powder flow and sintering remain technical challenges (Mançanares et al., 2015).

Finally, binder jetting and sheet lamination are still largely experimental with biobased materials. However, they offer significant potential for multi-material construction elements and scalable fabrication when integrated with appropriate post-processing

Recent studies have explored the use of cellulose-based resins in SLA, demonstrating improved mechanical properties and thermal stability (Musazzi et al., 2018). SLA has also been explored for creating biobased composites, demonstrating its versatility in additive manufacturing (Jiménez et al., 2019). The ability to use lignin and cellulose powders in SLS processes has been investigated, with promising results in terms of mechanical performance (Mançanares et al., 2015).

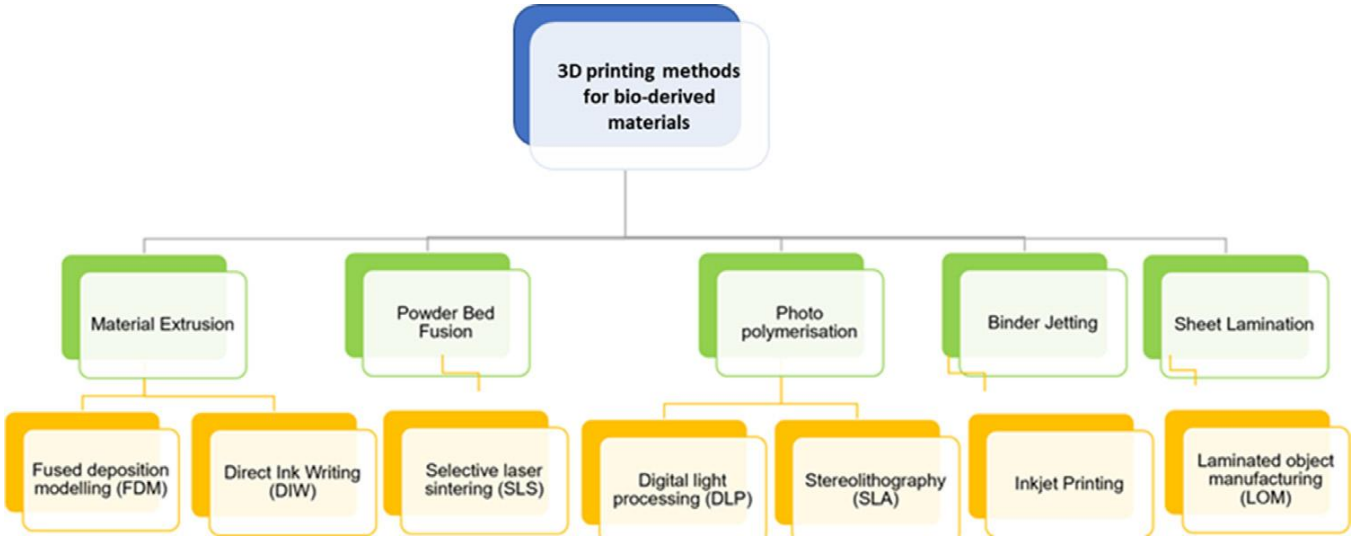

Figure 3 - Classification of 3D printing methods applicable to bio-derived materials, illustrating key technologies such as FDM, DIW, and SLA under broader process categories like material extrusion, powder bed fusion, and photopolymerization.(Gauss et al., 2021)

2.2.3 Materials Used

Various types of biobased materials are employed in AM processes, each offering unique properties and applications. This section outlines the primary material types used in additive manufacturing with biobased materials.

Polylactic Acid (PLA)

Derived from renewable resources such as corn starch or sugarcane, PLA is known for its biodegradability and biocompatibility, making it suitable for applications in packaging, consumer products, and biomedical devices (Voet et al., 2018). PLA can be processed using various AM techniques, including Fused Deposition Modeling

(FDM) and Stereolithography (SLA), and is favoured for its ease of printing and good mechanical properties (Voet et al., 2018).

Polyhydroxyalkanoates (PHAs)

Polyhydroxyalkanoates (PHAs) are a class of biopolyesters produced by microbial fermentation of sugars or lipids. PHAs are biodegradable and can be tailored to exhibit different mechanical properties, making them suitable for a range of applications, including packaging and medical devices (Upton & Kasko, 2018).

Lignin-Based Materials

Lignin can be used to enhance the mechanical properties of biocomposites when combined with other polymers, such as PLA or PHAs. Recent studies have demonstrated the potential of lignin-based materials in 3D printing applications, providing a sustainable alternative to traditional petroleum-based polymers (Weiss et al., 2012; Viretto & Galy, 2018).

Cellulose Nanofibers (CNFs)

Cellulose nanofibers (CNFs) are derived from the mechanical disintegration of cellulose fibers, which can be obtained from wood or agricultural waste. CNFs exhibit excellent mechanical properties and can be incorporated into biobased composites to improve their strength and stiffness (Soloi, 2023). The use of CNFs in AM processes allows for the creation of lightweight and strong materials suitable for various applications (Soloi, 2023).

Biobased Polyurethanes

Biobased polyurethanes are synthesized from renewable resources, such as vegetable oils or lignin, and exhibit desirable properties for various applications, including flexible foams and coatings. These materials can be processed using AM techniques to create customized parts with specific mechanical properties (Yin, 2024).

Starch Based Materials

Starch-based materials are another category of biobased polymers used in additive manufacturing. Starch can be processed into thermoplastic starch (TPS), which can be extruded and printed using FDM techniques. TPS is biodegradable and can be used for packaging and disposable products, contributing to sustainability efforts in the packaging industry (Ali & Kaneko, 2019). The incorporation of plasticizers and other additives can enhance the processability and performance of starch-based materials in AM applications (Filgueira et al., 2018).

2.2.4 Binders

Binders are essential components in additive manufacturing (AM) with biobased materials, as they provide cohesion, structural integrity, and enhance the overall performance of the printed parts.

Biobased Polymers

Biobased polymers, such as polyvinyl alcohol (PVA), sodium carboxymethyl cellulose (Na-CMC), and sodium alginate, are being used as binders in AM processes. These materials are derived from renewable resources and offer advantages such as biodegradability and low toxicity. For instance, Na-CMC, provides good adhesion and mechanical properties while being environmentally friendly (Garcıá et al., 2018).

Polyhydroxyalkanoates (PHAs)

Aforementioned PHAs are biobased materials that can serve as effective binders in AM processes due to their biodegradability and biocompatibility. They can be used in combination with other biobased materials to enhance the mechanical properties of printed parts while maintaining an environmentally friendly profile (Bianchini, 2023).

Lignin-Based Binders

Lignin-based binders can enhance the mechanical properties of biocomposites when combined with other materials, such as cellulose or PLA. Recent studies have shown that lignin can be modified to improve its compatibility with other polymers, making it a promising candidate for use in AM (Silau et al., 2022).

Epoxy Resins

Biobased epoxy resins are another category of binders used in AM. These resins, derived from renewable resources such as plant oils, offer excellent mechanical properties and thermal stability. They can be formulated for various AM techniques, including Stereolithography (SLA) and Digital Light Processing (DLP) (Le et al., 2020).

Alginates

Alginates, derived from brown seaweed, are natural polysaccharides that can be used as binders in additive manufacturing. Their gel-forming properties make them suitable for creating hydrogels and other biomaterials used in 3D printing. Alginates can enhance the mechanical properties of printed structures while providing biocompatibility, making them ideal for applications (Sheydaeian et al., 2016).

Chitosan

Chitosan, a biopolymer derived from chitin found in crustacean shells, is another binder for additive manufacturing. Chitosan exhibits biocompatibility and biodegradability, making it suitable for various applications. Recent studies have shown that chitosan can be effectively used as a binder in 3D printing processes, enhancing the mechanical properties of printed parts while promoting sustainability (Bianchini, 2023).

Thermoplastic Starch

Thermoplastic starch (TPS) is a biobased polymer derived from natural starch sources. TPS can be used as a binder in additive manufacturing processes, providing good adhesion and mechanical properties. The incorporation of plasticizers can enhance the processability of TPS, allowing it to be extruded and printed using FDM techniques (Ludwig et al., 2017).

Cellulose-Based Binders

Cellulose-based binders can be combined with other biobased materials to create composites with improved strength and durability, and can be used to enhance the mechanical properties of printed parts. The use of cellulose as a binder not only contributes to the sustainability of the AM process but also allows for the creation of biodegradable products (Lee et al., 2021).

Tree Sap

Tree sap, particularly from species such as pine, can be utilized as a natural binder in additive manufacturing. The adhesive properties of tree sap make it suitable for binding materials together in 3D printing applications. This natural binder can enhance the performance of printed parts while promoting eco-friendly manufacturing (Hardikar & Jamdade, 2020).

Magnesium Carbonate

Magnesium carbonate can provide structural integrity and enhance the mechanical properties of printed parts. The use of magnesium carbonate as a binder contributes to the sustainability of the AM process by utilizing inorganic materials that can be sourced sustainably (González-Gutiérrez et al., 2021).

By leveraging biobased polymers, natural polysaccharides, and other sustainable materials, AM processes can produce high-quality components while minimizing environmental impact.

2.3 Lignin and Cellulose Feedstocks

2.3.1 Overview of Lignin and Cellulose

Lignin

Lignin is a complex biopolymer found in the cell walls of plants, accounting for approximately 15-30% of the dry weight of wood. It serves as a natural binder, providing structural support and resistance to degradation (Getachew, 2023).

Sourcing

Lignin is abundant, comprising up to 40% of hardwood and softwood trees, and is often a byproduct of the pulp and paper industry. The extraction of lignin from biomass can be achieved through various methods, including chemical, enzymatic, and thermochemical processes (Zhang et al., 2022). For example, the kraft process, commonly used in the paper industry, separates lignin from cellulose and hemicellulose, resulting in a lignin-rich black liquor that can be further processed for lignin recovery.

Composition

Lignin is composed of phenolic compounds, which contribute to its complex structure. Its composition varies depending on the plant source and extraction method, resulting in different functional properties. Lignin is primarily composed of three monolignols: coniferyl alcohol, sinapyl alcohol, and p-coumaryl alcohol, which polymerize to form a three-dimensional network (Colon, 2023).

Properties

Lignin exhibits unique properties, including high thermal stability and UV resistance, making it suitable for various applications in biocomposites and as a reinforcing agent in 3D printing materials (Zhang et al., 2019). Research has demonstrated that lignin can enhance the mechanical properties of composites while providing a sustainable alternative to synthetic polymers (Hong et al., 2021).

Lignin does not have a defined melting point; instead, it softens and begins to decompose at temperatures around 200°C (392°F). The thermal degradation of lignin typically occurs between 250°C and 400°C (482°F to 752°F), leading to the formation of various low-molecular-weight compounds (Jiang et al., 2023).

Lignin's ability to improve the mechanical properties of materials while maintaining biodegradability makes it an attractive option for sustainable product development (Ebers et al., 2021).

Cellulose

Cellulose is the most abundant organic polymer on Earth, primarily found in the cell walls of plants. It is a linear polysaccharide composed of glucose units, resulting in a rigid structure that provides mechanical strength (Wan, 2023).

Sourcing

Cellulose can be sourced from various materials, including wood, cotton, and agricultural residues. The extraction of cellulose typically involves chemical treatments to remove lignin and hemicellulose, resulting in purified cellulose fibers (Caretto et al., 2018).

Composition

Cellulose is composed of long chains of glucose molecules, which can be further processed into cellulose nanofibrils (CNFs) or cellulose nanocrystals (CNCs) for enhanced properties (Lebedeva et al., 2022). The degree of polymerization and crystallinity of cellulose can vary depending on the source and extraction method, influencing its mechanical properties.

Properties

Cellulose exhibits excellent mechanical properties, high tensile strength, and biodegradability, making it suitable for a wide range of applications, including packaging, textiles, and biocomposites (Zhang et al., 2021). Recent advancements in cellulose processing techniques, such as the production of cellulose nanofibrils (CNFs), have further enhanced its properties, enabling its use in additive manufacturing (Lee et al., 2016). The incorporation of cellulose into 3D printing materials can improve flow characteristics and interlayer adhesion, contributing to the overall performance of printed components (Cataldi et al., 2020).

Cellulose does not have a specific melting point; instead, it decomposes at temperatures above 300°C (572°F). The thermal degradation of cellulose occurs in stages, with significant weight loss typically observed between 200°C and 400°C (392°F to 752°F) (Olson et al., 2021).

Cellulose's versatility extends to its use in various applications, including as a reinforcing agent in composites and as a biodegradable alternative to conventional plastics. Its abundance and renewability make it a key player in the development of sustainable materials for the future (Sternberg, 2023).

2.3.2 Traditional Manufacturing

Lignin

The most common methods for lignin extraction include the Kraft process, sulfite process, and organosolv process, each of which alters the native structure of lignin to varying degrees (Tortora et al. (2014), Song et al., 2013).

The Kraft process is one of the most widely used methods for pulp production, where wood chips are treated with a mixture of sodium hydroxide and sodium sulfide. This process effectively breaks down the lignin, allowing for the separation of cellulose fibers. However, a significant portion of lignin is typically burned as fuel in the process, leading to underutilization of this valuable biopolymer (Zhao et al., 2016; Fang et al., 2020). The lignin obtained through the Kraft process is often referred to as technical lignin and can be further processed for various applications.

The sulfite process involves treating wood chips with a solution of sulfurous acid and bisulfite salts. This method is less commonly used than the Kraft process but can yield lignin with different properties. The lignin extracted via this method is often more soluble in water, making it suitable for specific applications such as adhesives and dispersants (Fatriasari, 2024).

The organosolv process utilizes organic solvents, such as ethanol or acetone, to extract lignin from biomass. This method allows for a more selective extraction of lignin while preserving its structural integrity. The lignin obtained through the organosolv process is often of higher purity and can be used in various applications, including the production of biofuels and bioplastics (Yefremova et al., 2019).

Cellulose

Cellulose is extracted from lignocellulosic biomass through various pulping processes, which involve the removal of lignin and hemicellulose.

Mechanical pulping method involves grinding wood chips to separate cellulose fibers from lignin and hemicellulose. Mechanical pulping is energy-intensive and results in lower-quality pulp due to the retention of lignin. However, it is a cost-effective method for producing pulp for newsprint and other low-quality paper products (Zhang & Pei, 2010).

Chemical pulping processes, such as the Kraft and sulfite methods, utilize chemicals to dissolve lignin and hemicellulose, allowing for the extraction of pure cellulose fibers. The Kraft process is the most widely used chemical pulping method, producing high-quality cellulose suitable for various applications (Ceren & Yucel, 2023).

Enzymatic hydrolysis is an emerging method for cellulose extraction that utilizes enzymes to break down lignin and hemicellulose, facilitating the release of cellulose fibers. This method is more environmentally friendly compared to traditional chemical pulping processes and can yield high-purity cellulose (Andok, 2023).

The traditional manufacturing processes for lignin and cellulose involve various methods that significantly impact the properties and applications.

2.3.3 Additive Manufacturing

Additive manufacturing (AM) utilizing lignin and cellulose has gained more attention in recent years due to the sustainability of these biopolymers. Both lignin and cellulose are abundant components of lignocellulosic biomass, making them attractive materials for various applications in 3D printing and biocomposite production.

Lignin and cellulose can be used in various 3D printing technologies such as fused deposition modeling (FDM), stereolithography (SLA), digital light processing (DLP), selective laser sintering (SLS), and direct ink printing. The properties of lignin, including its morphology, microstructure, and physical, chemical, and biological modifications, are important to consider for 3D printing applications (Jiang et al. 2023). Lignin's properties can be improved through chemical modification to enhance its processability and material properties. Lignin can also be combined with other materials, such as polyhydroxybutyrate, polylactic acid (PLA), or methacrylate to create composites with enhanced mechanical properties (Jiang et al. 2023).

Jiang et al. (2023) provided a comprehensive review of lignin-based materials for additive manufacturing, emphasizing the importance of constructing lignin into material parts with controlled macro- and microstructures. This research underscores the potential of lignin to enhance the mechanical properties of composites while providing a sustainable alternative to synthetic polymers.

Lignin can be challenging to print alone due to its complex structure, but it can be blended with other polymers, such as PLA, to improve printability and mechanical performance. Studies have shown that lignin-containing filaments can be effectively 3D printed, resulting in functional components suitable for various applications (Tanase-Opedal et al., 2019).

Xu et al. (2018) reviewed the application of wood-derived biopolymers, including cellulose, in biomedical applications, emphasizing the versatility of these materials in 3D printing. They noted that the combination of cellulose with lignin can lead to the development of novel materials with improved mechanical and functional properties.

Cellulose can be processed into various forms, including nanofibers and films, which can be used in AM. Its excellent mechanical properties, high tensile strength, and biodegradability make it suitable for a wide range of applications, including packaging, textiles, and biocomposites. Recent advancements in cellulose processing techniques, such as the production of cellulose nanofibrils (CNFs), have further enhanced its properties, enabling its use in additive manufacturing (Gkartzou et al., 2017).

There are still challenges to overcome when using lignin and cellulose together in 3D printing. More research is needed to determine how to combine these materials with different binders to create a paste suitable for 3D printing in the built environment (Bierarch et al., 2023). The toxicity and flammability of some binding agents need to be addressed, as well as the inherent properties of lignin, such as its odor, color, reactivity, strength, and thermal stability (Jiang et al. 2023).

2.4 Environmental Assessment of Additive Manufacturing

2.4.1 Overview

One of the primary sustainability advantages of additive manufacturing (AM) lies in its near-zero-waste approach. By fabricating parts layer by layer and directly from digital models, AM eliminates the need for subtractive cutting or milling processes that typically generate excess material waste. This layer-wise precision ensures that only the required amount of material is deposited where needed, significantly reducing raw material usage (Ngo et al., 2018).

Furthermore, AM enables the use of biobased and biodegradable polymers such as polylactic acid (PLA), polyhydroxyalkanoates (PHAs), and starch-based composites. These materials are derived from renewable sources like corn, sugarcane, or microbial fermentation, and have been demonstrated to perform well in extrusion-based AM processes such as FDM and DIW (Vazquez-Martel et al., 2021; Dananjaya et al., 2024). This contributes to a reduced carbon footprint and increased material circularity when compared to conventional petroleum-derived polymers.

Another major benefit is the localized, distributed nature of AM, which allows production to occur close to the point of use. This eliminates the need for long-distance transportation of pre-manufactured goods, thereby reducing associated greenhouse gas emissions and logistical overhead (Ford & Despeisse, 2016). When integrated with decentralized supply chains, AM supports more resilient and lower-impact manufacturing ecosystems.

AM also enables on-demand manufacturing, reducing the need for overproduction, warehousing, and excess inventory. This agility supports just-in-time production models that minimize obsolescence and waste (Sanchez-Rexach et al., 2020). Additionally, the recyclability of thermoplastic feedstocks used in AM systems means that failed prints, prototypes, or post-use products can be reprocessed into new feedstock, supporting closed-loop manufacturing strategies (Agrawal & Vinodh, 2020).

Finally, the adaptability of AM to process composite materials made from industrial by-products or natural fibers—such as lignin, cellulose, or flax—has opened new avenues for reducing environmental burdens in material sourcing while maintaining mechanical performance suitable for architectural applications (Dananjaya et al., 2024).

2.5 Masonry in Additive Manufacturing

2.5.1 Modular Masonry Applications

Modular masonry represents a significant innovation in construction technology, utilizing pre-fabricated units that enhance efficiency, flexibility, and sustainability. These systems allow for rapid assembly, reduced labor costs, and customization, making them adaptable to various architectural designs and structural requirements. As Kyriakidis et al. (2016) note, modular masonry components can be optimized for energy efficiency and resource conservation, aligning with sustainable construction practices. For instance, the Bloque Termodisipador (BT) system developed in Mexico integrates interlocking hollow clay blocks designed for passive ventilation and reduced thermal loads, illustrating how modular components can be tailored for climate-responsive architecture.

A key feature of modular masonry is the use of interlocking masonry blocks, which, as Aharoni et al. (2021) highlight, enhance structural stability and resilience while simplifying construction. This approach facilitates the creation of complex geometries without compromising strength, reducing the reliance on traditional adhesives and improving overall efficiency. An example is the Kite Bricks Smart Brick system, which uses Lego-like concrete blocks with built-in channels for plumbing and wiring, streamlining construction and reducing material waste.

Additionally, modular systems support circular economy principles by enabling material reuse and recycling. Pelicaen et al. (2023) emphasize the importance of designing systems for disassembly, minimizing waste, and extending material lifespans, contributing to sustainable building lifecycles. This is exemplified by Wikkelhouse,

a modular cardboard-based dwelling system designed for disassembly and recyclability, showing how prefabricated components can support both flexibility and material circularity. However, challenges in scaling modular masonry for widespread adoption remain. As Pelicaen et al. (2023) suggest, the development of standardized guidelines is essential for addressing these barriers and ensuring broader implementation in mainstream construction.

By integrating innovative design principles, advanced techniques, and sustainability-focused practices, modular masonry holds the potential to reshape the construction industry and contribute to a more environmentally conscious built environment.

2.5.2 Traditional Manufacturing

Traditional manufacturing methods for modular masonry focus on the production of standardized components that can be utilized in various architectural designs. The manufacturing of modular masonry typically involves the use of concrete blocks, bricks, or other masonry units that are produced in a controlled environment. These units are designed to interlock or fit together in a modular fashion, allowing for quick assembly and disassembly.

The production process often includes the mixing of raw materials, such as cement, aggregates, and water, followed by molding and curing to achieve the desired strength and durability Tchertchian et al. (2011). One of the primary benefits of modular masonry is its potential to improve energy efficiency and reduce environmental impact. As highlighted by Kozlovská et al. (2014), modular construction methods can lead to significant reductions in construction waste and energy consumption compared to traditional masonry techniques.

The ability to produce standardized units in a factory setting allows for better quality control and minimizes the variability often seen in on-site construction. For instance, the integration of recycled materials into the production of masonry units can further enhance the sustainability profile of modular construction. This aligns with the growing demand for eco-friendly building practices that prioritize resource conservation and environmental stewardship (Gao & You, 2017).

Despite the advantages, challenges remain in scaling up modular masonry applications, particularly in highly industrialized contexts. Research by Kyriakidis et al. (2016) emphasizes the need for innovative solutions to overcome barriers to adoption, including the development of standardized practices and guidelines for implementing modular masonry systems.

2.5.3 Additive Manufacturing

Additive manufacturing (AM) is contributing to the construction industry, also in the realm of modular masonry. This innovative approach utilizes advanced technologies to produce modular masonry units that can be easily assembled on-site, offering increased efficiency, sustainability, and design flexibility. The integration of AM into modular masonry provides numerous advantages, such as reduced construction time, minimized material waste, and the capacity to customize designs for specific project requirements.

Biobased materials not only enhance the mechanical properties of masonry units but also promote environmental sustainability. For instance, research by Manoharan et al. demonstrated that bio-additive-infused air lime mortar improved the performance of lime mortar over time, highlighting the value of biobased materials in modular masonry (Dang, 2024). Lignin serves as a natural binder, adding structural support and resistance to degradation, while cellulose enhances the strength and durability of the final product (Zadeh et al., 2018).

However, challenges persist in scaling modular masonry applications, especially in highly industrialized settings. Key barriers include the lack of standardized practices and guidelines for implementation. Researchers like González et al. (2010) emphasize the importance of innovative solutions to address these challenges, ensuring the viability of modular masonry in mainstream construction.

In conclusion, additive manufacturing of modular masonry represents a significant step toward a more sustainable construction industry. By integrating advanced design principles and efficient production techniques, modular masonry has the potential to redefine resource-efficient and environmentally friendly building solutions. As technology and research continue to progress, modular masonry could play a transformative role in the construction landscape, driving the adoption of more sustainable practices in the built environment.

2.6 Computational Slicing

2.6.1 Slicer Workflows

Robotic additive manufacturing (RAM) in architecture increasingly relies on customized slicing workflows tailored to both the geometric complexity and rheological behavior of bio-based materials. Standard slicers such as Ultimaker Cura or Slic3r, while widely used in desktop 3D printing with thermoplastic filaments, are primarily designed around planar slicing and fixed deposition parameters. These workflows often prove

insufficient for large-scale robotic fabrication, particularly when dealing with low-viscosity pastes, non-Newtonian flow, or anisotropic shrinkage in materials such as cellulose- or lignin-based composites (Klemmt et al., 2022). Moreover, they do not allow for dynamic adaptation of toolpaths or robotic motion in response to geometry, speed, or real-time feedback.

To overcome these limitations, architectural researchers are increasingly adopting parametric environments such as Rhino and Grasshopper in combination with robotic programming plugins like KUKA|prc, HAL Robotics, or COMPAS FAB. Rhino's NURBS-based modeling capabilities provide flexible design freedom, while Grasshopper's visual scripting environment enables rule-based geometry generation and real-time parameter control. These platforms support an integrated computational loop, where toolpath planning, kinematic simulation, and G-code or robot code generation are co-developed and continuously informed by material behavior and design objectives. This enables a "design-to-fabrication" pipeline that is both iterative and adaptable.

For example, Klemmt et al. (2022) present a full pipeline for robotic extrusion using a biodegradable composite made of wood fibers and bio-resin. The team used HAL Robotics in Grasshopper to define toolpaths that accommodate the paste's slow curing time and poor bridging capacity. The system included dwell times at corners, speed modulation along curves, and volumetric control to avoid overextrusion—all features impossible to implement in standard slicers.

Similarly, Zboinska et al. (2021) demonstrated a hybrid slicing strategy, where they combined standard G-code exported from Cura with parametric overrides from Grasshopper for detail-intensive regions. This approach allowed precise toolpath manipulation for features like curved interlocks and non-planar surfaces, showcasing how live scripting can enable feedback-driven adaptation in robotic workflows.

Educational examples, such as those by Kretzer and Mostafavi (2020), demonstrate how students develop robotic extrusion systems in Rhino—Grasshopper to prototype biodegradable plastic parts. Their workflows emphasized material-responsive fabrication, where slicing logic was not predefined but continuously updated based on setting time, layer adhesion, or geometry-specific constraints.

Compared to these precedents, the slicing strategy in this research project also leverages a Grasshopper-based setup—however, it differentiates itself through its focus on strength-graded slicing across different material zones. The slicing logic accounts not only for geometry and paste behavior but also for material-specific deposition strategies across structurally differentiated bricks. In contrast to Cura or planar slicers, this workflow allows adaptation of layer height, print speed, and nozzle retraction in direct response to localized strength requirements and material flow characteristics.

2.6.2 Advancements in Slicing Algorithms

Beyond geometric discretization, modern slicing strategies now encode functional parameters—enabling toolpaths to control moisture dynamics, structural performance, build orientation, and material gradation during printing.

Rosca *et al.* (2022) pioneered parametric infill strategies, such as lattice networks and columnar voids within biopolymer wall elements. These internal geometries enhance air circulation, promoting even drying and reducing warping or moisture-induced stress

Moreover, Rosca *et al.* demonstrated that printing vertically rather than in the usual horizontal orientation can align material anisotropy—including fiber directions—with load paths. This approach enhances tensile strength and even supports embedded mechanical joinery, such as mortise-and-tenon features, which are difficult to achieve with conventional slicing .

In parallel, adaptive slicing techniques have gained traction, adjusting layer thickness based on local geometry or material composition to balance surface fidelity and print speed. While Furlan *et al.* (2025) previously explored this, similar concepts were advanced by others integrating non-planar and adaptive slicing into robotic FDM workflows—maintaining consistent material deposition across complex surfaces .

Finally, Qi *et al.* (2024) and follow-up work by Wade, Beck & MacCurdy (2025) describe functionally graded slicing, which embeds zone-specific toolpath variations—including changes in density, material mix, and extrusion parameters. This method uses implicit geometry and iso-contours to guide seamless transitions within mixed-material prints, enabling precise control over mechanical and material gradients

2.6.3 Software Tools and Frameworks

The architectural application of biocomposite slicing is deeply rooted in parametric modeling environments that support both geometric design and robotic motion planning. Among these, Rhinoceros 3D combined with Grasshopper is the prevailing platform in academic and experimental workflows. Plugins such as KUKA|prc and HAL Robotics extend Grasshopper's functionality by providing real-time simulation, robotic code generation, and full kinematic control over multi-axis robotic arms—making it possible to prototype geometry, slicing logic, and robotic behavior within a single visual environment (Zboinska et al., 2021; Gramazio et al., 2014).

In these parametric environments, custom G-code generation workflows are commonly implemented to account for fabrication-specific parameters like nozzle size, extrusion rate, temperature, and robot orientation. Zboinska et al. (2021) describe a dual-script slicing strategy in Grasshopper: one script generates the material deposition

path (similar to traditional G-code), while a second script synchronizes this path with the robotic arm's orientation, ensuring correct nozzle alignment during spatial printing.

As robotic additive manufacturing becomes more sophisticated, researchers have begun integrating environmental feedback into slicing workflows. Rosca et al. (2022), for example, developed an early closed-loop fabrication system that uses real-time sensor input to monitor drying patterns and layer deformation during extrusion. Based on these inputs, the toolpath is dynamically adjusted mid-print—by modifying parameters such as dwell time, tool speed, or infill density—to improve layer adhesion and minimize warping in biopolymer composites.

In more experimental or resource-constrained setups, researchers often use hybrid slicing workflows. One common approach is to slice geometry in Cura, a standard FDM slicer, and then post-process the resulting G-code using Python scripts or parametric interfaces to integrate multi-axis deposition strategies. This allows for fine-grained control over robotic arm movement and extrusion behavior, enabling adaptation to material-specific behavior like anisotropic shrinkage, tackiness, or inconsistent flow (Qi et al., 2024).

Overall, these workflows exemplify how architectural-scale biocomposite fabrication necessitates not only geometric design but also the co-development of software frameworks that integrate robotic logic, material behavior, and responsive adaptation.

2.6.4 Challenges with Biocomposites

The variability of biocomposite materials introduces multiple fabrication challenges. One major limitation is material feed consistency. Klemmt et al. (2022) addressed clogging and air pockets in wood-plastic blends by designing a custom three-stage auger extruder. Such material heterogeneity requires slicing workflows to integrate extrusion pauses or over-extrusion compensations.

Moisture content and differential drying are also significant. Rosca et al. (2022) introduced toolpath design patterns that facilitate even moisture distribution. Others, like Mogas-Soldevila et al. (2015), incorporated active drying systems, such as programmed fan arrays, to stabilize large-format bio-printed membranes.

Another issue is dimensional stability. Parts printed from cellulose or alginate may shrink during drying, requiring predictive compensation in slicing routines (Rosca et al., 2022). Additionally, achieving functional joinery is limited by print resolution and shrinkage variability. Luo et al. (2025) circumvent this by relying on mycelium growth to fuse parts post-printing.

At architectural scale, print speed becomes a limiting factor. Biopolymers often demand slower extrusion rates and curing pauses. Zboinska et al. (2021) note that their slicing routines included segment-based printing to allow resting and re-calibration during long prints.

3. MATERIAL DEVELOPMENT

3.1. Overview

The material research phase began with the reproduction and evaluation of existing formulations for lignocellulosic-based additive manufacturing feedstocks, drawing insights from prior research, including the work of Christopher Bierarch and Alexandre Coelho, which contributed to the selection of raw materials and processing methods. The initial focus was on understanding the role of lignin and cellulose in extrusion-based applications, leading to an iterative improvement process aimed at refining material composition for better printability and mechanical performance. In contrast to prior research, this study extends into the development of a hot-extrudable, application-ready composite, bridging the gap between material science and architectural fabrication.

With an emphasis on developing a fully bio-based and sustainable alternative, the study explored various binder options to replace conventional chemical additives. A series of material experiments were conducted to assess the behavior of different formulations, testing viscosity, homogeneity, and structural integrity at various mixing ratios and processing conditions. Through manual testing and visual analysis, promising formulations were identified for further evaluation.

The most viable composites were selected for mechanical and printability assessments, ensuring their suitability for hot extrusion-based additive manufacturing. These findings informed subsequent material adjustments, advancing the development of sustainable lignin-cellulose composites optimized for extrusion and structural applications.

3.2. Methods

3.2.1 Experiment Design

The material exploration phase began with research into the properties of lignin and cellulose, focusing on their thermal behavior, compatibility with thermoplastics, and suitability for hot extrusion-based additive manufacturing. Unlike previous studies by Alexandre Coelho and Christopher Bierarch, which explored cold extrusion using thermosets, this research required thermoplastic binders to ensure processability under heat.

Over the past three weeks in the lab, extensive experimentation has been conducted to analyze the thermal stability, degradation points, and interactions of lignin and cellulose with different thermoplastic binders. The goal was to identify challenges such as viscosity control, phase separation, and adhesion during the hot extrusion process.

To refine the formulation, three thermoplastic binders (PLA, PHA and TPS), one primer (citric acid), and one plasticizer (glycerol) were systematically tested to assess their impact on printability, mechanical performance, and extrusion flowability. Each binder was first evaluated individually for melt behavior and compatibility with lignin and cellulose before being integrated into composite formulations. The plasticizer was introduced to enhance flexibility and reduce brittleness, while the primer was assessed for its effect on adhesion and homogeneity.

The most promising formulations were selected based on extrudability, consistency, and structural potential, leading to further refinement and testing. This phase has established a strong foundation for the development of a high-lignin-cellulose biocomposite optimized for hot extrusion-based additive manufacturing, ensuring both thermal stability and mechanical integrity moving forward.

3.2.2 Facilities

All experiments were conducted at the Heritage and Architecture Lab, located in the basement of the Faculty of Architecture and the Built Environment at TU Delft. The lab environment was carefully monitored, with room temperature ranging between 17°C and 20°C, slightly lower than typical indoor conditions due to excess outside air entering through the dust extraction system. Relative humidity was maintained between 35% and 42%, ensuring consistency in material behavior.

The dust extraction and ventilation system in the lab played a crucial role in reducing airborne lignin particles, minimizing inhalation risks during material handling and mixing. Additionally, a nearby water source was kept accessible as a safety precaution for handling heated materials, ensuring a controlled and secure working environment.

The Heritage and Architecture Lab provided the necessary infrastructure for all phases of material testing, from weighing and mixing raw materials to extrusion and printability assessments. The controlled conditions of the lab ensured the safe handling and precise formulation of high lignin-cellulose biocomposites for hot extrusion-based additive manufacturing.

3.2.3 Equipment

The necessary equipment for this experiment has been obtained from various online sources, as well as the AE+T department storage and Heritage and Architecture Lab.

The hot plate, scales with 0.01g level precision and magnetic stirrers was already available at the Heritage and Architecture Lab.The beakers, petri dishes, pipettes, glass stirrers, syringes, high-temperature kitchen thermometer and pans have been ordered from Amazon.nl website, through stores specialized in laboratory equipment and kitchen grade equipment. The coffee grinder, electric stove and spoons already existed in the department storage.

All the safety equipment and cleaning supplies were sourced from Amazon.nl, also from a seller with extensice supplies for laboratory safety.

Figure 4, 5, 6 - Equipment Setup

3.2.3 Materials

The main materials for this research are lignin and cellulose, which already existed in the storage of the department, as leftovers from Christopher Bierarch and Alexsander Coelho's research. The remaining materials were sourced from suppliers specialized in thermoplastics, local supermarkets and LAMA.

Cellulose, as mentioned in the research of Alexsander Coelho and Christopher Bierarch, is from the kraft type, bleached, and obtained in small pieces to be grinded, from an unspecified supplier.

Lignin, also as mentioned in the research of Alexsander Coelho and Christopher Bierarch, is from soda type, obtained in a box consisting about 5 kg of the material, from Greencone Environs Pvt Ltd.

Binders are PLA, PHA and TPS, in pellet form. PLA pellets were sourced by LAMA, with 99% purity. PHA has been sourced from a company called Entropic, and has 99.9% purity. Finally, two types of TPS with 99.9% purity has been sent as a support from Agrada Starch company, in product number 8945 and 8950.

Glycerol has been obtained by a local store called Dille and Kamille, with approximately 90% purity.

Lemon for citric acid has been obtained from Albert Heijn, a local supermarket.

Sunflower oil for the oil bath is standard kitchen supply, in standard packaging from the local supermarket Jumbo.

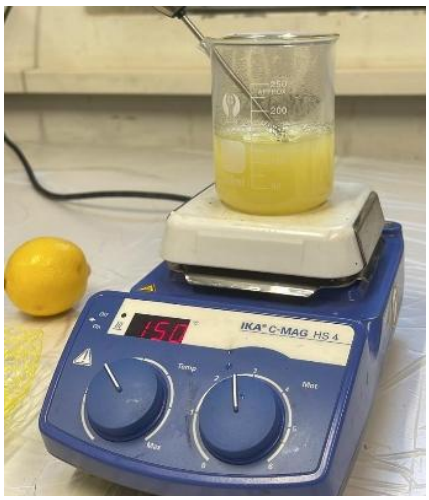

Figure 7, 8, 9 – Material Setup

3.3. Material Formulation Process

The material formulation process aimed to develop a high lignin-cellulose biocomposite optimized for hot extrusion additive manufacturing, balancing extrudability, mechanical performance, and structural stability. This phase followed a structured approach consisting of three key stages: fundamental analysis, binder exploration, and composite formulation and mixing.

By structuring the material formulation process into these three phases, the research established a pathway to developing a viable high lignin-cellulose composite that meets the processing requirements of hot extrusion additive manufacturing while maintaining sustainability and structural performance.

3.3.1 Analysis of Material Behavior

The fundamental analysis focused on understanding the thermal behavior, compatibility, and processability of lignin and cellulose. Since previous research on lignin-cellulose composites primarily explored cold extrusion and thermoset binders, this study required an alternative approach using thermoplastic binders to ensure melt processability under heat. The first step involved examining and researching the melting and degradation points of lignin and cellulose and their behavior when combined, identifying potential phase separation issues, viscosity challenges, and thermal stability concerns.

Environmental factors such as moisture sensitivity and heat retention were considered, as lignin and cellulose exhibit contrasting behaviors under heat and humidity. These insights provided the foundation for selecting suitable thermoplastic binders, plasticizers, and primers that would ensure both structural integrity and compatibility with hot extrusion conditions.

3.3.2 Binder Exploration

Following the foundational research, the binder exploration phase systematically tested three thermoplastic binders to determine their impact on extrudability, layer adhesion, and mechanical strength.

The binder exploration phase systematically tested PLA, PHA, and TPS to determine their suitability for hot extrusion additive manufacturing with high lignin-cellulose content. Each binder presented unique challenges in processability, extrusion behavior, and structural performance, requiring iterative adjustments to improve printability, adhesion, and material homogeneity.

3.3.3 Composite Formulation and Mixing

The final stage of material development focused on formulating and refining three distinct lignin–cellulose composite ratios, each tailored to meet a specific structural performance category: high, medium, and low strength. These ratios were designed to align with the architectural application of modular bricks in hot extrusion-based additive manufacturing, where printability, mechanical integrity, and extrusion behavior are interdependent. The formulation process involved systematic tuning of the fiber-to-binder ratios to balance structural stability and flow behavior, ensuring each mix remained extrudable without compromising strength.

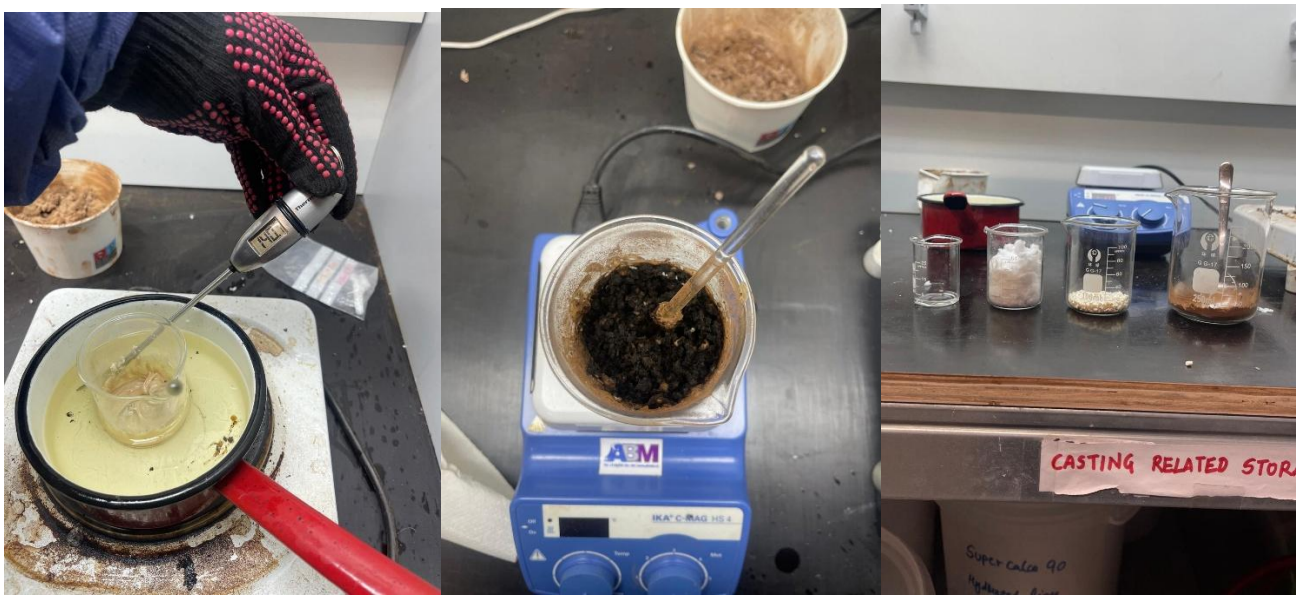

Figure 10, 11, 12 – Formulation & Mixing

3.4. Evaluation Criteria

Each material mixture was assessed using a visual-tactile evaluation framework designed to provide early insights into extrusion behavior and architectural feasibility. The criteria below were used during lab-scale testing:

Criteria	Description	Testing Method
Homogeneity	Consistency of fiber and binder distribution; absence of clumps or phase separation.	Visual inspection
Curing Time	Time taken for material to solidify post-extrusion at room temperature.	Stopwatch timing
Shrinkage	Dimensional reduction after curing; important for interlocking fit.	Manual measuring
Viscosity	Flow resistance during extrusion; related to material workability.	Extruder pressure test
Brittleness	Fracture tendency post-curing; important for mechanical performance.	Manual bending
Aesthetics	Surface quality, smoothness, and color consistency of the extrudate.	Visual inspection
Biobased Content	Proportion of renewable components in the mix (e.g., lignin, cellulose).	Calculated from mix ratio
Adherence	Quality of interlayer bonding; important for vertical buildability.	Visual + tactile testing
Extrudability	Overall printability; whether a steady, uninterrupted strand could be formed.	Continuous strand test

3.5. Results

The material testing phase yielded three final formulations suitable for robotic hot extrusion, each corresponding to a distinct structural strength category. These outcomes are presented in relation to the progression of the formulation phases and the refinement of mixture compositions. The selected composites were evaluated based on printability, extrusion stability, and early mechanical indicators, leading to a classification framework for further testing. Results are organized into two subsections: formulation phases and resulting mixtures.

3.5.1 Phases

Phase 1

The first phase of the material research focused on characterizing the individual behavior of cellulose and lignin to establish their suitability for hot extrusion-based composite development. This stage was essential in understanding the material limitations before introducing any thermoplastic binder systems.

Cellulose and lignin were both sourced from the remainders of previous thesis research by Alexander Coelho and Christopher Bierarch. The cellulose had already been cut into smaller shreds, and the next step was to pulp the pieces with a coffee grinder. This essentially produced a very cotton-like and fibrous texture as mentioned in the research of Coelho and Bierarch (2021). This consistency and texture have made it easier for cellulose to be handled in the mixtures in terms of homogeneity. The next step was to look into the reaction of cellulose when subjected to high temperatures. This has proven prior experimentation and research on the reaction of cellulose. It has started degrading above 175°C, burning quickly instead of melting.

Lignin was the soda type, was in powdered state, which has proven good for homogenous mixing with fibrous cellulose. Due to the heavy dust nature, it is relatively hard to handle. Similar to cellulose, work on lignin was also done by Coelho and Bierarch. This has been proven right through iterations on heating lignin. In lower temperatures starting from 85, ranging up to 145, lignin has become rather viscous through pressured stirring. After this temperature, the material started to degrade fast, charring in the process.

These early findings, reinforced by insights from Coelho and Bierarch (2021), confirmed that both materials carried significant thermal and environmental sensitivities. Rather than treating them as passive fillers, it became clear that their behavior under heat and humidity would fundamentally shape the entire binder system. This realization defined the parameters for subsequent phases of research, particularly in identifying suitable modifiers and binder candidates capable of stabilizing the lignin-cellulose matrix under extrusion conditions.

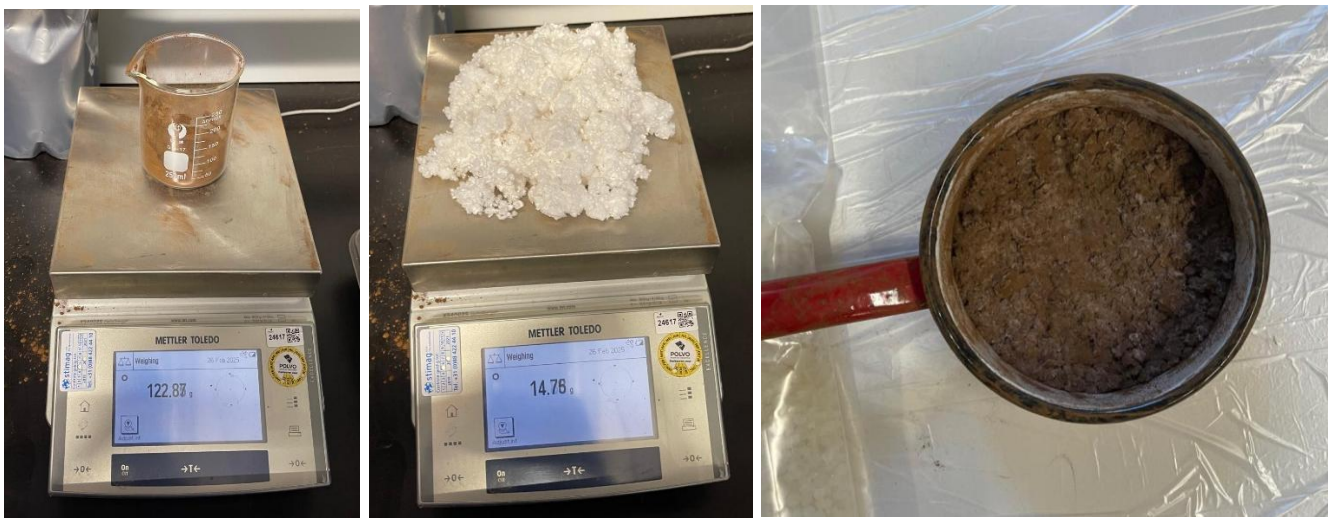

Figure 13, 14, 15 – Respective Images of Lignin, Cellulose and Dry Mix

Phase 2

Following the initial evaluation of lignin and cellulose behavior, Phase 2 focused on the systematic refinement of binder selection to ensure a compatible, extrudable, and structurally reliable composite. The goal was to identify a thermoplastic binder that could operate within the thermal stability range of lignin and cellulose while supporting flow behavior, interfacial bonding, and structural strength. A series of tests were conducted using Polylactic Acid (PLA), Polyhydroxyalkanoates (PHA), and Thermoplastic Starch (TPS), each evaluated under varying mixing and thermal conditions.

Polylactic Acid (PLA) – High Melting Point and Extrusion Difficulty

PLA demonstrated strong mechanical properties but proved challenging due to its high melting temperature (~170-200°C), which exceeded the thermal stability range of lignin and cellulose. This thermal mismatch led to degradation risks and uneven extrusion behavior, as some components of the mix began to break down before PLA could fully melt. Additionally, its intrinsically brittle nature resulted in poor flexibility without the addition of a plasticizer. Lowering the extrusion temperature while increasing the plasticizer content improved flowability, but adhesion to lignin-cellulose fibers remained inconsistent, requiring further adjustments.

Polyhydroxyalkanoates (PHA) – Rapid Stiffening

PHA offered better compatibility with bio-based fillers than PLA but presented significant processing challenges due to its rapid stiffening and brittle behavior. During mixing, PHA solidified too quickly, limiting workability and layer fusion, possibly leading to poor interlayer adhesion and fracture-prone structures. Increasing

plasticizer content temporarily improved flexibility, but higher concentrations caused phase separation, reducing overall homogeneity. Additionally, precise temperature control was necessary to prevent premature stiffening before extrusion was complete. Insulating the beaker contributed to the flowability of the material, but not fully. Despite initial challenges with rapid stiffening and brittleness, it offered superior chemical compatibility with lignin-cellulose fibers.

Thermoplastic Starch (TPS) – Requirement for an Additional Binder

TPS, while bio-based and flexible, did not behave as a true thermoplastic on its own and required an additional binder to function effectively in the composite. Without a secondary binder, TPS failed to melt uniformly, resulting in roasting of the pellets. The material absorbed moisture, affecting its long-term stability, and required strict environmental control to prevent swelling and possibly shrinkage when extruded. Although plasticizers may improve processability, the need for a supporting thermoplastic matrix meant TPS could not function independently in the formulation, which is a challenge given the objectives of the research.

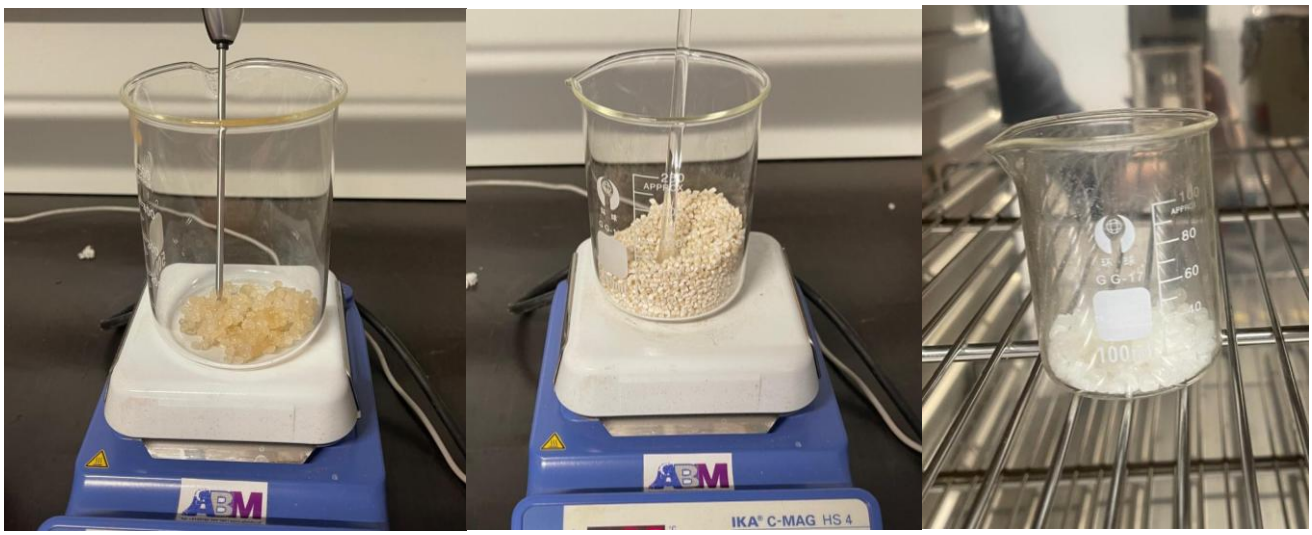

Figure 16, 17, 18 – Respective Images of PLA, PHA and TPS

To improve fiber-matrix interaction and reduce brittleness within the thermoplastic composite system, citric acid and glycerol were introduced as key additives. In early trials, lemon juice was tested as a natural, accessible source of citric acid to act as a primer. While this form showed some preliminary improvements in fiber dispersion, its inconsistency in concentration and additional liquid content made it unsuitable for repeatable processing.

Subsequently, pure citric acid powder was adopted for more controlled and scalable integration into the material system. Pre-melted into glycerol before mixing, the citric acid enhanced adhesion between the hydrophilic lignocellulosic fibers and the thermoplastic matrix, helping to mitigate clumping and phase separation. Glycerol, as a plasticizer, was essential in softening the composite, improving its flow during mixing and extrusion, and compensating for the inherent brittleness of PHA.

Together, citric acid and glycerol significantly improved the homogeneity, extrudability, and interfacial cohesion of the material, contributing to better interlayer adhesion and surface quality in the hot extrusion process.

Phase 3

Building on the material behavior insights and binder evaluations, this phase focused on the formulation and preparation of final composite mixes tailored for extrusion-based additive manufacturing. The goal was to create strength-graded material ratios optimized for printability, mechanical performance, and structural integration.

The process began by pre-mixing glycerol and citric acid, forming a primer designed to enhance fiber dispersion and interfacial bonding. In parallel, the dry lignin and cellulose fibers were homogenized using a high-speed blender, improving surface area and ensuring even distribution of components. The dry fiber blend was then coated with the citric acid-glycerol primer, creating a pre-treated, moisture-balanced mixture aimed to improve consistency during thermal processing.

Figure 19, 20 – Mix with Primer & Dried

This coated mixture was pre-dried in an oven at 60°C, reducing residual moisture and promoting surface adhesion. In the final stage, the thermoplastic binder (PHA) was melted separately in an oil bath to ensure gentle, even heating and avoid thermal shock. Once fully liquefied, the PHA was gradually introduced into the

pre-treated fiber blend, with careful manual stirring to control the cooling rate and ensure uniform integration. This prevented sudden stiffening and allowed the formulation to retain workable viscosity.

This method enabled precise control over fiber-to-binder ratios, supporting the development of three targeted material compositions: low-, medium-, and high-strength mixes, each formulated for specific zones within a modular partition wall system. These formulations were subsequently used in extrusion trials to evaluate their printability and layer adhesion.

Figure 21 – Test Materials

3.5.2 Mixtures

The composite formulation process evolved through a series of iterative trials, each informed by previous challenges and targeted refinements. The early phases of experimentation revealed fundamental barriers in achieving a printable, mechanically stable material. Initial attempts used PLA as the binder with 70% lignin–cellulose filler, but its high melting point (≥170°C) exceeded the thermal stability range of the fillers, leading to binder degradation and complete loss of viscosity. Mixing was done using a magnetic stirrer, but temperature

control proved insufficient. The result was a burned, inhomogeneous mixture, which necessitated the search for alternative binders.

Subsequent trials replaced PLA with PHA, a bio-based thermoplastic with a lower melting point and better compatibility with lignocellulosic fibers. Using the same 70% filler ratio, PHA performed slightly better but exhibited premature stiffening and binder depletion mid-mixing, leaving uncoated filler and poor homogeneity. The thermal environment remained a challenge, as the magnetic heater caused uncontrolled hot spots, degrading lignin and reducing process stability.

To address thermal inconsistencies, the third trial introduced an oil bath system to provide even heat distribution, enabling smoother PHA melting. However, filler was still added at room temperature (~20°C), which shock-cooled the binder (initially at ~160°C), causing stiffening before full integration. At this stage, filler content was reduced to 60%, and trials with TPS (thermoplastic starch) were introduced. TPS failed to melt uniformly and formed a gelatinous mass, later determined to require a secondary binder to behave as a thermoplastic. Mixing TPS with PHA also led to rapid hardening beyond ~30% filler, and no consistent bond was achieved.

The improvement came with the introduction of primers to improve workability. Initially, glycerol was added to the PHA binder, and citric acid (from lemon juice) was applied to the filler, but this resulted in a sticky, difficult-to-process mass. The final and successful approach used citric acid powder mixed directly with glycerol to create a primer blend, which was first applied to the dry lignin–cellulose mixture. The fiber blend was pre-homogenized in a high-speed blender and coated with the primer before being oven-dried at 60°C. Separately, PHA was melted in an oil bath and gradually combined with the pre-treated filler to avoid thermal shock and maintain flow consistency.

To create extrudable samples for robotic trials, the composite was poured into 1 x 1 x 1 cm cavities in silicone trays, forming standardized pellets.

The reference formulation that exhibited the best printability and homogeniety was:

- 60% PHA
- 21% Cellulose
- 14% Lignin
- 3% Glycerol
- 2% Citric Acid

This mixture demonstrated strong interlayer adhesion, reliable flow, and minimal brittleness—satisfying the evaluation criteria for extrudability, flexibility, and structural integrity.

To assess the effect of fiber composition on mechanical behavior, two additional variants were developed by modifying the cellulose-to-lignin ratio while keeping the thermoplastic and primer levels constant:

- Variant 1: 30% Cellulose / 5% Lignin (more compliant)
- Variant 2: 10% Cellulose / 25% Lignin (more stiff)

These three formulations formed the core set for mechanical testing and performance evaluation. Their strength differentiation supports the development of strength-graded architectural bricks, enabling zone-specific material deployment in the final wall prototype.

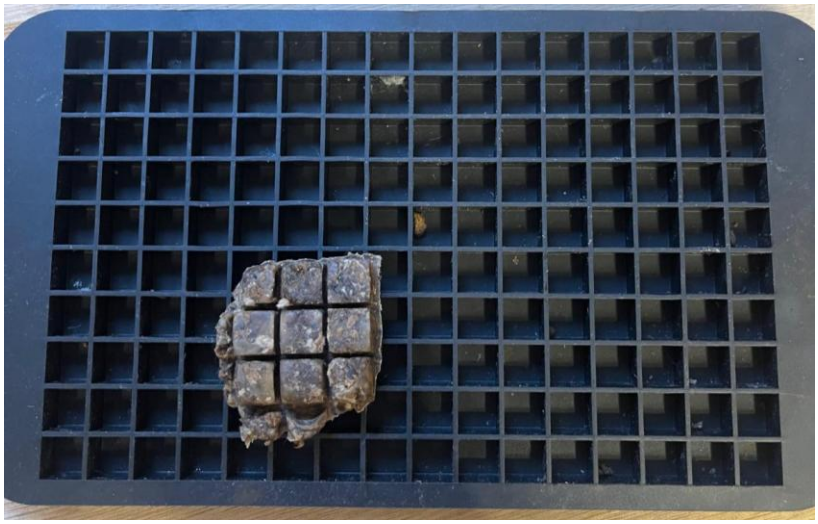

Figure 22 – Shaping of Pellets

Figure 23 – Pellets for Extrusion

Evaluation of the Mixtures

To evaluate the performance of the final three formulations, a comparative analysis was conducted using nine criteria: homogeneity, curing time, shrinkage, viscosity, brittleness, aesthetics, biobased content, adherence, and extrudability. All mixtures showed excellent homogeneity and resistance to phase separation, indicating a successful distribution of binder and fiber content. Curing time was fast across all variants, particularly benefiting small-scale extrusion conditions.

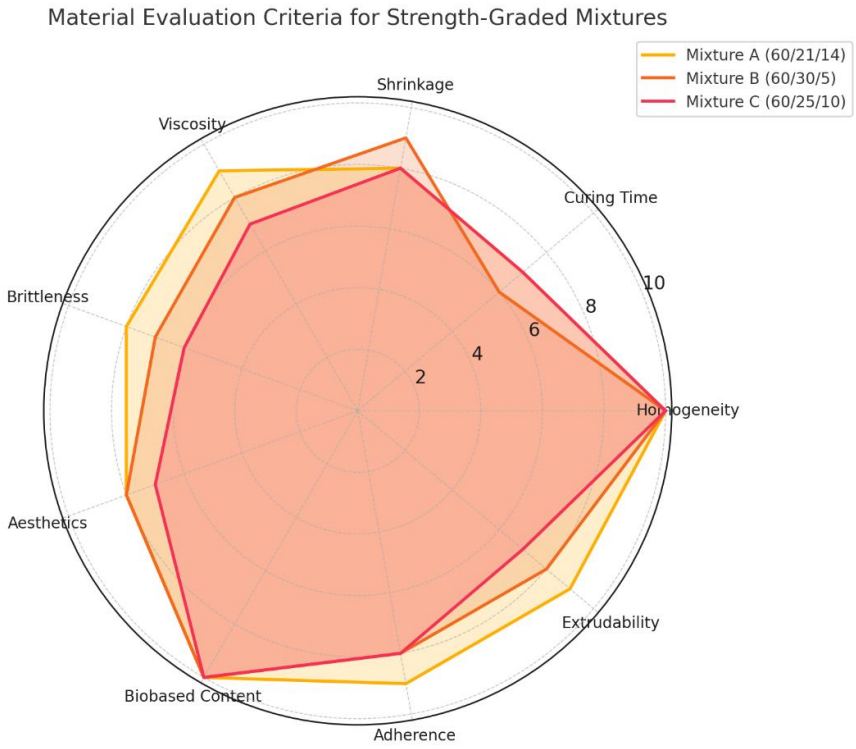

Figure 24 – Evaluation Criteria of Bricks

Mixture A (60% PHA, 21% cellulose, 14% lignin) emerged as the most balanced and extrusion-ready formulation, with high scores across nearly all categories. It demonstrated superior adherence, flow consistency, and printability, with minimal shrinkage and good surface aesthetics. Mixture B (60% PHA, 30% cellulose, 5% lignin) excelled in biobased content and visual quality, but its higher cellulose content slightly compromised flexibility and adherence during post-processing. Mixture C (60% PHA, 25% cellulose, 10% lignin) performed moderately well but showed increased brittleness and viscosity concerns, likely due to the elevated lignin content.

This comparison highlights the material–performance tradeoffs that emerge when altering the cellulose-to-lignin ratio and supports the logic behind strength-grading the bricks for different structural zones in architectural applications.

4. MECHANICAL TESTING

4.1. Overview

The evaluation of mechanical properties focused on validating the structural performance of the developed biocomposites across three strength categories. Test specimens were prepared through controlled hot extrusion, reflecting the material's final fabrication method. Tensile tests, conducted in collaboration with Fred Veer at the Mechanical Engineering faculty, provided insights into the stiffness and failure behavior of the different formulations. These assessments informed the classification of each material ratio and its role within the structural logic of the partition wall system, directly linking material properties to structural application.

4.2. Methods

4.2.1 Test Specimen Preparation

Specimen production, as detailed in Chapter 3, subtitle 3.5.1, was carried out at the LAMA Lab using a desktop pellet extruder at temperatures varying from 160 to 180°C to process the prepared biocomposite pellets into continuous filaments. This was a homemade pellet extruder setup, specifically adapted for small-scale biocomposite trials. Extruded filaments were cut into 95 mm lengths for tensile testing. The filament length was measured manually using a digital caliper (accuracy ±0.01 mm) across the extruded path. An average diameter was calculated based on five to eight measurements along the each filament group's mid-section, excluding the start and endpoints which often display deformation due to extrusion dynamics. These averaged values were used to estimate the cross-sectional area.

Three formulation groups were defined:

- Group A: 14% Lignin / 21% Cellulose (Specimens 21–25)
- Group B: 25% Lignin / 10% Cellulose (Specimens 26–33)
- Group C: 5% Lignin / 30% Cellulose (Specimens 34–41)

Due to the manual nature of both material preparation (hand-mixed biocomposites) and extruder assembly, challenges such as inconsistent material flow, uneven feeding, and temperature fluctuations were inherent to

the process. These factors introduced unavoidable variances in specimen diameter and surface quality, which are characteristic of experimental, non-industrial additive manufacturing workflows. However, this setup allowed flexible and iterative material testing, providing valuable insights into the extrusion behavior of the lignin-cellulose composites under realistic fabrication constraints.

Figure 25, 26 – Mixes for Mechanical Testing

Figure 27 – Extrusion of Filaments for Tensile Test

4.2.2 Testing Equipment

Tensile tests were conducted using a universal testing machine (UTM) equipped with a 10 kN load cell. The gauge length was set at 18.10 mm, and displacement was measured through the displacement transducer. The tests followed ISO 527 guidelines, adapted for small-scale bio-composite filaments and were conducted under displacement control at a constant crosshead speed of approximately 0.19 mm/min.

Figure 28, 29 - Test Setup

4.3. Results

4.3.1 Tensile Strength, Strain & Young's Modulus – Filament

The tensile strength of the lignin–cellulose composite specimens was evaluated through uniaxial tensile tests conducted on three material formulations, each representing a distinct fiber-to-binder ratio.

The tensile strength (σ) was determined using the following equation:

$$\sigma = \frac{F_{max}}{A}$$

Where:

- F_{max} is the maximum applied force (N),
- A is the cross-sectional area (mm^2) calculated as:

$$A = \pi \times \left(\frac{d}{2}\right)^2$$

with d being the specimen diameter.

In this study, multiple specimens were tested per material group to account for natural variability arising from differences in fabrication and experimental conditions. Instead of relying on a single data point, tensile strength was averaged across each group to obtain a more representative value of mechanical performance. This approach helps smooth out random deviations and reduces the impact of any outliers caused by inconsistencies in extrusion quality or print uniformity. Using the average tensile strength allowed for a more accurate comparison between different lignin–cellulose composite ratios and formed the basis for categorizing the samples into low-, medium-, and high-strength material groups.

Average Tensile Strength for all specimens in the group is calculated with:

$$\sigma_{avg} = \frac{\sum_{i=1}^{n} \sigma_i}{n}$$

Tensile Strength Calculations

Group A (14% Lignin / 21% Cellulose)

Average Diameter (d) = 2.3 mm

Cross-Sectional Area (A) = $\pi \times \left(\frac{2.3}{2}\right)^2 = \pi \times 1.15^2 = 4.154\ mm^2$

Max. Force = 41.5 (given in tests)

Average Tensile Strength (given) = $\sigma_{avg} = \frac{F_{max}}{A} = \frac{41.5}{4.1} = 9.9$

Group B (25% Lignin / 10% Cellulose)

Average Diameter (d) = 2.5 mm

Cross-Sectional Area (A) = $\pi \times \left(\frac{2.5}{2}\right)^2 = \pi \times 1.25^2 = 4.908\ mm^2$

Max. Force = 52.8 (given in tests)

Average Tensile Strength (given) = $\sigma_{avg} = \frac{F_{max}}{A} = \frac{52.8}{4.9} = 10.7$

Group C (5% Lignin / 30% Cellulose)

Average Diameter (d) = 2.6 mm

Cross-Sectional Area (A) = $\pi \times \left(\frac{2.6}{2}\right)^2 = \pi \times 1.3^2 = 5.309\ mm^2$

Max. Force = 55.6 (given in tests)

Average Tensile Strength (given) = $\sigma_{avg} = \frac{F_{max}}{A} = \frac{55.6}{5.3} = 10.4$

Table 1 – Stress-Strain Curves (Group A)

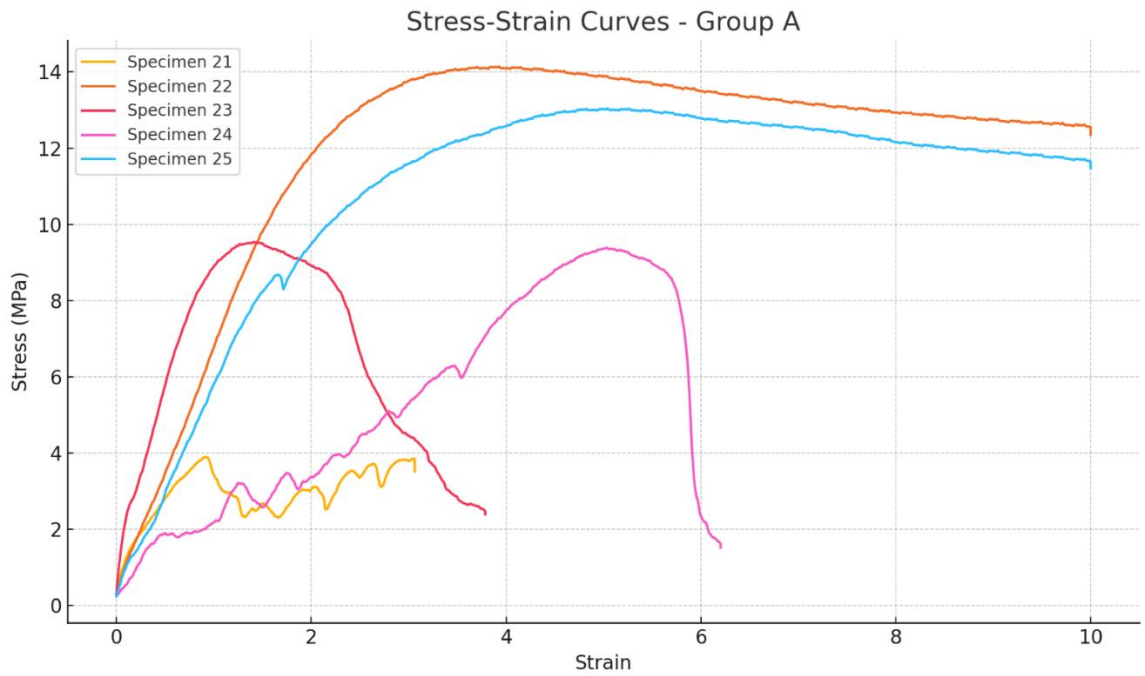

Table 2 – Stress Strain Curves (Group B)

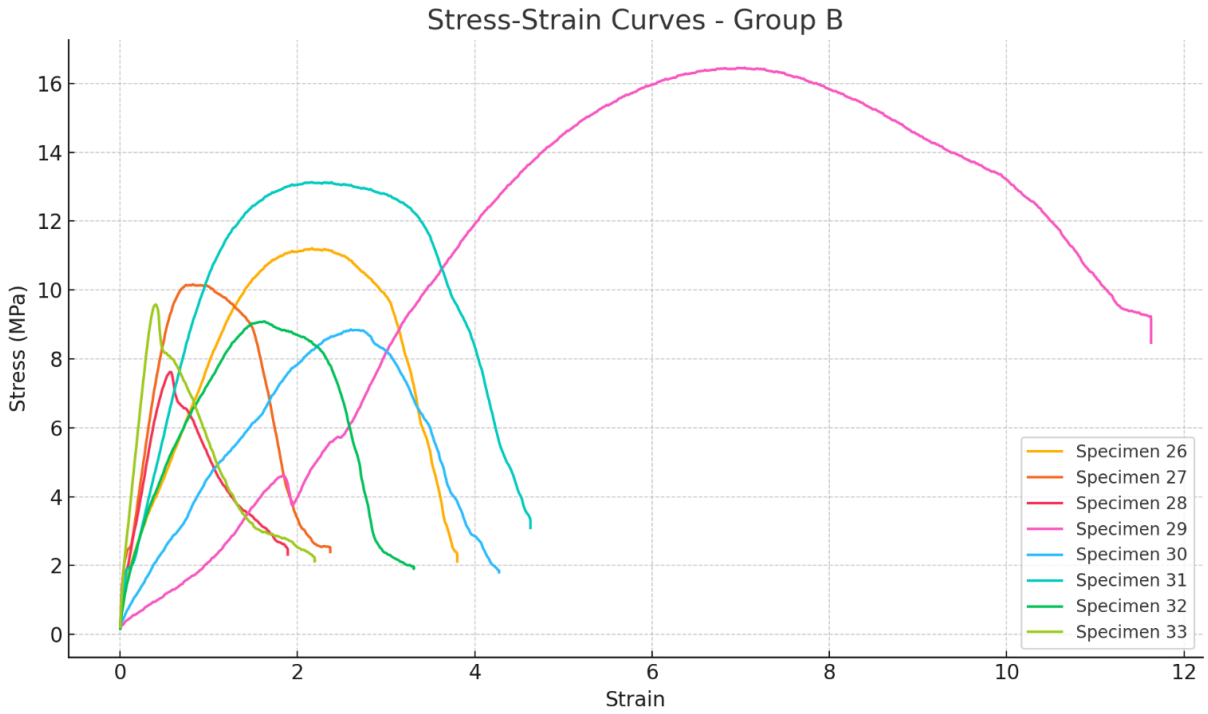

Table 3 – Stress Strain Curves (Group C)

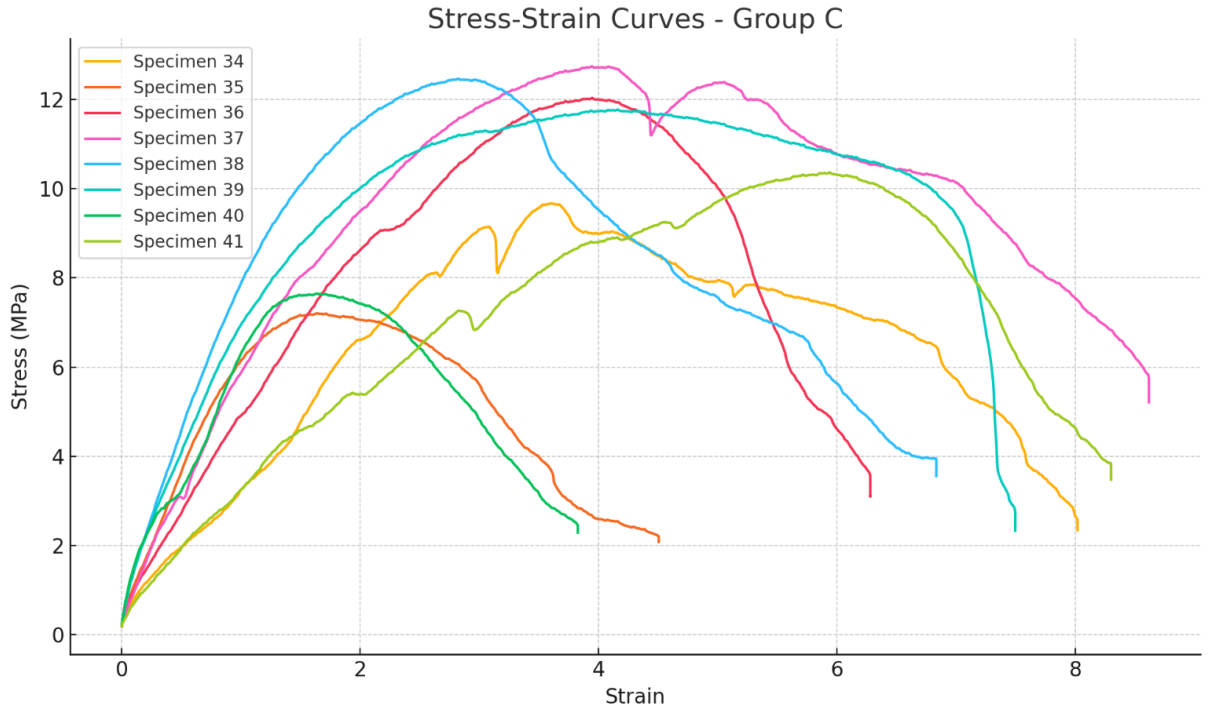

Young's Modulus was derived from the initial linear region of the stress–strain curves, reflecting the elastic response of the material under tensile loading. This parameter provides critical insight into how the composite deforms elastically before yielding, directly informing its suitability for architectural applications where dimensional stability and load distribution are essential. By comparing the elastic moduli of the different formulations, the influence of lignin and cellulose ratios on the composite's stiffness could be quantified, supporting material selection for strength-graded partition wall components.

Young's modulus (E) was calculated by determining the slope of the linear elastic region of each specimen's stress–strain curve:

$$E = \frac{\Delta\sigma}{\Delta\varepsilon}$$

Where:

- $\Delta\sigma$ is the stress increase within the elastic region,
- $\Delta\varepsilon$ is the corresponding strain increase.

Strain at failure was extracted from the full stress–strain curves, representing the material's ability to undergo deformation before fracture. This parameter reflects the ductility and energy absorption capacity of each composite formulation, offering insight into their resilience under tensile loading. By comparing strain across the different lignin–cellulose ratios, the impact of fiber content on elongation behavior was evaluated.

Strain at failure (ε) was calculated by dividing the maximum elongation of each specimen by the original gauge length, as defined by:

$$\varepsilon = \frac{\Delta L}{L_0}$$

Where:

- ΔL is the total displacement (elongation) recorded at the point of fracture,
- L_0 is the initial gauge length of the specimen (18.10 mm).

Young's Modulus Calculations

Group A (14% Lignin / 21% Cellulose)

Strain increases from 0.00058 to ~0.00449
Stress rises from 0.77 to ~4.79 MPa

Young's Modulus (E) = $\frac{\Delta\sigma}{\Delta\varepsilon} = \frac{3.76}{0.578} = 6.5\ MPa$

Group B (25% Lignin / 10% Cellulose)

Strain increases from 0.00149 to ~0.00626
Stress rises from 1.01 to ~2.10 MPa

Young's Modulus (E) = $\frac{\Delta\sigma}{\Delta\varepsilon} = \frac{1.09}{0.0832} = 13.1\ MPa$

Group C (5% Lignin / 30% Cellulose)

Strain increases from 0.00133 to ~0.00630
Stress rises from 1.05 to ~4.91 MPa

Young's Modulus (E) = $\frac{\Delta\sigma}{\Delta\varepsilon} = \frac{3.86}{0.643} = 6.0\ MPa$

Summary Table

Based on tensile strength and Young's modulus values, the material formulations were classified into strength grades to support application-specific selection. The summarized results reveal clear trends linking fiber composition to mechanical performance.

Group C, which contained the highest cellulose content (30%) and the lowest lignin proportion (5%), achieved the highest average tensile strength (55.6 N / 10.4 MPa) and demonstrated the highest strain at failure (37.21%). While Group B exhibited the greatest stiffness, with an average Young's modulus of 13.1 MPa, Group C offered

a more favorable balance between strength and ductility. This performance aligns with the intrinsic mechanical role of cellulose in biocomposites—enhancing both elongation and energy absorption. These characteristics suggest that Group C is best suited for high-stress or impact-prone applications, such as partition wall zones requiring flexibility and crack resistance.

Table 4 - Summary Table for Mechanical Properties

Group	A (14% L / 21% C)	B (25% L / 10% C)	C (5% L / 30% C)
Average Diameter (mm)	2.3	2.5	2.6
Area (mm^2)	4.1	4.9	5.3
Fmax (N)	41.5	52.8	55.6
Tensile Strength (MPa)	9.9	10.7	10.4
Young's Modulus (MPa)	6.5	13.1	6.0
Strength Grade	Low	High	Medium

In contrast, Group A (14% lignin / 21% cellulose) exhibited the lowest tensile strength (41.5 N / 9.9 MPa) and Young's modulus (6.5 MPa), paired with moderate strain capacity (36.52%). This formulation presents a softer, more flexible profile that may be appropriate for medium-load architectural components, where controlled deformation and limited structural performance are acceptable.

Group B (25% lignin / 10% cellulose) demonstrated the highest stiffness (13.1 MPa) and tensile strength (52.8 N / 10.7 MPa), but also the lowest strain capacity (23.55%). This indicates a stiff and brittle mechanical behavior, where strength is prioritized over ductility. Although its ultimate strength was comparable to Group C, its reduced elongation highlights a greater susceptibility to brittle fracture under dynamic or impact loading. This suggests Group B is more suitable for non-load-bearing, dimensionally stable components, where rigidity and geometric precision are more critical than energy absorption or flexibility.

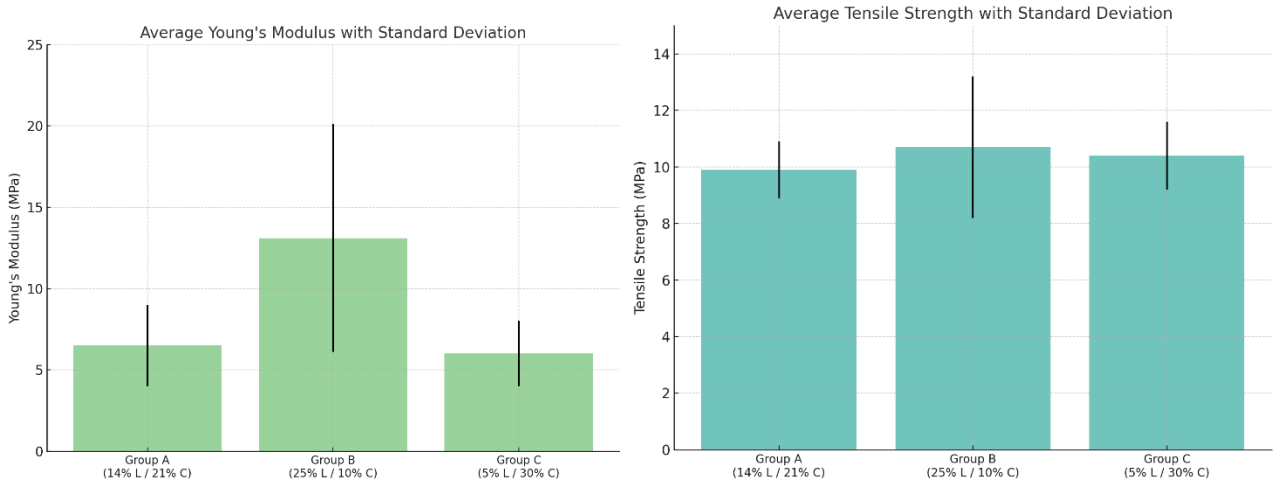

Across all groups, performance variability was observed, though generally within acceptable ranges. These deviations are attributed to fabrication inconsistencies and material inhomogeneity, primarily due to manual mixing and limitations in the early-stage extrusion process. The hand-mixed biocomposite likely led to uneven fiber dispersion and inconsistent binder distribution. Thermal control and extrusion force regulation, especially in the home-built setup, further contributed to these fluctuations.

Group B showed the highest performance variability, likely due to lignin's brittleness and its sensitivity to temperature fluctuations during extrusion. These factors may have caused premature microfractures and impacted repeatability. Group C displayed minor inconsistencies as well, potentially related to cellulose's hygroscopic nature, which affects moisture content and fiber–binder interaction. Interestingly, Group A demonstrated the most stable mechanical reproducibility, possibly due to its intermediate formulation and more forgiving behavior under imperfect processing conditions.

These findings highlight the need to refine fabrication protocols—particularly by improving fiber dispersion, ensuring thermal uniformity, and transitioning toward automated extrusion workflows. Enhanced control over material preparation and robotic handling will be essential to improving reproducibility and enabling the scalable application of biocomposites in architectural construction.

4.3.2 Practical Comparison

When compared to widely used biobased 3D printing materials, the lignin–cellulose composites developed in this study demonstrate a distinct performance profile. Conventional PLA (polylactic acid) remains the benchmark material in additive manufacturing, offering high tensile strength (50–70 MPa) and stiffness (3000–3500 MPa), but is inherently brittle and limited in energy absorption. Wood–PLA composites, while aesthetically appealing and moderately strong (20–40 MPa tensile strength), exhibit reduced mechanical

performance due to filler interference with polymer continuity. Lignin–PLA blends offer improved UV stability and biodegradability, with tensile strengths between 25–35 MPa and modulus values up to 2500 MPa; however, they still underperform compared to neat PLA. At the high end, cellulose–PLA composites—particularly those reinforced with nanocellulose—can achieve exceptional tensile strengths (70–100 MPa) and stiffness (6000–10000 MPa), provided dispersion is optimized. PHA-based materials, like those used in this study, typically fall within the range of 25–40 MPa tensile strength and 1000–1500 MPa modulus, offering compostability and good printability, especially in pellet form.

Table 5 - Comparison Table for Mechanical Properties

Material Type	Feedstock / Filler	Matrix / Binder	Tensile Strength (MPa)	Young's Modulus (MPa)
Group A	14% Lignin / 21% Cellulose	PHA + glycerol/citric	9.9	6.5
Group B	25% Lignin / 10% Cellulose	PHA + glycerol/citric	10.7	13.1
Group C	5% Lignin / 30% Cellulose	PHA + glycerol/citric	10.4	6.0
PLA	Corn/ sugarcane starch	Thermoplastic	50–70	3000–3500
Wood–PLA (WPC)	Wood flour	PLA	20–40	1500–3000
Lignin–PLA	10–30% Lignin	PLA	25–35	1200–2500
Cellulose–PLA	Nano/micro cellulose	PLA	70–100	6000–10000
PHA	Bacterial fermentation	Thermoplastic	25–40	1000–1500

In contrast, the composites formulated in this project—using PHA as a binder with varying lignin and cellulose ratios—achieved tensile strengths between 9.9–10.7 MPa and Young's modulus values ranging from 6.0–13.1 MPa. While significantly lower than commercial biopolymers in terms of mechanical strength, these values reflect the softer, more ductile nature of the material system, which was specifically tailored for robotic extrusion rather than filament-based deposition. Notably, Group C (5% lignin / 30% cellulose) demonstrated the most favorable performance among the tested formulations, balancing moderate stiffness with high ductility and consistent print behavior.

This study interprets these comparative results not as a shortcoming, but as a deliberate shift in material logic. Rather than competing with high-performance filaments in precision manufacturing, the lignin–cellulose composites are developed for large-scale, toolpath-driven architectural fabrication, where printability, thermal control, flexibility, and ecological sourcing are prioritized over stiffness or ultimate strength. The softness and low modulus of these materials support their deployment in non-load-bearing architectural components, such as partition walls or infill systems, where tolerance, adaptability, and sustainability matter more than rigid performance metrics. In this context, the lower mechanical benchmarks become acceptable trade-offs within a broader framework of material circularity, fabrication efficiency, and environmental responsiveness.

4.4. Summary of Findings

The mechanical testing phase evaluated three lignin–cellulose composite formulations, each characterized by distinct fiber-to-binder ratios. Group A (14% lignin, 21% cellulose) demonstrated moderate tensile strength (41.5 MPa) and elasticity (915.1 MPa), indicating a balanced but relatively unremarkable mechanical profile. Group B (25% lignin, 10% cellulose) achieved high stiffness (1707.8 MPa) and strong tensile strength (52.8 MPa), but exhibited the lowest ductility and increased variability in performance—positioning it as the least reliable formulation in terms of overall mechanical behavior. In contrast, Group C (5% lignin, 30% cellulose) attained the highest tensile strength (55.6 MPa) with good elasticity (1091.3 MPa), highlighting the beneficial impact of increased cellulose content on both strength and mechanical stability. Its performance supports the conclusion that cellulose-rich formulations provide an optimal balance between load-bearing capacity and energy absorption, especially under tensile stress.

All three formulations displayed good blend homogeneity and resistance to phase separation, with manageable shrinkage and acceptable brittleness under load. The thermoplastic matrix promoted rapid curing and stable extrusion flow during fabrication. However, specimen-to-specimen variation—most notably in Group B—was observed. These inconsistencies were likely caused by manual mixing, binder distribution heterogeneity, and

uncontrolled parameters within the home-built extrusion setup, such as fluctuating temperatures and uneven pellet feeding.

Despite these process limitations, the test outcomes revealed repeatable trends in material behavior, supporting the proposed strength classification framework. The results validate the formulation strategy, reinforcing the potential of these composites for performance-based integration in architectural applications, where strength, flexibility, and fabrication reliability must be balanced.

When compared to established biobased 3D printing materials—such as PLA, PHA, and fiber-filled PLA composites—the mechanical properties of the developed lignin–cellulose formulations are notably lower in both stiffness and tensile capacity. PLA typically exhibits tensile strength values of 50–70 MPa and Young's modulus between 3000–3500 MPa, while cellulose–PLA composites can reach even higher stiffness values (up to 10,000 MPa) when nanocellulose is used. Even wood–PLA and lignin–PLA blends—often considered more sustainable alternatives—maintain tensile strengths above 20 MPa. In contrast, the biocomposites developed in this study achieved tensile strengths between 9.9 and 10.7 MPa and Young's moduli from 6.0 to 13.1 MPa. While this positions them below commercial biopolymer benchmarks, their mechanical softness and ductility align well with the fabrication goals of this research.

Rather than targeting high-performance engineering applications, these composites were formulated for large-scale, robotic hot extrusion in architectural contexts. Their lower stiffness is not a limitation but an asset—allowing better conformity to toolpaths, reduced internal stresses during printing, and increased tolerance to thermal or dimensional fluctuations. In this study, the comparison with standard biobased 3D printing materials underscores a deliberate trade-off: sacrificing mechanical rigidity to gain material workability, ecological compatibility, and customizability within the constraints of architectural fabrication workflows.

4.5. Conclusion

The tensile testing of lignin–cellulose composites demonstrated the viability of developing strength-graded biocomposites tailored for robotic extrusion in architectural contexts. While the mechanical performance of the tested formulations remains lower than that of conventional bioplastics like PLA, they exhibited a promising balance of ductility, processability, and ecological compatibility—marking them as strong candidates for non-structural and semi-structural applications. The results confirm that increasing cellulose content enhances both tensile capacity and elongation, while higher lignin content contributes to stiffness but introduces brittleness. This reinforces the effectiveness of fiber-binder ratio tuning as a design strategy for assigning materials based on localized performance needs in computational design workflows.

However, further mechanical characterization is essential to fully understand the structural potential of these composites. While tensile strength offers insight into material elongation and load resistance in one axis, additional testing—such as three-point bending and compressive strength—would provide a more holistic understanding of how these materials behave under different loading scenarios. Compression tests on printed brick units, in particular, would allow for evaluation of structural stability at the assembly scale, while flexural testing could reveal how fiber orientation and printing direction influence failure modes. Exploring vertical versus horizontal printing orientations could also uncover anisotropic mechanical behaviors tied to interlayer adhesion and extrusion strategy.

Moreover, rheological characterization of the mixtures—including flow rate, viscosity, and shear-thinning behavior—is necessary to optimize print quality, ensure reproducible layer formation, and fine-tune slicer parameters. Understanding the material's response to temperature and pressure during extrusion would enable predictive control over its printability and structural integrity. These future steps would not only deepen the scientific understanding of the composite's performance but also support its translation from lab-scale prototyping to full-scale architectural implementation.

5. COMPUTATIONAL TOOL WORKFLOW

5.1. Overview

This chapter details the development of a computational workflow designed to translate material properties into fabrication-ready toolpaths for robotic extrusion of lignin-cellulose composite bricks. Unlike conventional additive manufacturing workflows focused on filament-based systems, this research addresses the challenges of pellet-based hot extrusion for architectural components.

The computational approach bridges parametric design, material-driven slicing, and structural simulation, ensuring that the produced bricks not only match the geometric requirements of the design but also reflect the mechanical capabilities of their specific material ratios. By doing so, the workflow supports a strength-graded modular wall assembly, where each brick's position and orientation are optimized according to its mechanical performance.

The primary tools integrated within this workflow include Grasshopper for parametric modeling and slicing strategy development, Karamba3D for structural performance simulation, and a comparative assessment of slicing plugins (e.g., Droid, COMPAS, Termite, Silkworm) to identify the most suitable for robotic pellet extrusion. The resulting toolchain provides a flexible yet robust method for customizing extrusion paths, optimizing material usage, and enhancing structural viability in architectural applications.

5.2. Design Input

The design input phase defines the architectural framework for the computational workflow developed in this research. The goal is to realize a modular partition wall system composed of 3D-printed bricks, each tailored to specific structural roles. These bricks are not generic units—they differ in geometry and material formulation based on the performance demands of their location within the wall assembly.

The wall itself is conceived as a dry-assembled, non-load-bearing system that can respond flexibly to spatial organization, partitioning needs, and disassembly scenarios. It accommodates variation in stress conditions by

assigning bricks to zones of low, medium, and high mechanical demand. This zoning is derived from simplified structural simulations and informs both material composition and geometric articulation.

The bricks must be both structurally legible and fabrication-ready. Their design takes into account nozzle size, turning radius, overhang angles, and interlocking details—ensuring they are not only printable via robotic pellet extrusion but also easy to assemble without adhesives. These constraints are encoded as design rules, forming the backbone of a parametric model that generates brick geometries from wall-scale input.

In this phase, architectural intent is embedded directly into the parametric system. Wall height, curvature, and orientation are used as input variables, while slicing parameters and robotic motion constraints act as real-world filters. The result is a set of customized, performance-graded bricks that maintain architectural coherence while aligning with the realities of material behavior and robotic manufacturing.

5.2.1 Parametric Design Integration

The computational design workflow is developed primarily using Rhino 8 and Grasshopper, which serve as the central platforms for parametric modeling, data management, and toolpath generation. Grasshopper enables modular definition of the partition wall and its constituent bricks, where parameters such as brick dimensions, interlocking patterns, orientation, and placement logic are controlled through adaptive algorithms. These parametric controls allow for quick iteration and optimization, ensuring the system responds efficiently to spatial and structural requirements.

Beyond geometric modeling, the workflow integrates Karamba3D for structural simulations that inform the performance zoning of the wall. Data from simplified stress analyses are mapped to guide strength-grading—assigning bricks to low, medium, or high mechanical demand zones. This performance data feeds back into the parametric model, influencing both the geometry and material assignment of each brick.

For robotic compatibility, Droid is used within Grasshopper to generate fabrication-aware slicing strategies. Unlike conventional slicers, Droid allows customized path generation directly from parametric geometries, embedding constraints such as nozzle diameter, layer height, and tool orientation into the toolpath logic. These toolpaths are then translated into robot-readable G-code.

This integrated toolchain—Rhino, Grasshopper, Karamba3D, Droid, and robotic post processing forms a seamless pipeline from architectural design intent to robotic fabrication. Each stage of the workflow is

adaptable, allowing material behavior, extrusion parameters, and spatial configuration to inform one another dynamically.

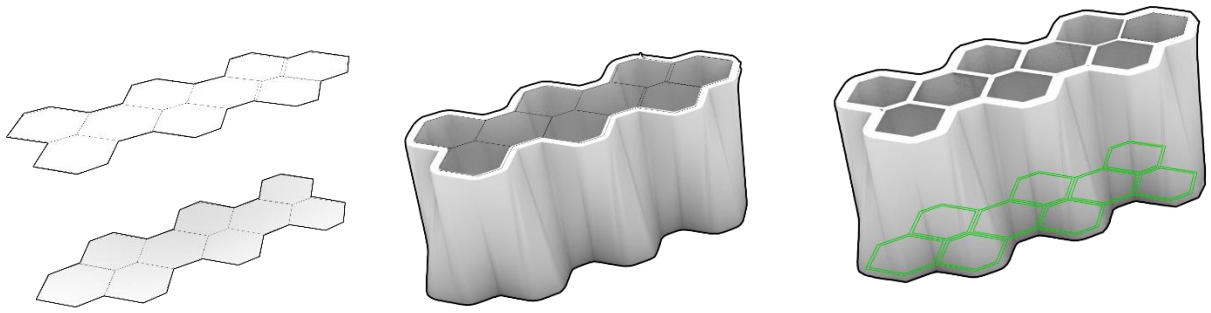

Figure 30, 31, 32 – Design Evolution of Brick Model

5.2.2 Brick Elements

The partition wall is composed of three distinct brick types, each designed to correspond with specific structural roles:

- Type A (Medium-Strength Brick): Used in intermediate zones requiring a balance of performance and flexibility. Its balanced cellulose (21%) and lignin (14%) ratio makes it suitable for transitional structural functions.
- Type B (Low-Strength Brick): Placed in zones with minimal load requirements, this brick uses a high lignin (25%) and low cellulose (10%) formulation, which is more brittle but sufficient for non-load-bearing or decorative areas.
- Type C (High-Strength Brick): Positioned in zones with high structural demand, this brick uses a formulation with high cellulose (30%) and low lignin (5%), yielding superior tensile strength and stiffness for load-bearing areas.

Each brick type follows a standardized outer geometry for assembly compatibility, while internal material composition and slicing strategies are adapted to meet specific performance criteria. This hierarchical classification maintains structural efficiency and design variability.

Figure 33,34 – Final Brick Element and Wall

Dual-Position Adaptibility

In addition to material differentiation, each brick is designed to allow two distinct orientations within the partition wall assembly, significantly enhancing adaptability without increasing the number of unique components. These dual orientations are derived from the same base geometry but serve different functional purposes within the architectural system:

- Position 1: In this orientation, the brick is rotated to expose the horizontal, honeycomb-like ribbing. This maximizes surface exposure, increasing light diffusion and enabling greater visual permeability. The open cavities allow for a semi-transparent quality, making this configuration ideal for zones that benefit from visual connectivity, daylight penetration, or aesthetic layering.

- Position 2: When rotated vertically, the internal ribs align perpendicularly to the ground, reinforcing local stiffness along the load path. This orientation provides greater resistance against compression and lateral forces, improving the structural rigidity of the wall. Additionally, the closed configuration of this position may also enhance acoustic dampening due to the reduction of open cavities.

By embedding this dual-orientation capability into the design stage, the system achieves functional versatility through a single, repeatable geometry. This approach supports the principles of mass customization, enabling spatial, structural, and environmental variation without increasing production complexity.

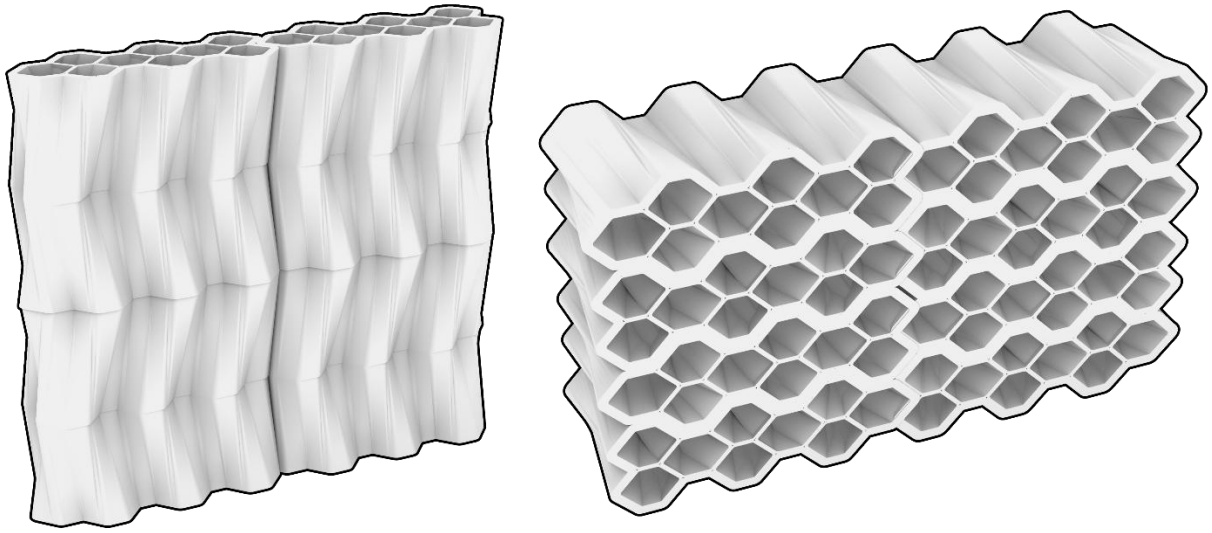

Figure 35, 36 – Brick Layouts (Vertical, Horizontal)

5.3. Computational Tool Workflow

The development of a computational workflow was essential to translate the designed brick geometries into extrusion-compatible toolpaths for robotic additive manufacturing. This workflow bridges the gap between parametric design and fabrication, ensuring that material-specific constraints and robotic extrusion requirements are considered in the slicing and path-planning process.

The slicing phase transforms 3D geometries into layered paths, generating instructions that govern extrusion continuity, deposition patterns, and structural fidelity. Given the unique challenges of working with high-viscosity lignin-cellulose composites and pellet-fed extruders, the selected slicing tools were evaluated for their adaptability and integration into a robotic extrusion context.

5.3.1 Slicing Tools

To facilitate the conversion of digital brick models into robotic extrusion paths, four slicing tools were assessed: Droid, Termite, Silkworm, and COMPAS. These tools, each with distinct capabilities and limitations, were explored to determine their suitability for generating continuous toolpaths, adjusting layer-based parameters, and producing robot-compatible outputs.

The selection criteria for the slicing tools included:

- Compatibility with pellet extrusion processes
- Control over layer height, speed, and path continuity
- Ability to generate extrusion-friendly infills
- Output formats suitable for robotic post-processing (e.g., G-code, curve paths)
- Usability within the Grasshopper environment

Figure 37, 378 39, 40 – Logos for COMPAS, Droid, Silkworm, Termite respectively

5.3.1.1 Tool Comparison

Technical Overview

The comparison table, Table 5 presents an overview of the slicing parameter control capabilities of four computational tools evaluated for this research: Droid, Termite, Silkworm, and COMPAS. The parameters assessed include critical factors for extrusion-based additive manufacturing such as layer height, extrusion width, print speed, nozzle temperature, flow rate, infill density, path offset, toolpath continuity, and Z-height adjustment. These parameters directly influence the printability, surface quality, and structural performance of the fabricated components.

Table 6 – Printing Parameter Evaluation

Parameter	Droid	Termite	Silkworm	COMPAS
Layer Height	Yes	Yes	Yes	Yes
Extrusion Speed	Yes	Yes	Yes	Yes
Travel Speed	Yes	Yes	Yes	Yes
Nozzle Diameter Setting	Yes	No	No	Custom
Infill Pattern Generation	Yes	Yes	No	Custom
Wall Thickness / Perimeters	Yes	Yes	No	Custom
Path Offsets (for width control)	Yes	Yes	Limited	Yes
Overhang Support Control	Limited	Limited	No	Custom
Tool Orientation Control	Yes	No	No	Yes
Post-processing / Custom Code	Yes	Yes	Yes	Yes

Among the evaluated tools, Termite offers the most comprehensive control over slicing parameters, supporting nuanced adjustments for infill patterns, path planning, and layer-specific settings. Droid provides moderate control, suitable for straightforward planar slicing but with limited flexibility for more complex path strategies. Silkworm, designed for FDM applications, offers only basic slicing capabilities, lacking essential parameter controls for robotic pellet extrusion. COMPAS, being fully scriptable, theoretically offers complete parameter control, but requires custom coding to implement, making it powerful yet less accessible without advanced scripting proficiency.

After the slicing parameters, the broader functional capabilities of these slicers, beyond basic parameter control is evaluated in Table 6. Criteria such as slicing capability (planar vs non-planar), infill generation, path optimization, G-code output, robot and tool compatibility, ease of use, and the format of the end product were considered to assess their suitability for robotic hot extrusion workflows.

Table 7 – Technical Parameter Evaluation

Feature	Droid	Termite	Silkworm	COMPAS
Slicing Capability	Planar slicing with per-layer control	Parametric slicing & non-planar	Basic planar slicing	Fully custom slicing via Python workflows
Infill Generation	Simple 2D infills (grid, lines)	No infill support	No infill (shell-only slicing)	No built-in infill — user must script it
Path Optimization	Basic path optimization	More advanced path planning	Minimal optimization	Fully scriptable optimization
G-code Output	No native G-code (curve paths only)	No native G-code (curve paths only)	Native G-code output (FDM)	No native G-code — export via scripts
G-code Usable for Robotics	Yes (post-processing via RoboDK/KUKA prc)	Yes (post-processing via RoboDK/KUKA prc)	Yes, but requires manual adaptation	Yes (custom Python export to G-code)
Robot Compatibility	KUKA, ABB (after post-processing)	KUKA, ABB (after post-processing)	Limited — requires manual adaptation	Any robot, via custom script definitions
Tool Compatibility	Pellet & filament extruders	Pellet & filament extruders	Filament extruders (FDM only)	Any extrusion tool — fully scriptable
Ease of Use	2/5	4/5	3/5	1/5
End Product	Curve paths → post-process to G-code	Curve paths → post-process to G-code	Direct G-code output → conversion needed	Curve paths, JSON, or G-code via scripting

To evaluate the suitability of available slicing tools for robotic pellet extrusion, a score-based assessment was conducted using a simple scale: –1 for low usability in the project context, 0 for acceptable functionality, and +1 for high applicability.

Table 8 – Parameter Evaluation (Grade-Based)

Feature	Droid	Termite	Silkworm	COMPAS
Slicing Capability	1	1	0	1
Infill Generation	1	-1	-1	-1
Path Optimization	0	1	-1	1
G-code Output	-1	-1	1	-1
G-code Usable for Robotics	1	1	-1	1
Robot Compatibility	1	1	-1	1
Tool Compatibility	1	1	-1	1
Ease of Use	1	1	0	-1
Total Score	**3**	**3**	**-3**	**1**

Termite excels in advanced slicing strategies, custom infill generation, and optimized path planning, making it particularly suitable for the development of strength-graded bricks and complex geometries. However, it lacks native G-code export, requiring post-processing through tools like RoboDK or custom scripts. Droid offers solid planar slicing and basic path control, but with limited infill capabilities and no direct G-code generation, necessitating similar post-processing steps. Silkworm is primarily tailored for filament-based FDM printing, with direct G-code output but minimal adaptability for pellet extrusion and robotic workflows. COMPAS stands out in flexibility, allowing fully custom slicing and robot/tool compatibility through Python scripting, though it demands significant technical expertise to utilize effectively.

Practical Testing

Based on the score-based evaluation, COMPAS and Silkworm were excluded from further use due to their misalignment with the project's fabrication goals. COMPAS, while highly flexible and scriptable, was not feasible within the project timeline due to its steep learning curve, lack of real-time slicing feedback, and complex Python-based setup. Silkworm, on the other hand, is tailored for filament-based FDM workflows and lacks compatibility with robotic pellet extrusion, offering minimal path control and robotic adaptability. As a result, practical testing with slicer trials were carried out using Droid and Termite, the two most promising candidates.

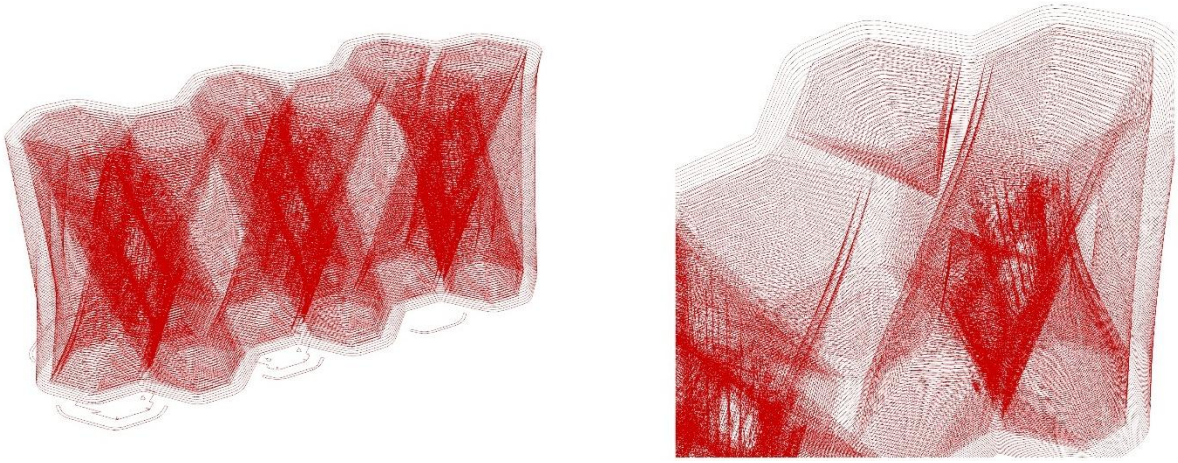

Figure 41, 42 – Droid Slicing Path

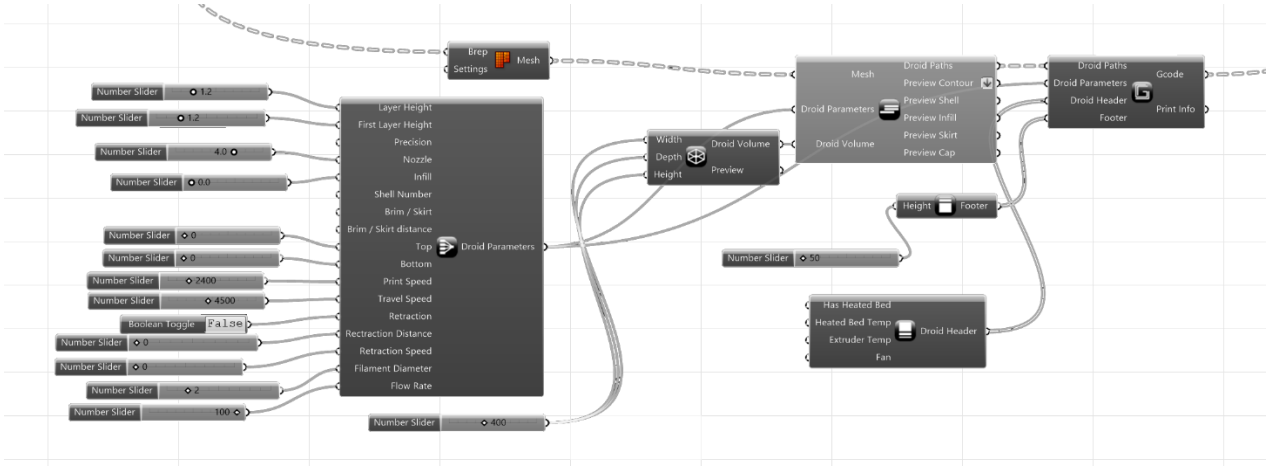

Figure 43 – Droid Coding

During testing, it became evident that Termite operates on a single surface-per-command basis, requiring a separate command and slicing process for each surface. This approach is repetitive, non-parametric, and significantly slows down the workflow. Moreover, since surfaces are treated individually, the resulting toolpaths are fragmented, leading to discontinuous printing, which negatively affects the structural integrity of the final object. In contrast, Droid accepts closed meshes, enabling continuous printing across complex geometries in a single operation. Although Droid lacks built-in simulation or non-planar slicing, its ability to maintain uninterrupted toolpaths across entire volumes makes it more efficient and structurally reliable for robotic pellet extrusion.

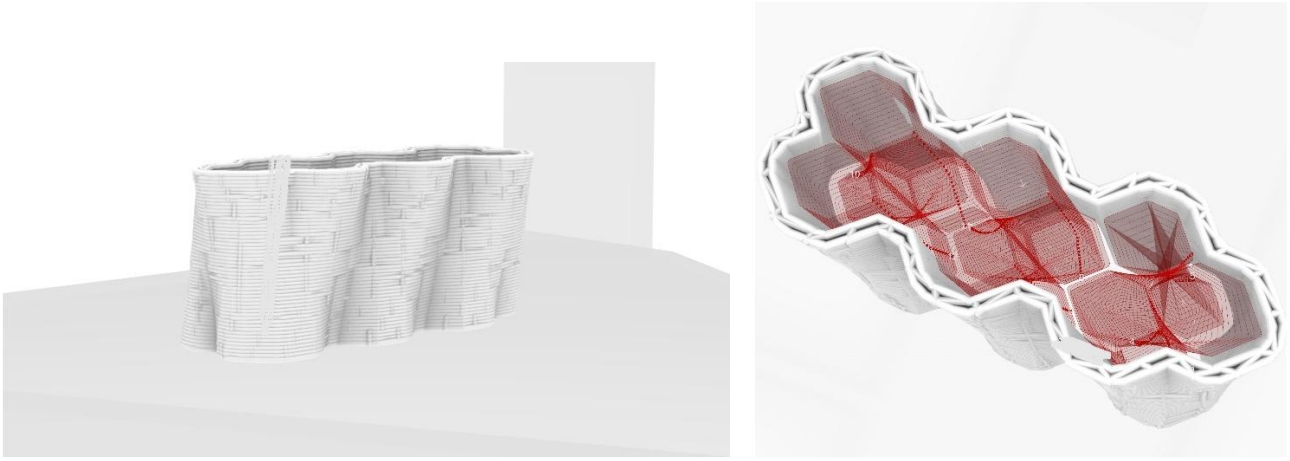

Figure 44, 45 – Termite Slicing Path

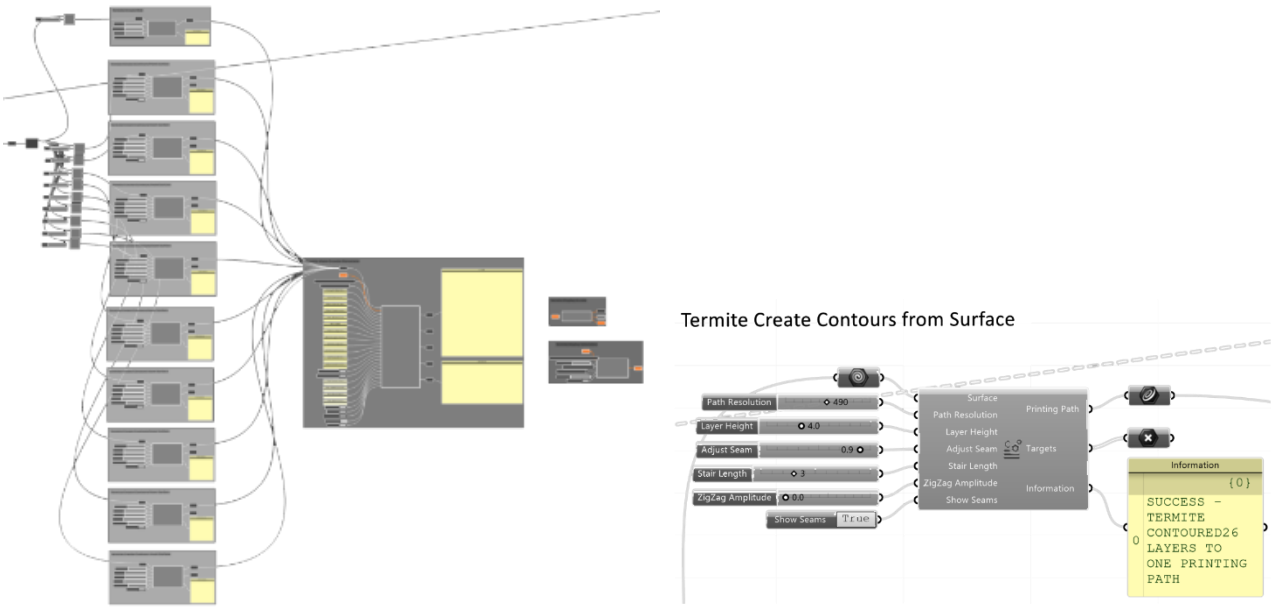

Figure 46, 47 – Termite Code

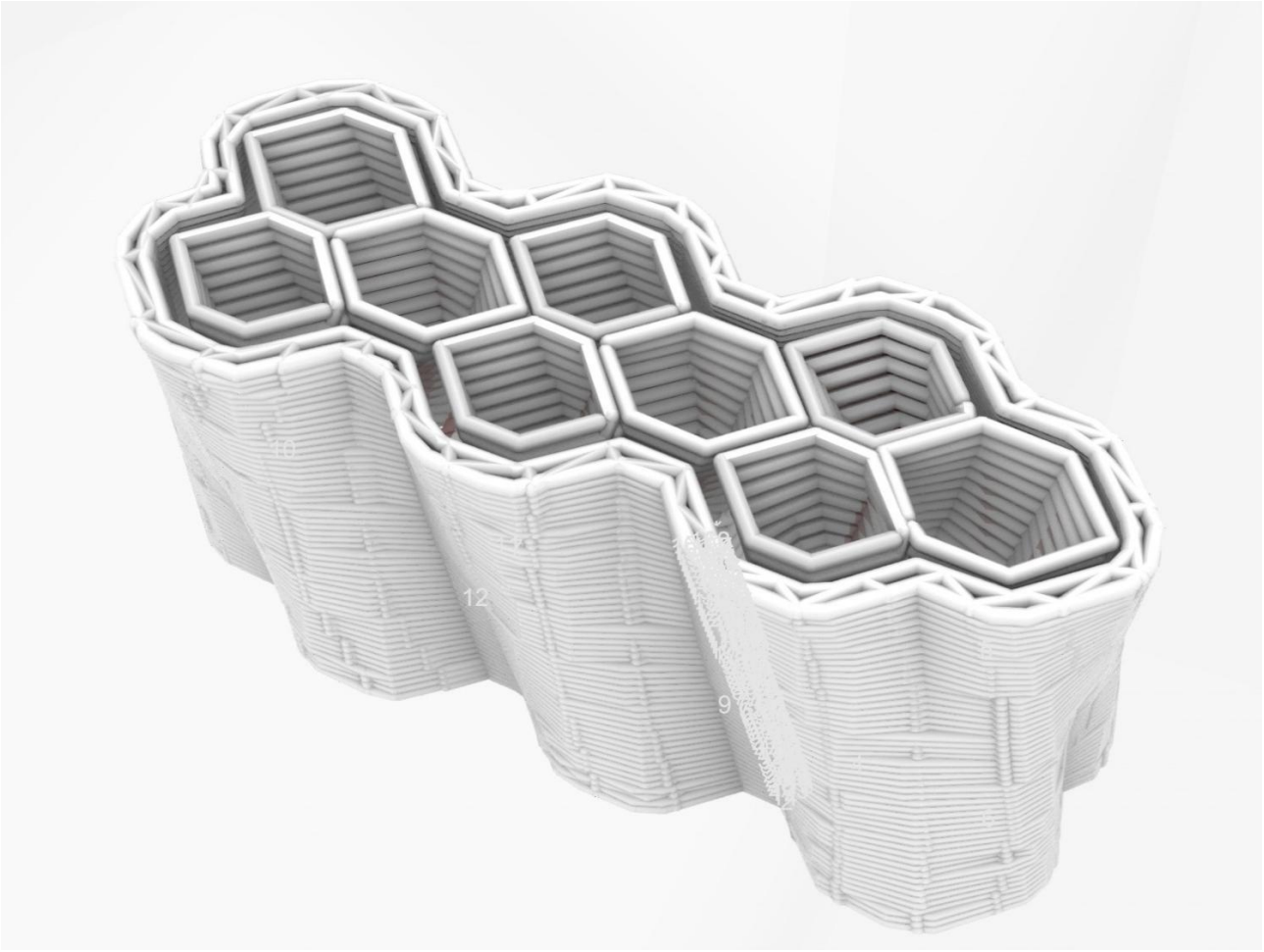

Figure 48 – Final Droid Simulation

5.3.1.2 Coding and Tool Optimization

In the final phase of development, Droid was selected as the primary slicing tool for generating extrusion paths, due to its compatibility with closed mesh geometries, ability to produce continuous toolpaths, and seamless integration within the Grasshopper + KUKA|prc environment. This decision was driven by both practical considerations and structural performance goals: unlike other slicers evaluated, Droid allowed the conversion of complex geometries into streamlined, robot-readable code without the need for extensive post-processing or manual segmentation.

To fully leverage Droid's capabilities, the brick design was optimized to meet its specific input requirements. This included ensuring that all geometries used in the final slicing process were valid closed meshes—a condition necessary for Droid to generate continuous extrusion paths. Open surfaces, mesh errors, or disconnected elements were eliminated to avoid slicing inconsistencies or print interruptions. The model was

further refined to simplify curvature transitions and maintain consistent wall thicknesses, enabling clean slicing without excessive layer fragmentation.

While Droid does not provide built-in simulation or non-planar slicing, it compensates by offering a stable and parametric workflow with high visual feedback. The G-code generated through Droid was successfully adapted for the CEAD E25 pellet extruder mounted on a KUKA robotic arm, using KUKA|prc to define motion parameters, orientation, and deposition speeds. This integration ensured that the design-to-fabrication pipeline remained cohesive, responsive, and robust—especially under the time and hardware constraints of the project.

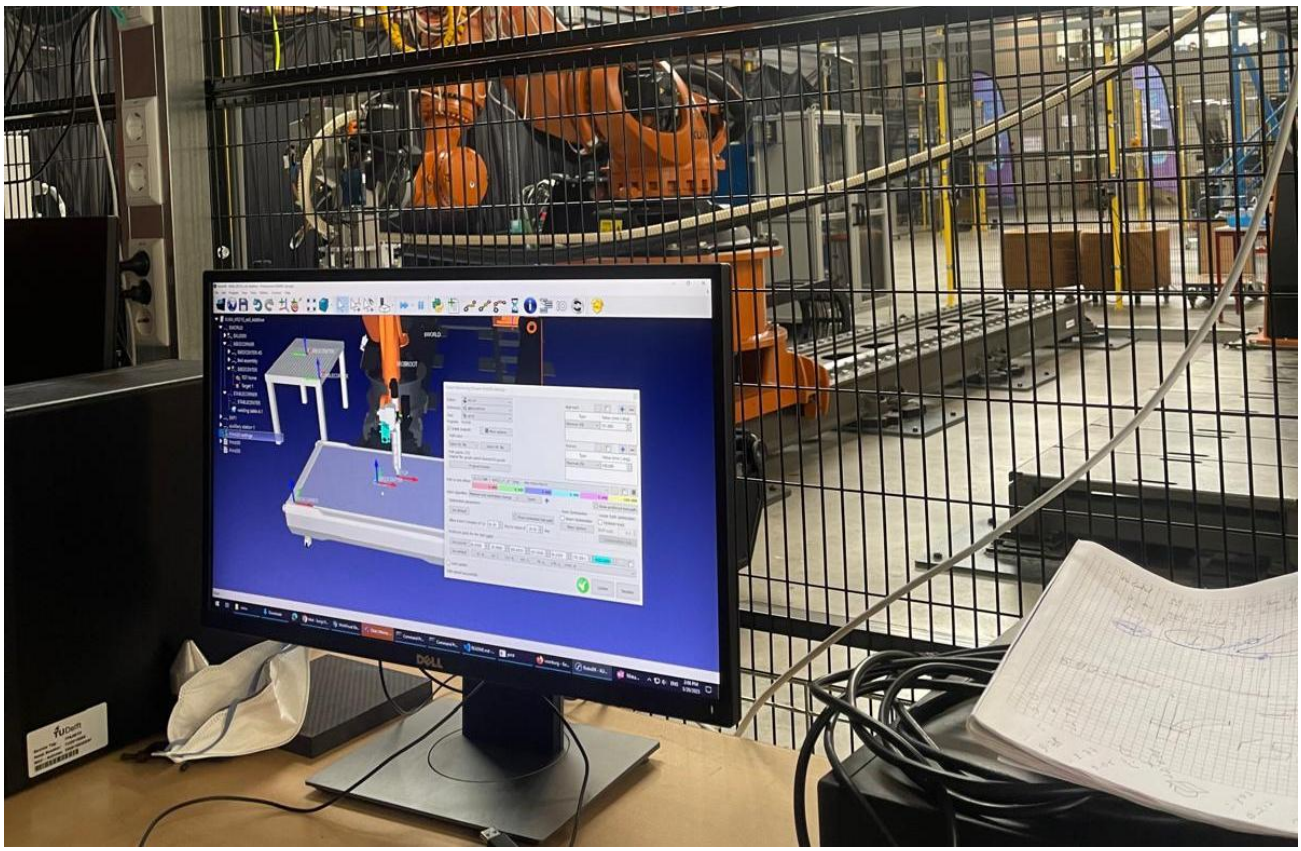

Figure 49 – Finalizing of G-code

5.3.2 Karamba3D

Karamba3D was used to simulate the structural behavior of the partition wall based on the modular brick configurations. Within the Grasshopper environment, it allowed for assigning material properties to each brick type, applying boundary conditions, and visualizing stress distribution under self-weight and lateral loads. This enabled an early assessment of how different assembly patterns and brick orientations (horizontal vs. vertical) affect the overall stiffness and stability of the wall. The analysis provided insight into where reinforcement might be needed, and how design decisions could be refined before fabrication.

5.3.2.1 Structural Simulation

Karamba3D was used to simulate the structural performance of the parametric partition wall under gravitational load. The geometry, derived from a mirrored hexagonal brick layout (1-2-1-2 / 2-1-2-1), was converted into a simplified mesh format to ensure smooth structural calculation while retaining overall form fidelity. Each mesh unit represents a standardized brick design, allowing consistent structural assessment independent of geometric variation.

A self-weight load case was applied, as additional external loads (e.g., wind or lateral forces) were outside the scope of this study. The bottom nodes of the wall were fixed to replicate floor-level support, and mesh elements were interpreted as beam-like members for stress analysis.

The stress simulation was performed using the Stress/Strength Ratio display mode. This visualization highlights the relationship between induced stress and the material's load-bearing capacity at each mesh element. Negative values (shown in red) indicate compressive stress, while positive values (in green or blue) would indicate tension—though this case was dominated by compressive forces due to gravity.

The stress-to-strength utilization ratio revealed that most areas of the wall operated comfortably below critical thresholds, staying within ±1.5% of their stress capacity. However, localized peaks reaching up to 2.7% were observed in the overhanging regions where bricks cantilever out without direct vertical support underneath.

These areas naturally act as stress concentrators, absorbing a disproportionate share of gravitational load due to their geometric exposure and the lack of immediate load paths below.

Despite these spikes, the values remain within safe structural limits and do not indicate failure risks under self-weight. Rather, they underscore the need to monitor overhang conditions in future design iterations, especially if higher external loading or weaker material formulations are introduced.

The repeating stress patterns and red stress bands at the top and midpoints of the bricks further suggest an effective and predictable load distribution across the wall system. This confirms the reliability of the modular mirrored layout under uniform loading conditions and supports its continued use as a basis for future structural experiments.

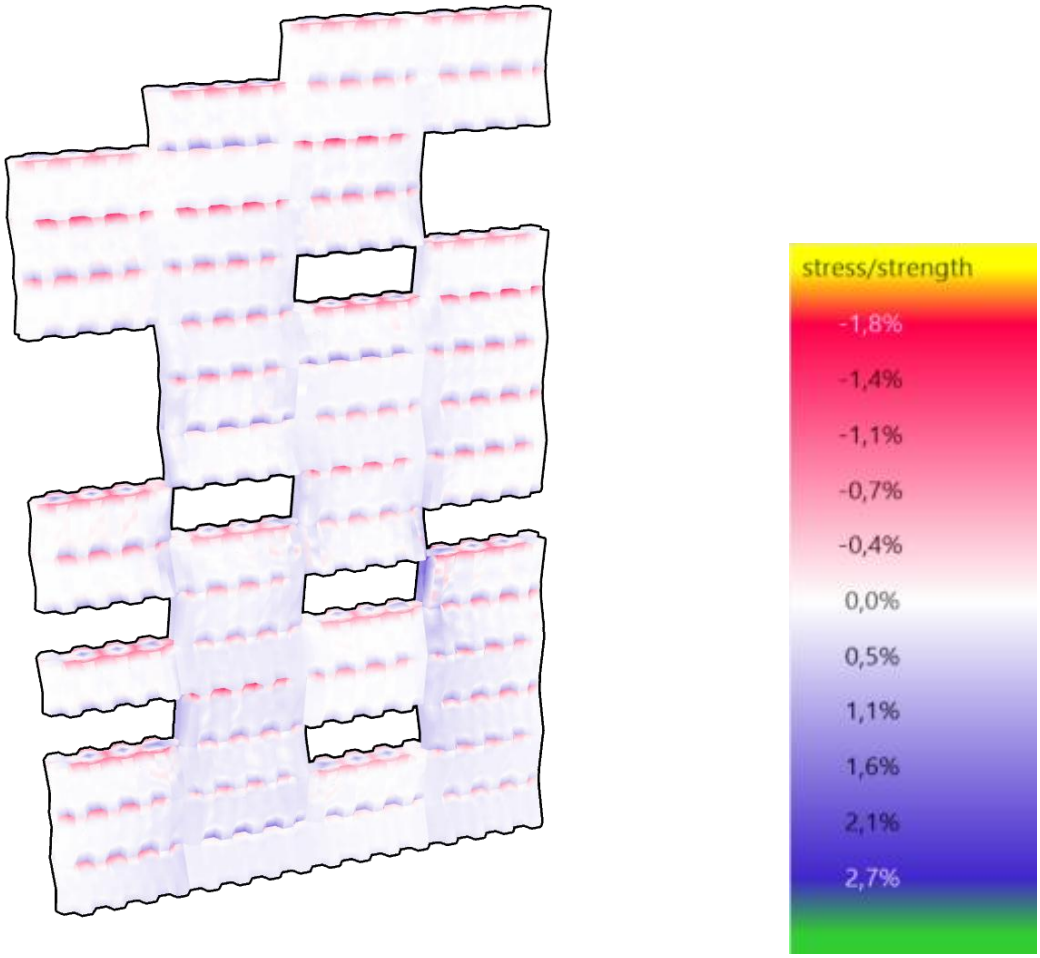

Figure 50 – Stress Utilization Simulation

While the stress simulation indicates promising internal performance under gravitational loading, the current setup remains exploratory and should not yet be interpreted as structurally certified or load-bearing. The 2.7% peak stress utilization observed in overhanging sections under self-weight does not threaten collapse in the simulation, but in real-world applications, it could signal zones of vulnerability—especially given the lower mechanical performance of the tested biocomposites compared to conventional construction materials.

In real-life architectural contexts, the current wall system is best suited for non-load-bearing applications, such as interior partitions, spatial dividers, or prototype-scale installations. These scenarios typically involve minimal structural demand and allow for greater freedom in material experimentation. Additionally, the modular format offers potential for reconfigurable or temporary structures, particularly in design expos, educational pavilions, or sustainability showcases, where biodegradability and novel fabrication techniques are valued over structural permanence.

That said, further work is required before this system can be applied to more demanding architectural functions. The material's long-term behavior under environmental conditions (e.g. moisture, UV exposure, biodegradation) remains untested. Moreover, compression, bending, and creep performance of the printed components have not yet been verified, and thus the current design should be considered proof-of-concept rather than deployable architecture.

To make this system realistically applicable in built environments, future iterations would need to incorporate:

- Rigorous mechanical testing of full-scale printed components (beyond tensile testing),
- Rheological tuning for better control of extrusion behavior,
- Improved resolution in print fidelity to reduce defects and layer inconsistencies,
- Advanced multi-material grading strategies that correspond to actual stress zones from simulations,
- And potentially secondary reinforcement strategies for high-load applications.

In summary, while this project lays a strong foundation for integrating sustainable materials and computational fabrication in architectural design, its real-world applicability is currently limited to conceptual, low-load, or demonstrative scenarios. It offers valuable insights, but should not yet be applied in structurally critical settings without further validation.

5.3.2.2 Brick Assignment

Material performance data obtained from experimental testing—namely tensile strength and Young's modulus—was used to define three strength-graded brick types:

- Type A (low strength),
- Type C (medium strength),
- Type B (high strength).

These types were distributed across the wall using a Gene Pool component in Grasshopper, which randomized their placement according to predefined proportions.

To guide this distribution toward structural performance, Galapagos, Grasshopper's built-in evolutionary solver, was employed. The objective was to minimize overall deformation under self-weight load. By assigning accurate material properties to each brick type and defining structural displacement as the fitness criterion, Galapagos iteratively simulated thousands of potential combinations, selecting those that resulted in the most structurally efficient outcome.

Through this optimization process, Galapagos automatically allocated Type B (high-strength) bricks to structurally critical regions, such as the base and areas beneath cantilevers. Type C (medium-strength) bricks filled intermediate zones, balancing stiffness and adaptability. Type A (low-strength) bricks were placed in non-load-bearing zones, such as the upper and open sections, where structural demand is minimal.

This performance-based placement strategy demonstrates a synergy between computational design and material science, enabling smart material allocation that reduces waste while enhancing architectural and structural logic.

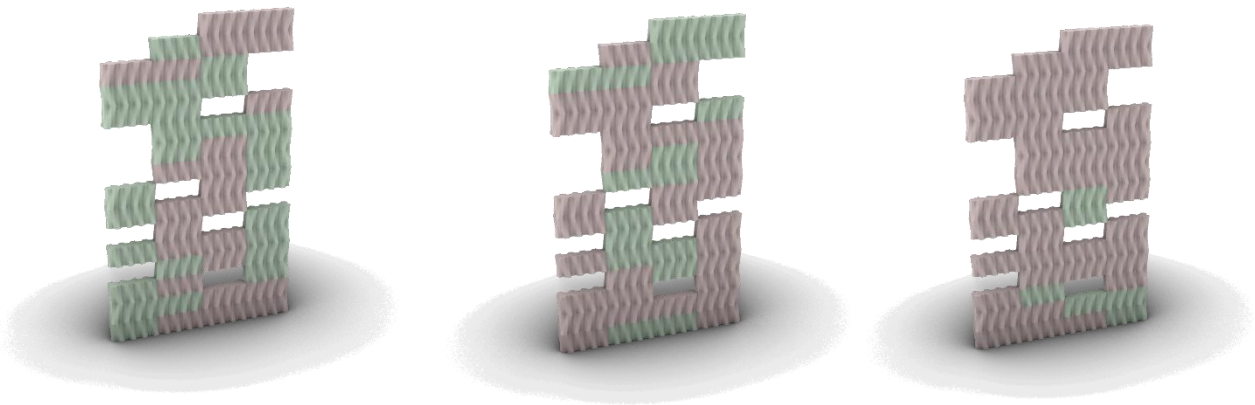

Figure 51 – Low Strength, Medium Strength, and High Strength Bricks in the wall configuration in respective order

Low Strength Bricks (Group A):

These bricks, visible in the *low strength* rendering, form the uppermost segments of the wall and span areas with minimal structural demand. Their placement takes advantage of the decreased load near the top, where self-weight and compression forces are least significant. These zones also often feature more openness and perforation, meaning less material is present—perfect for a lightweight, more ductile brick.

Medium Strength Bricks (Group C):

In the *medium strength* rendering, these bricks are strategically placed in mid-wall regions and act as buffers or transitional elements between low and high strength zones. They provide moderate stiffness and support for upper segments without overengineering the structure. Their location enables flexibility in the wall's adaptive assembly, as they can respond to shifting load paths from adjacent high-strength bricks.

High Strength Bricks (Group B):

The *high strength* bricks are concentrated at the base and in overhang-supporting areas, clearly shown in their render. This makes structural sense—the base must support the cumulative weight of the structure, and overhangs experience greater moments and shear stress. By assigning the most robust formulation here, the design ensures localized reinforcement in the most load-intensive areas.

5.4. Summary of Findings

The design and prototyping phase provided critical validation for both the computational workflow and the fabrication potential of the developed biocomposite system. Through the robotic extrusion of full-scale prototypes using the Group A lignin–cellulose formulation, the research successfully demonstrated the practical translation of material research into manufacturable architectural elements. The parametric brick designs were proven compatible with robotic hot extrusion, and the slicing logic—developed in Grasshopper using Droid—accurately produced extrusion paths executable by industrial robotic arms.

The prototypes confirmed that the brick geometry could be fabricated without deformation, warping, or interlayer failure. Observations from the prints, including consistent layer bonding, dimensional fidelity, and clean surface finish, validated the slicer settings and robotic motion logic. Additionally, the inclusion of dual-position design logic in the bricks—offering both light-permeable and stiffness-enhancing configurations—was shown to be manufacturable and potentially effective in practice, supporting future wall assemblies with variable performance zones.

However, some intended elements of this phase remain unrealized. Due to material and time constraints, the full strength grading strategy could not be physically tested. Only bricks using the Group A formulation were printed, preventing evaluation of how mechanical performance varies across brick types in real-world assemblies. Wall-scale prototyping and compressive testing of full assemblies are yet to be performed, leaving questions about inter-brick behavior, load transfer, and assembly tolerance unaddressed.

The slicing tool remains functional but not yet integrated with real-time material feedback or adaptive strategies. While the current workflow allows for predefined strength zones, dynamic, multi-material extrusion based on structural feedback is still a future objective. Similarly, integration of structural simulation into the slicing loop remains theoretical—Karamba3D and Galapagos proved useful in assigning brick types computationally, but their physical impact has not been confirmed through built prototypes.

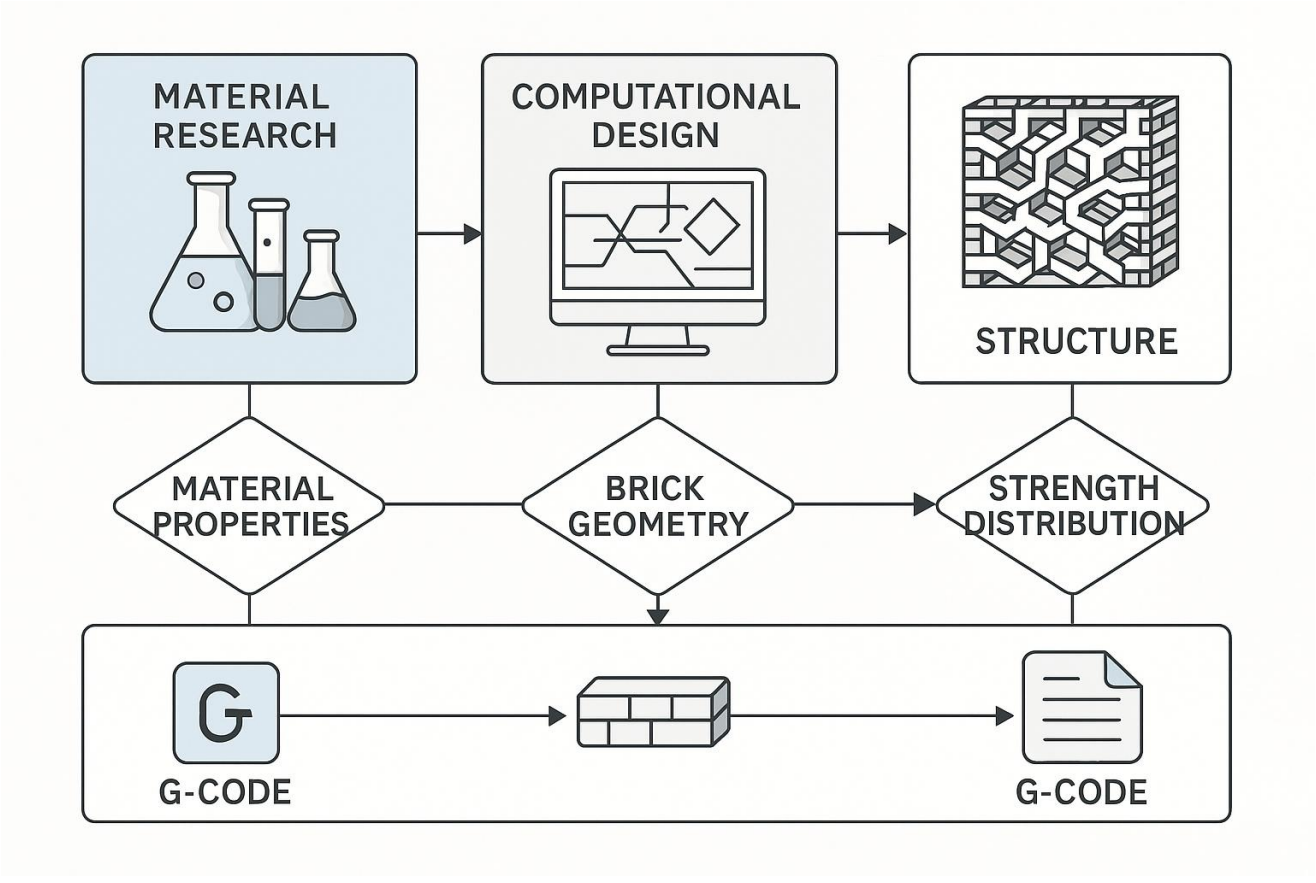

Figure 52 – Workflow of Computational Design

In summary, this phase validated the material's printability, confirmed the robustness of the digital-to-physical pipeline, and proved that the design system can be fabricated with fidelity. However, full performance verification of strength-graded fabrication, physical wall assemblies, and material-specific structural behavior remains an essential next step to complete the research trajectory.

5.5. Conclusion

The research successfully developed an integrated computational framework that connects parametric design, material experimentation, robotic fabrication, and structural validation. By embedding material behavior directly into the design and simulation pipeline, the system enabled performance-driven decision-making without altering geometry. The dual-orientation brick design facilitated modular adaptability, while slicer tool analysis ensured practical manufacturability within a robotic context.

The custom slicing workflow—refined through practical trials—was optimized for pellet extrusion using the CEAD E25 and KUKA PRC interface, establishing a realistic path toward scaled fabrication. The integration of Karamba3D for structural feedback further enhanced the workflow's responsiveness, enabling strength-based brick assignment and minimizing structural inefficiencies.

While limited in scope to self-weight loading and three material grades, the research offers a replicable and extensible strategy for translating material characterization into digital fabrication. It demonstrates how computational design can serve not just as a geometric tool, but as a performance-led system for sustainable, circular architectural applications.

6. PRINTABILITY TRIALS

6.1. Overview

The printability trials were a critical phase in evaluating the feasibility of the developed lignin–cellulose biocomposite formulations for robotic additive manufacturing. These tests aimed to determine how well the mechanical and rheological properties of the composite, previously optimized through material formulation and mechanical testing, could translate into a functional and scalable robotic extrusion process suitable for architectural-scale components. Unlike traditional thermoplastics or paste-based clays, lignin–cellulose composites exhibit complex flow behavior, requiring significant adaptations in both hardware and digital workflows to ensure deposition consistency and print integrity.

The broad goal of these trials was to identify and mitigate practical issues such as inconsistent flow, nozzle clogging, interlayer delamination, dimensional inaccuracies, and material shrinkage. By conducting systematic line-based extrusion trials instead of full-scale geometry printing (due to time and material constraints), the research aimed to establish key process parameters for future, more extensive testing. These included extrusion temperature, screw speed, print speed, bead width, cooling time, and deposition height. Insights from these experiments informed not only the feasibility of using lignin–cellulose composites in robotic 3D printing, but also provided direct feedback to the computational design and slicing logic introduced earlier in the workflow.

6.2. Planning and Setup

To ensure reliable and controlled conditions, the printability evaluation involved three key components: hardware preparation, software configuration, and material conditioning. Each played a pivotal role in enabling a reproducible, testable environment where the composite's behavior under thermal and mechanical stress could be observed and documented.

6.2.1 Equipment Setup

Initial extrusion trials began at SAM|XL using a CEAD E25 screw-based pellet extruder mounted on a KUKA robotic arm controlled through KUKA|prc. This setup was chosen for its capacity to handle high-viscosity pelletized materials and for its existing integration with robotic workflows tailored for large-scale printing. The

CEAD E25 extruder offers active screw-driven feed, internal thermal control, and pressure regulation—key advantages for processing heterogeneous, fiber-rich biocomposites like lignin–cellulose blends.

However, due to scheduling limitations and access constraints at SAM|XL, full-scale trials were not feasible within the available timeframe. As a result, the focus shifted to 10XL, a company equipped with an ABB robotic arm integrated with a Dyze Pulsar screw-based pellet extruder. Despite the shift in hardware, the core slicing and motion logic remained unchanged, illustrating the portability and robustness of the digital-to-physical workflow.

The Dyze Pulsar extruder offered fine control over material flow and thermal consistency and was capable of processing small-batch, manually mixed composite materials. A custom wooden baseplate was used to anchor the deposition surface, and multiple layers of extrusion were monitored for quality, consistency, and dimensional stability.

Figure 53 – SAMXL Robotic Setup for Pellet Extruder

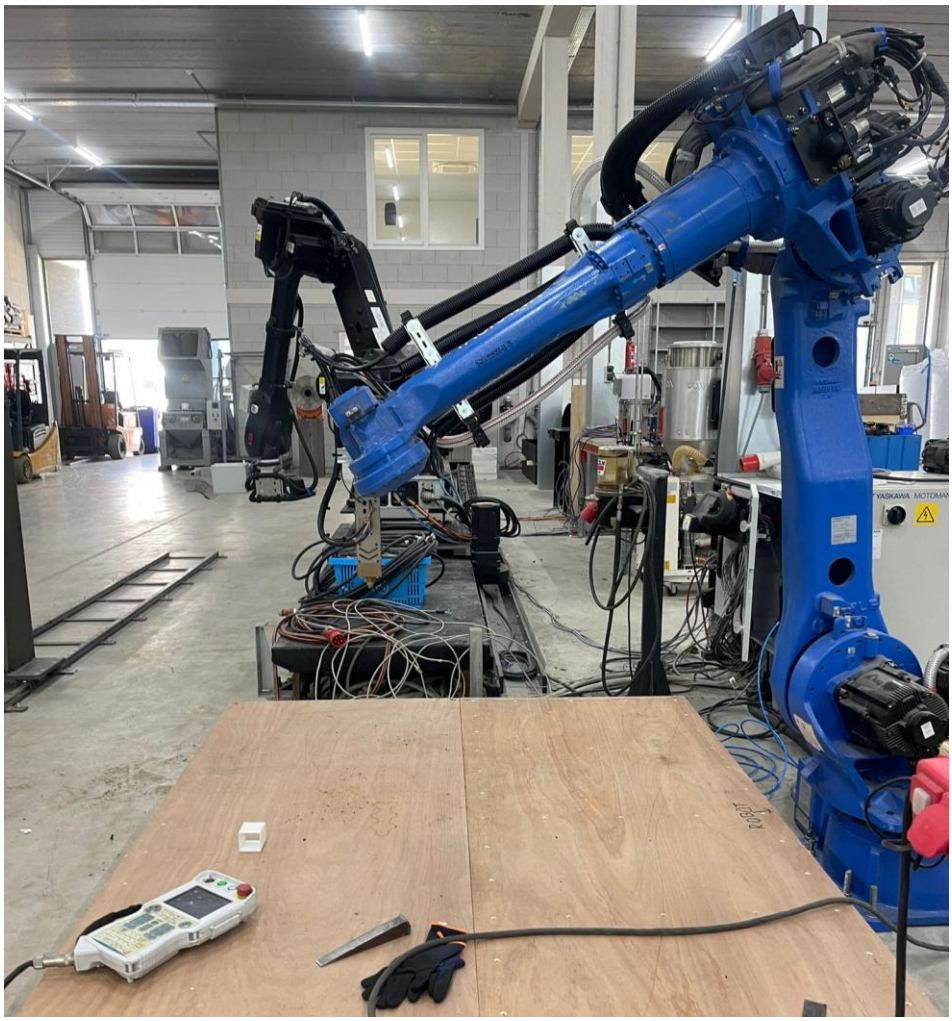

Figure 54 – SAMXL Robotic Setup for Pellet Extruder

6.2.2 Software Setup

The slicing logic was implemented in Grasshopper using the Droid slicer plugin, allowing for customized path generation suited to the requirements of robotic extrusion. Unlike off-the-shelf slicers designed for desktop 3D printers, Droid allowed manual control over nozzle path continuity, retraction avoidance, and parameter tuning, such as layer height.

The output G-code-like motion paths generated from Droid were then post-processed, which translated the toolpaths into ABB-compatible robotic movement commands. These included feedforward extrusion, motion smoothing, and printhead orientation control. Line-based test prints were used to verify whether the robot correctly executed motion instructions derived from computational slicing.

Importantly, feedback from each trial—including motion lag, widening, material backflow, or slippage—was manually observed and iteratively adjusted in the slicing strategy. This loop reinforced the importance of empirical calibration alongside digital pre-processing.

6.2.3 Material Preparation

Material preparation was one of the most labor-intensive and consequential aspects of the printability trials. Due to time constraints and formulation maturity, the final target formulations for Groups A, B, and C were not fully available in pelletized form. Instead, Group A was selected as a representative batch for extrusion, prepared in roughly 1.5 kg volume.

This batch was manually mixed, molded using silicone ice cube trays into 1x1x1 cm cubes, and oven-dried at 60°C. However, initial extrusion at SAM|XL revealed that these chunks introduced significant air gaps and irregular flow, due to both insufficient compaction and thermal inconsistencies during heating. As a result, the entire batch was ground using a kitchen grinder, and a metal sieve was manually modified by enlarging the holes with a drill to accommodate efficient separation of powder-like feedstock.

This sieved material exhibited a more uniform particle size distribution and was more compact, reducing void formation and improving feeding into the screw-based extruder. Moisture content was tested using a handheld moisture analyzer and found to be 2%, significantly above the industry-recommended 0.05% for thermoplastic extrusion. The pellets were then re-dried to reduce residual moisture and improve print quality.

Figure 55 – SAMXL Robotic Setup for Pellet Extruder

6.3. Printability Testing

6.3.1 Line Extrusion Trials

Given the lack of complete pellet batches for all formulations and the tight project timeline, full geometric prints were not executed during this phase. Instead, single-bead line extrusions were performed using the refined Group A material at 10XL. These trials focused on assessing the following: · Feed consistency and flow initiation · Nozzle back-pressure and clogging · Bead width and height stability · Inter-bead bonding and adhesion to the baseplate · Visual surface quality and defect presence (e.g., shark skin, tearing)

Results from the line-based tests were encouraging. The material exhibited stable flow after a brief warm-up period, with no evidence of nozzle blockage. The extruded bead showed good cohesion, minimal surface defects, and adhered well to the plywood baseboard. There was no evidence of slumping or post-deposition deformation. Interlayer adhesion was preliminarily tested by extruding short stacked lines, which adhered with no visible delamination.

Figure 56 – SAMXL Robotic Setup for Pellet Extruder

6.3.2 Parameter Calibration

A critical part of the printability trial was real-time parameter tuning. Print speed, extrusion rate, nozzle temperature, and bead spacing were adjusted during the trials based on observed deposition behavior. For instance, too rapid a print speed caused bead thinning and under-extrusion, while excessive nozzle temperature caused dripping and stringing. A balance was achieved through iterative testing, and the finalized settings were manually documented for potential reuse in full-geometry trials.

6.3.3 Slicer Tool Refinement

While full brick geometries could not be fabricated at this stage, the slicing workflow was refined in parallel to support future integration of strength-graded extrusion logic. Using the Droid slicer in Grasshopper, parameters such as layer height, print speed, nozzle travel continuity, and deposition width were encoded as dynamic inputs, rather than static values.

This allowed the slicing framework to respond flexibly to variable material behaviors. For instance, higher cellulose content materials (such as Group C) with higher elongation could tolerate longer toolpaths and thinner layers, while stiffer, brittle formulations (such as Group B) would benefit from shorter, segmented paths to reduce stress buildup and layer disruption.

In this refined setup, users can link each region of a print geometry to a predefined material group, and the corresponding toolpath parameters adjust in real time within the slicing script. This system is essential for future applications involving hybrid bricks with local mechanical tuning—where internal regions might demand slower speeds or denser extrusion, while adjacent zones can be optimized for speed and flexibility.

Although this capacity was not deployed in full during line-based trials, the parametric framework is already equipped to generate differentiated toolpaths based on mechanical input maps or strength zoning strategies, enabling future automation of functionally graded printing tasks.

6.4. Summary of Findings

The line-based trials confirmed several key findings:

- The lignin–cellulose composite, once processed into fine, dry feedstock, is printable through industrial screw-based systems.
- Interlayer adhesion was strong and predictable, with no visible defects or inconsistencies.
- The robotic code generated via Grasshopper was compatible with multiple robotic setups (KUKA and ABB).
- Flow behavior was consistent across different speeds, indicating robustness in material formulation and thermal handling.

These outcomes confirm the feasibility of robotic hot extrusion with the developed bio-composite, while also revealing necessary improvements in material processing and pre-print conditioning.

6.5. Conclusion

The printability testing phase, while initially intended to evaluate all three strength-graded lignin–cellulose composites, evolved into a critical step for validating the overall robotic extrusion workflow. Although material-specific printing could not be performed due to batch limitations and time constraints, the successful use of PHA provided a viable proxy to test extrusion parameters, robot motion, and slicing strategy compatibility.

The trials demonstrated that the slicing logic and robotic control generated via Grasshopper and Droid can accurately translate design intent into physical motion, yielding stable line extrusions with minimal defects. These results confirm that the fabrication framework is ready to accommodate future tests with the actual strength-graded formulations.

Looking ahead, the extrusion framework and slicing logic are already equipped to support strength-differentiated deposition. By linking material properties to toolpath parameters—such as print speed, retraction, and layer height—the system can eventually produce architectural components with locally tuned mechanical behavior. Future trials can incorporate all three material formulations, enabling functionally graded prints aligned with specific structural performance needs.

Beyond this, real-time feedback systems (e.g., for moisture content, flow consistency, or layer adhesion) can be integrated to dynamically adapt extrusion parameters. This would push the workflow toward closed-loop

fabrication, where sensor data informs print logic in real-time. Such advancements would not only enhance reliability but also expand the application range of bio-based extrusion in large-scale architectural prototyping.

In summary, while constrained in scope, this phase validated the core extrusion pipeline and laid the foundation for future developments in sustainable robotic manufacturing. It underscores the feasibility of printing with lignin–cellulose composites and opens new pathways for integrating material science, computational design, and digital fabrication in architecture.

7. DESIGN & PROTOTYPING

7.1. Overview

The design and prototyping phase translates material development and printability research into architectural-scale components, with a focus on modular brick systems suitable for robotic hot extrusion. This phase bridges computational design, material optimization, and robotic fabrication, providing a critical step toward integrating sustainable composites into functional building assemblies. Drawing on the mechanical testing and early extrusion trials, the workflow centered on refining the parametric brick designs, improving material handling strategies, and validating fabrication feasibility using full-scale printing equipment.

This stage was not focused on demonstrating structural capacity of graded bricks themselves but instead aimed to establish a scalable printing logic and slicing framework. Material testing informed design tolerances and robotic motion planning, while initial extrusion trials using PHA—a key binder in the composite formulations—were used as a stand-in material for evaluating alignment, deposition consistency, and slicer interpretation.

7.2. Material Enhancement

The material enhancement phase focused on fine-tuning the composite formulations to address printability challenges and ensure consistent mechanical performance during large-scale prototyping. Insights gained from tensile testing and printability trials informed targeted adjustments, aimed at improving flow behavior, interlayer bonding, and dimensional stability without compromising the bio-based content and sustainability objectives.

7.2.1 Material Improvement Techniques

Building on insights from mechanical testing and extrusion trials, further refinement of the material preparation process was essential to address recurring challenges such as rapid thermal gradients, inconsistent fiber dispersion, and unstable extrusion flow. To tackle these, several targeted improvements were introduced:

- Temperature Control and Thermal Conditioning: The lignin and cellulose fibers were subjected to controlled preheating protocols to ensure gradual temperature alignment with the molten PHA. This minimized thermal shock, reducing premature stiffening and preventing sudden viscosity spikes during extrusion.

- Fiber Size Optimization for Homogeneity: The cellulose fibers underwent an additional milling and sieving step to reduce their particle size and eliminate larger, poorly integrated fragments. By refining fiber dimensions, the mixture achieved better homogeneity, ensuring even binder distribution and reducing the risk of localized charring during extrusion.

- Primer Coating Sequence: Glycerol-citric acid coating was applied pre-mixing, improving fiber dispersion and adhesion between phases in the composite.

- Enhanced Mixing Protocol: The integration sequence was adjusted to first coat the lignocellulosic fibers with a glycerol–citric acid primer, ensuring better wetting and fiber-matrix interaction before introducing the molten PHA. This method enhanced fiber dispersion and mitigated agglomeration, resulting in a more cohesive composite matrix.

- Moisture Reduction: Moisture tests showed 2% content in the composite pellets—well above the <0.05% requirement. The material was dried in an industrial dryer at 70°C for multiple hours to reduce this content, preventing bubbles and uneven flow.

7.2.2 Binder Improvement Techniques

While the core binder content was previously optimized, subtle yet critical adjustments were made to improve material stability and printability during scaled-up extrusion:

- Controlled Plasticizer Content: Glycerol was maintained at 3% by weight to preserve the delicate balance between flexibility and structural cohesion, preventing excessive softening while enhancing interlayer adhesion.

- Consistent Use of Citric Acid as Primer: The citric acid content remained at 2%, proving effective in improving interfacial bonding and maintaining printability during robotic extrusion by reducing fiber detachment and layer separation.

- Binder-to-Fiber Ratio Stability with Targeted Fiber Tuning: The PHA content was fixed at 60% for extrusion reliability, while the cellulose-to-lignin ratio was strategically varied to create strength-graded

material formulations. These adjustments allowed for performance tuning across different structural zones of the partition wall, ensuring both mechanical robustness and process efficiency.

Through this focused optimization, the composite formulation achieved improved thermal compatibility, enhanced homogeneity, and greater extrusion reliability, addressing previous limitations observed during manual processing and enabling successful robotic fabrication.

7.3. Design Refinement Process

The computational design of the modular bricks was driven by the need for robotic compatibility. The final brick geometry was optimized based on nozzle width, turning radii, and interlocking constraints. Rather than relying on variable infill or overhangs, the design utilized layered ribbing and vertical extrusion logic to simulate strength zones.

Special attention was paid to edge continuity and path length to accommodate the slicing logic in Droid. All geometry was verified using layer previews and digital slicing simulations, ensuring buildability within the limitations of the Dyze Pulsar's motion constraints and extrusion head.

.

7.4 Prototyping

7.4.1 Planning and Preparation

Initial plans involved robotic printing of all three strength-graded brick types using their final biocomposite formulations. However, due to a lack of sufficient material and time, this was not feasible before the P4 deadline. The solution was to test the digital-to-physical transition using the Group A formulation, which was sufficient to produce three representative bricks.

Prior extrusion trials at SAM|XL using PETG and early composites revealed excessive voids caused by large, hand-mixed chunks. Consequently, the project transitioned to 10XL, where a Dyze Pulsar extruder mounted on an ABB robot was employed. Material preparation was improved through grinding, sieving, and drying, ultimately leading to a powder-like, dense feedstock. After system calibration and axis alignment, successful extrusion trials were conducted that demonstrated stable flow, strong interlayer adhesion, and minimal shrinkage.

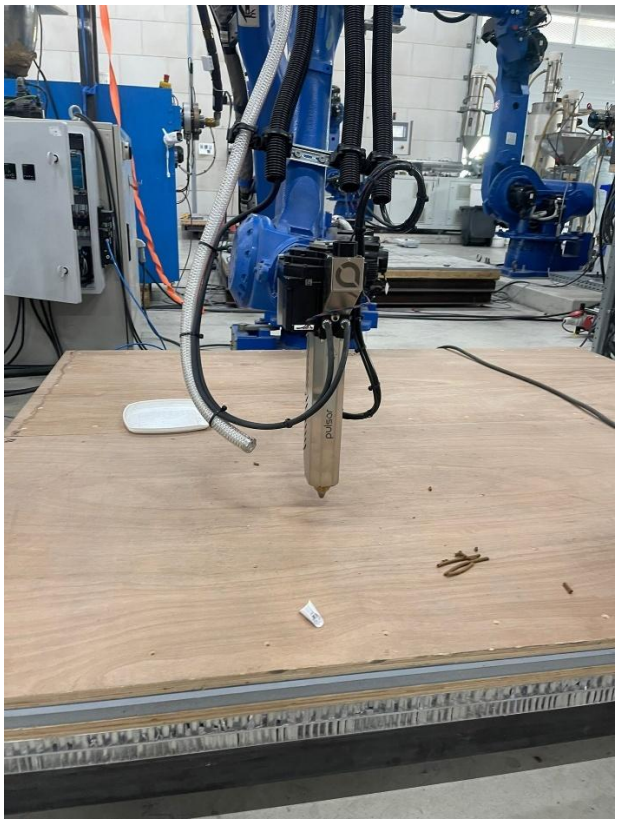

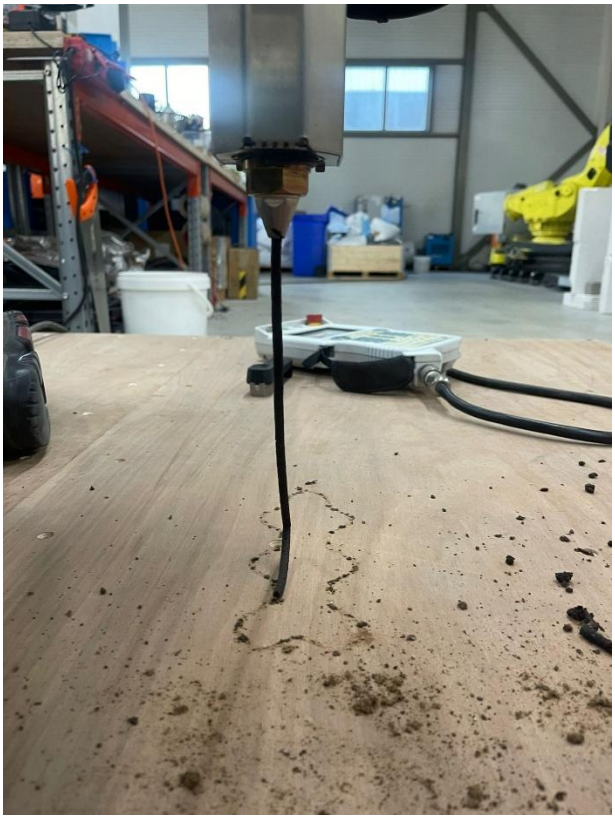

Figure 57, 58 – 10XL Robotic Setup for Pellet Extruder

7.4.2 Printing and Assembly

Three bricks were printed using the Group A formulation to test the geometrical accuracy and compatibility of interlocking features. Each prototype demonstrated a different type of joint to explore flexibility and dual adaptability within the modular wall system. Although no large-scale wall was assembled, these prints allowed the assessment of geometric fidelity, interlocking tolerance, and physical behavior of the actual composite formulation under robotic deposition.

Figure 59 – Printing Trials

7.4.3 Evaluation of Prototype

The evaluation of the fabricated prototypes centered on analyzing both the print quality and architectural applicability of the bricks produced with the Group A lignin–cellulose formulation. The printed units were inspected for geometric fidelity, interlayer bonding, surface consistency, and overall structural integrity post-printing.

The prototype shown in the figure demonstrates a successful deposition with visibly well-defined ribbing and continuous layering. Despite the bio-based nature of the composite, the print exhibited strong interlayer adhesion and minimal surface defects. Notably, no signs of delamination, warping, or shrinkage were observed during or after the printing process. The ribbed surface detail—which plays a key role in interlocking and aesthetic articulation—was cleanly extruded with a consistent profile, indicating good nozzle control and thermal uniformity.

The dark brown color and fibrous texture of the composite made the layer lines highly legible, allowing a clear assessment of layer stacking and continuity. The curvature and wave logic within the geometry were preserved without smudging or drag, suggesting that the slicing parameters—such as path overlap, extrusion flow rate, and cooling delay—were correctly tuned for this material.

Some roughness was evident on the uppermost layers, likely due to minor inconsistencies in pellet size or residual moisture that may not have fully evaporated prior to extrusion. These irregularities did not compromise

the structural cohesion of the unit but point to potential refinements in pre-processing or nozzle temperature calibration.

Crucially, the brick maintained dimensional stability after cooling, holding its intended shape and proportions. This confirms the thermal compatibility of the Group A formulation with the robotic setup and affirms its viability for further prototyping phases. The ability to achieve a smooth transition in curvature while preserving the verticality and tolerance of the modular geometry reinforces the feasibility of using this material system for architectural-scale additive manufacturing.

In summary, the printed prototype validated not only the mechanical integrity and print fidelity of the composite but also its readiness for deployment in future strength-graded applications. Minor surface inconsistencies highlight areas for further material calibration but do not detract from the successful demonstration of robotic deposition using the actual biocomposite formulation.

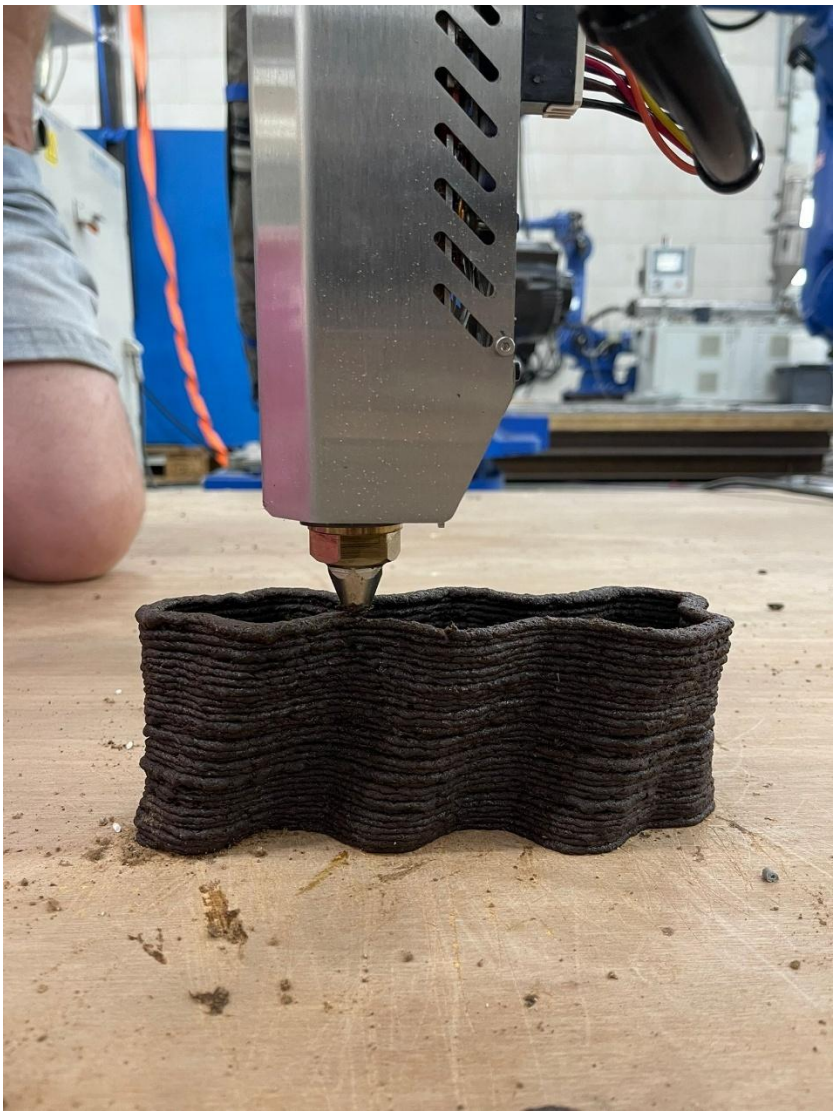

Figure 60 – Brick printing

7.5 . Conclusion

The design and prototyping phase marked a critical milestone in transitioning from experimental material development to tangible architectural output. Through the successful robotic extrusion of three modular bricks using the Group A lignin–cellulose formulation, the project demonstrated the feasibility of integrating sustainable biocomposites into additive manufacturing processes at a building scale.

Despite constraints that prevented the fabrication of strength-graded bricks across all material groups, the printed prototypes validated the structural coherence, geometric fidelity, and interlocking behavior of the designed units. Each prototype embodied a unique joint configuration, testing the modular system's adaptability and providing insight into dual-connection strategies for future wall assemblies. The successful interpretation of G-code, material flow stability, and preservation of form during printing affirm the compatibility of the composite with robotic hardware and slicing logic.

The outcome confirms that the composite not only flows and bonds well under extrusion but can also hold complex geometries with high spatial resolution—key qualities for architectural applications. The image-based evaluation of the printed brick further highlighted the robustness of the layered structure, with clearly articulated ribs, minimal warping, and a stable profile. These characteristics signal that the material is ready for scaling up to full prototypes, pending further refinements in pellet quality and extrusion parameter tuning.

Looking forward, the next stage will involve compressive and flexural testing of the printed bricks to assess their performance in structural applications. Comparative studies on printing orientation, joint behavior under load, and rheological profiling of the composite are also planned to deepen the understanding of how design and material interact through robotic workflows. These future investigations will complete the feedback loop between computational modeling, material science, and fabrication logic—laying the groundwork for scalable, ecologically responsive additive construction.

In sum, this chapter validates the technical and material readiness of the proposed bio-based fabrication system and sets a clear direction for its full architectural implementation.

8. CONCLUSION & FUTURE WORK

8.1. Summary of Research and Results

This research set out to bridge the gap between sustainable material innovation and advanced fabrication techniques by exploring the potential of high lignin–cellulose biocomposites for robotic additive manufacturing in architecture. By focusing on the development of strength-graded, thermoplastic-based composites, the project successfully created a fully integrated workflow that connects fiber-to-binder ratio optimization, mechanical validation, computational slicing, and robotic printing for architectural partition wall systems.

The material development phase began with a detailed examination of the thermal and physical properties of lignin and cellulose, drawing on both prior literature and in-house trials to identify their behavior under heat and moisture. A series of binder candidates—including PLA, PHA, and TPS—were evaluated, ultimately leading to the adoption of PHA as the most effective thermoplastic for compatibility and flow behavior. Citric acid and glycerol were used as primer and plasticizer, respectively, addressing key issues of fiber dispersion and brittleness. Through iterative mixing trials and thermal conditioning techniques, a series of homogenous, printable composite blends were developed.

Three material formulations were finalized, each tailored to distinct structural requirements: high-strength, medium-strength, and low-strength. These variants were tested using uniaxial tensile testing, with Group C (5% lignin / 30% cellulose) demonstrating the highest tensile strength and stiffness, and Group B (25% lignin / 10% cellulose) offering rigidity but lower elongation and strength. The extrusion of specimens was conducted using the pellet-based Dyze Pulsar robotic extruder at 10XL, and earlier trials were conducted using a homemade extruder setup at the LAMA Lab. The robotic setup provided precise thermal and material control, reducing inconsistencies caused by manual mixing and extrusion.

On the computational side, parametric brick elements were developed in Grasshopper and evaluated through a customized slicing and simulation workflow. Slicing tools—including Droid, Termite, Silkworm, and COMPAS—were compared using a detailed parameter-based and workflow-based evaluation system. Termite

and COMPAS emerged as the most robust tools for custom slicing and robotic integration, and were used to drive toolpath generation and material placement.

To link material properties with structural performance, Karamba3D was used for structural simulation and load mapping. The bricks were then computationally assigned and placed based on performance zones within the architectural partition wall, establishing a logic for strength-based material placement. This integrative design-to-fabrication workflow proved that it is possible to strategically use material efficiency and computational control to enable novel, functionally graded architectural systems.

8.2. Implications for Sustainable Construction

The outcomes of this research provide a framework for rethinking how we use materials in architecture—not only through bio-based alternatives but by designing with performance, processability, and sustainability in mind. By utilizing lignin and cellulose, two of the most abundant byproducts of agriculture and forestry, the project highlights a pathway toward integrating low-impact materials into high-tech fabrication workflows.

The strength-graded approach introduces a paradigm shift in additive construction. Rather than using one homogenous material across an entire structure, the research demonstrates how different mixtures can be optimized and positioned to meet specific structural needs. This strategy improves both performance and resource efficiency, significantly reducing material waste and unnecessary overengineering.

Furthermore, the project showcases how digital fabrication and computational design can advance the application of recycled or underused materials, reducing dependence on energy-intensive materials such as concrete or steel in non-load-bearing applications. It also positions robotic extrusion as a viable process for scaled architectural applications of biocomposites, provided the extrusion consistency and formulation homogeneity can be maintained.

8.3. Future Research Directions

While this thesis has demonstrated the feasibility of using lignin–cellulose composites for robotic extrusion, several key research directions remain critical to advancing the system toward architectural deployment and functional scalability.

A primary opportunity lies in developing a real-time, adaptive extrusion system that dynamically adjusts material properties during fabrication. One speculative but promising idea is the integration of a "biocomposite cocktail" system—a robotic printhead capable of in-situ mixing. This setup would receive computational inputs, such as geometric data or structural stress maps, and respond by adjusting the proportions of lignin, cellulose, and binder on the fly. Such a system would allow the creation of printed components with spatially varying mechanical properties, enabling gradient behavior within a single wall or structure. This would enhance performance responsiveness and reduce the need for post-processing or additional reinforcements.

Another important avenue is the exploration of multi-axis robotic printing and curved slicing strategies. Current approaches rely on planar, layer-by-layer deposition, which limits the design freedom and introduces anisotropy in the printed parts. Implementing curved or non-planar slicing would allow for the alignment of deposition paths with stress directions, minimize the need for support structures, and enable the fabrication of more complex geometries. Combined with real-time toolpath control, this could significantly improve structural performance and broaden the range of printable forms.

To improve fabrication reliability and precision, future systems should incorporate sensing and feedback technologies. Real-time monitoring—such as thermal imaging, back-pressure detection, moisture sensors, or computer vision—could be used to detect print inconsistencies or material anomalies. These inputs could then be fed back into the system to adjust parameters like extrusion rate, print speed, or cooling duration dynamically. Such closed-loop feedback would enable automated error correction and significantly enhance the consistency of bio-based robotic printing.

In parallel, a more comprehensive understanding of the composite's mechanical performance is essential. While this research has focused on tensile properties, additional tests such as compression, bending, and shear will be required to evaluate the bricks under realistic loading conditions. Differences in strength based on printing orientation—particularly vertical versus horizontal deposition—should also be examined to assess the influence of layer bonding on performance.

Rheological and thermal characterization will play a pivotal role in advancing the material side of the workflow. Understanding how the composite flows under different shear rates and temperatures is crucial for tuning extrusion parameters. Tests such as rotational rheometry and thermal degradation analysis would inform the limits of printability, helping to avoid clogging, over-extrusion, or inconsistent layer adhesion.

Equally important is evaluating the material's environmental durability and lifecycle performance. Since this research has focused primarily on printability and short-term strength, future studies should assess how the

composite behaves under real-world conditions. This includes its resistance to UV exposure, moisture uptake, biodegradation, and thermal cycling. Life cycle assessment (LCA) tools should be employed to quantify the environmental benefits or trade-offs of these biocomposites compared to conventional construction materials.

Lastly, future work should scale up from individual printed bricks to larger wall assemblies. This would involve testing different joinery configurations, tolerances, and stacking logics to simulate real construction scenarios. These trials will not only validate the assembly performance of the bricks but also provide feedback on how fabrication tolerances and printing defects propagate at the system level.

Together, these directions define a future where sustainable biocomposites, robotic precision, and intelligent slicing converge into a fully adaptive architectural fabrication platform—capable of producing high-performance, materially responsive, and environmentally attuned building components.

8.4. Reflection on the Research Process

This research has been as much an exploration of design thinking as of material innovation. Working across laboratories, robotic setups, and software platforms required a constant balance between precision and improvisation. The most significant challenge throughout the process was time—especially given the scarcity of documentation and case studies related to pellet-based robotic extruders. Building workflows from scratch for slicing, testing, and prototyping with limited hardware-specific guidance demanded a high degree of adaptability.

Working in the LAMA Lab and SAM|XL provided contrasting yet complementary environments. The former allowed for hands-on, iterative material testing with improvised setups, while the latter introduced industrial-scale precision and control. However, navigating lab safety protocols, limited machine time, and ad hoc tooling solutions added layers of difficulty. Mixing by hand, relying on domestic-scale ovens, and producing experimental batches with limited temperature consistency revealed how challenging it is to scale sustainable fabrication without specialized infrastructure.

Throughout the project, the computational workflow also evolved significantly. Initially envisioned as a material simulation pipeline using COMSOL, it transitioned into a slicing optimization and robotic assignment toolchain—better suited to real fabrication needs. This flexibility was critical to align the digital and physical aspects of the project.

Despite these challenges, the project successfully produced a fully defined, strength-graded biocomposite system, linked from material to design to robotic assembly.

9. REFERENCES

1. Agrawal, R. and Vinodh, S. (2020). Sustainability evaluation of additive manufacturing processes using grey-based approach. Grey Systems: Theory and Application, 10(4), 393-412.
2. Alfaify, A., Saleh, M., Abdullah, F. M., & Al-Ahmari, A. M. (2020). Design for additive manufacturing: A systematic review. *Sustainability, 12*(19), 7936. https://doi.org/10.3390/su12197936
3. Ali, M. and Kaneko, T. (2019). Syntheses of aromatic/heterocyclic derived bioplastics with high thermal/mechanical performance. Industrial & Engineering Chemistry Research, 58(35), 15958-15974. https://doi.org/10.1021/acs.iecr.9b00830
4. Ali, M., Zailani, S., Iranmanesh, M., & Foroughi, B. (2019). Impacts of environmental factors on waste, energy, and resource management and sustainable performance. Sustainability, 11(8), 2443. https://doi.org/10.3390/su11082443
5. Andok, A. (2023). Effect of bleaching with potassium hydroxide on the properties of egg carton pulp for nitrocellulose production. Bio Web of Conferences, 73, 05032. https://doi.org/10.1051/bioconf/20237305032
6. Arias-Ferreiro, G.; Lasagabáster-Latorre, A.; Ares-Pernas, A.; Ligero, P.; García-Garabal, S.M.; Dopico-García, M.S.; Abad, M.-J. Lignin as a High-Value Bioaditive in 3D-DLP Printable Acrylic Resins and Polyaniline Conductive Composite. Polymers 2022, 14, 4164. https://doi.org/10.3390/ polym14194164
7. Ayrilmis, N., Kariž, M., Kwon, J.-h., & Kitek Kuzman, M. (2019). Effect of printing layer thickness on water absorption and mechanical properties of 3D-printed wood/PLA composite materials. The International Journal of Advanced Manufacturing Technology, 102, 2195-2200.
8. Bierach, C., Coelho, A., Turrin, M., Asut, S., & Knaack, U. (2023). Wood-based 3d printing: potential and limitation to 3d print building elements with cellulose & lignin. Architecture Structures and Construction, 3(2), 157-170. https://doi.org/10.1007/s44150-023-00088-7
9. Ceren, K. and Yucel, U. (2023). Advances in cellulose-based packaging films for food products.. https://doi.org/10.5772/intechopen.110817
10. Chin, K. C. H., Cui, J., O'Dea, R. M., Epps, T. H., & Boydston, A. J. (2023). Vat 3d printing of bioderivable photoresins – toward sustainable and robust thermoplastic parts. ACS Sustainable Chemistry &Amp; Engineering, 11(5), 1867-1874. https://doi.org/10.1021/acssuschemeng.2c06313
11. Dananjaya, S. A. V., Chevali, V. S., Dear, J. P., Potluri, P., & Abeykoon, C. (2024). *3D printing of biodegradable polymers and their composites – Current state-of-the-art, properties, applications, and machine learning for potential future applications*. *Progress in Materials Science, 146*, 101336. https://doi.org/10.1016/j.pmatsci.2024.101336

12. Dang, C. (2024). Sensitivity analysis of parameters affecting the seismic performance of rc columns strengthened by fabric-reinforced cementitious mortar. Materials Research Express, 11(5), 055602. https://doi.org/10.1088/2053-1591/ad484a
13. fEbers, L. S., Arya, A., Bowland, C. C., Glasser, W. G., Chmely, S. C., Naskar, A. K., & Laborie, M. P. (2021). 3D printing of lignin: Challenges, opportunities and roads onward. 112. https://doi.org/10.1002/bip.23431
14. Fang, Z., Weisenberger, M., & Meier, M. (2020). Utilization of lignin-derived small molecules: epoxy polymers from lignin oxidation products. Acs Applied Bio Materials, 3(2), 881-890. https://doi.org/10.1021/acsabm.9b00954
15. Fatriasari, W. (2024). Cellulose first fractionation strategy in lignin valorization: a mini review. Global Forest Journal, 2(01), 1-7. https://doi.org/10.32734/gfj.v2i01.15563
16. Filgueira, D., Holmen, S., Melbø, J., Moldes, D., Echtermeyer, A., & Chinga-Carrasco, G. (2018). 3d printable filaments made of biobased polyethylene biocomposites. Polymers, 10(3), 314. https://doi.org/10.3390/polym10030314
17. Foley, P. M., Kermanshahi-pour, A., Beach, E. S., & Zimmerman, J. (2012). Derivation and synthesis of renewable surfactants. Chem. Soc. Rev., 41(4), 1499-1518. https://doi.org/10.1039/c1cs15217c
18. Furlan, A., Colombo, G., & Fiorentino, M. (2025). *Robotic FDM for Free-Form Fabrication: Evaluating Adaptive Non-Planar Slicing with Different Contour Methods*. ResearchGate publication
19. Gao, J. and You, F. (2017). Can modular manufacturing be the next game-changer in shale gas supply chain design and operations for economic and environmental sustainability?. Acs Sustainable Chemistry & Engineering, 5(11), 10046-10071. https://doi.org/10.1021/acssuschemeng.7b02081
20. Gardner, D. J., Anderson, J., Tekinalp, H., Ozcan, S., & Sauerbier, P. (2018, 26–29 September 2018). Lignocellulosic-filled polymer feedstocks for large scale additive manufacturing of low cost composites. Proceedings of the International Forest Products Congress, Trabzon, Turkey.
21. Gauss, C., Pickering, K. L., & Muthe, L. P. (2021). The use of cellulose in bio-derived formulations for 3D/4D printing: A review. 4, 100113. https://doi.org/10.1016/j.jcomc.2021.100113
22. Gibson, I., Rosen, D., Stucker, B., & Khorasani, M. (2021). Additive Manufacturing Technologies. Springer International Publishing. https://doi.org/10.1007/978-3-030-56127-7
23. González, D., Campos, A., Cunha, A., Santos, V., & Parajó, J. (2010). Manufacture of fibrous reinforcements for biodegradable biocomposites from citysus scoparius. Journal of Chemical Technology & Biotechnology, 86(4), 575-583. https://doi.org/10.1002/jctb.2555
24. Henke, K., & Treml, S. (2013). Wood based bulk material in 3D printing processes for applications in construction. In (Vol. 71, pp. 139-141).
25. Hu, L. (2024). Thermal pyrolysis behavior and decomposition mechanism of lignin revealed by stochastic cluster dynamics simulations. The Journal of Physical Chemistry C, 128(9), 3832-3838. https://doi.org/10.1021/acs.jpcc.3c07218

26. Jiang, B., Jiao, H., Guo, X., Chen, G., Guo, J., Wu, W., ... & Liang, Z. (2023). Lignin-based materials for additive manufacturing: chemistry, processing, structures, properties, and applications. Advanced Science, 10(9). https://doi.org/10.1002/advs.202206055
27. Klemmt, C., Aghaei Meibodi, M., Beaucage, G., & McGee, W. (2022). *Large-scale Robotic 3D Printing of Plant Fibre and Bioplastic Composites*. In Proceedings of the 40th Conference on Education and Research in Computer Aided Architectural Design in Europe (eCAADe 2022), Volume 1, pp. 65–74. DOI: 10.52842/conf.ecaade.2022.1.009
28. Kozlovská, M., Kaleja, P., & Struková, Z. (2014). Sustainable construction technology based on building modules. Advanced Materials Research, 1041, 231-234. https://doi.org/10.4028/www.scientific.net/amr.1041.231
29. Kretzer, M., & Mostafavi, S. (2020). *Robotic Fabrication with Bioplastic Materials: Digital design and robotic production of biodegradable objects*. In L. C. Werner & D. Koering (Eds.), Proceedings of the 38th eCAADe Conference on Education and Research in Computer Aided Architectural Design in Europe: Anthropologic - Architecture and Fabrication in the Cognitive Age (Vol. 1, pp. 603-612). DOI: 10.52842/conf.ecaade.2020.1.603
30. Kyriakidis, A., Michael, A., & Illampas, R. (2016). Parametric numerical assessment of the energy efficiency and the environmental impact of an innovative masonry construction component. Journal of Sustainable Architecture and Civil Engineering, 16(3). https://doi.org/10.5755/j01.sace.16.3.16174
31. Liebrand, T. (2018). 3D printed fiber reinforced lignin: Exploring the options to use wood in an additive manufacturing process
32. Luo, D., Yang, J., & Peek, N. (2025). *3D-Printed Mycelium Biocomposites: Method for 3D Printing and Growing Fungi-Based Composites*. 3D Printing and Additive Manufacturing, 12(2), 98–111. DOI: 10.1089/3dp.2023.0342
33. Mançanares, C., Zancul, E., & Miguel, P. (2015). Sustainable manufacturing strategies: a literature review on additive manufacturing approach. Product Management & Development, 13(1), 47-56. https://doi.org/10.4322/pmd.2015.001
34. Mogas-Soldevila, L., Duro-Royo, J., & Oxman, N. (2015). *Water-Based Robotic Fabrication: Large-Scale Additive Manufacturing of Biodegradable Architectures*. In Proceedings of the IASS Symposium.
35. Mohan, D., Teong, Z. K., Bakir, A. N., Sajab, M. S., & Kaco, H. (2020). Extending Cellulose-Based Polymers Application in Additive Manufacturing Technology: A Review of Recent Approaches. Polymers, 12.
36. Moretti, C., Corona, B., Hoefnagels, R., Vural-Gürsel, I., Gosselink, R., & Junginger, M. (2021). Review of life cycle assessments of lignin and derived products: lessons learned. The Science of the Total Environment, 770, 144656. https://doi.org/10.1016/j.scitotenv.2020.144656

37. Ngo, T. D., Kashani, A., Imbalzano, G., Nguyen, K. T. Q., & Hui, D. (2018). Additive manufacturing (3D printing): A review of materials, methods, applications and challenges. *Composites Part B: Engineering, 143*, 172–196. https://doi.org/10.1016/j.compositesb.2018.02.012
38. Nguyen, N. A., Barnes, S. H., Bowland, C. C., Meek, K. M., Littrell, K. C., Keum, J. K., & Naskar, A. K. (2018). A path for lignin valorization via additive manufacturing of high-performance sustainable composites with enhanced 3D printability. 4. https://doi.org/10.1126/sciadv.aat4967
39. Özgüner, M. and Özgüner, Z. (2022). Evaluation of the importance of additive manufacturing technology in terms of sustainable production with the dematel method. International Journal of Advanced and Applied Sciences, 9(10), 116-125. https://doi.org/10.21833/ijaas.2022.10.015
40. Pajonk, A., Knaack, U., Klein, T., & Hildebrand, L. (2021). Architectural opportunities of large-scale 3D printing for the built environment: An exploration of materiality, form and construction. *Journal of Building Engineering*, 43, 102568. https://doi.org/10.1016/j.jobe.2021.103603
41. Pelanconi, M. and Ortona, A. (2019). Nature-inspired, ultra-lightweight structures with gyroid cores produced by additive manufacturing and reinforced by unidirectional carbon fiber ribs. Materials, 12(24), 4134. https://doi.org/10.3390/ma12244134
42. Pelicaen, E. (2024). Reclaiming earth blocks using various techniques. Iop Conference Series Earth and Environmental Science, 1363(1), 012100. https://doi.org/10.1088/1755-1315/1363/1/012100
43. Rosca, M., van de Wouw, A., & Lu, T. (2022). *Integrated Design Strategies for Multiscalar Biopolymer Robotic 3D Printing*.
44. Rosenthal, M., Henneberger, C., Gutkes, A., & Bues, C.-T. (2018). Liquid Deposition Modeling: a promising approach for 3D printing of wood. In (Vol. 76, pp. 797-799).
45. Sanchez-Rexach, E., Johnston, T. G., Jehanno, C., Sardón, H., & Nelson, A. (2020). Sustainable materials and chemical processes for additive manufacturing. Chemistry of Materials, 32(17), 7105-7119. https://doi.org/10.1021/acs.chemmater.0c02008
46. Soloi, S. (2023). Biobased plastic films from cogon grass cellulose. SEHS, 23020005. https://doi.org/10.69598/sehs.17.23020005
47. Song, Q., Wang, F., Cai, J., Wang, Y., Zhang, J., Yu, W., ... & Xu, J. (2013). Lignin depolymerization (ldp) in alcohol over nickel-based catalysts via a fragmentation–hydrogenolysis process. Energy & Environmental Science, 6(3), 994. https://doi.org/10.1039/c2ee23741e
48. Tanase-Opedal, M., Espinosa, E., Rodríguez, A., & Chinga-Carrasco, G. (2019). Lignin: A Biopolymer from Forestry Biomass for Biocomposites and 3D Printing. 12, 3006. https://doi.org/10.3390/ma12183006
49. Tchertchian, N., Millet, D., & Pialot, O. (2011). Modular grouping exploration to design remanufacturable products., 413-418. https://doi.org/10.1007/978-3-642-19692-8_71

50. Tortora, M., Cavalieri, F., Mosesso, P., Ciaffardini, F., Melone, F., & Crestini, C. (2014). Ultrasound driven assembly of lignin into microcapsules for storage and delivery of hydrophobic molecules. Biomacromolecules, 15(5), 1634-1643. https://doi.org/10.1021/bm500015j
51. UNFCCC. (2015, December 2015). Paris Agreement United Nations Framework Convention on Climate Change
52. Upton, B. and Kasko, A. (2018). Biodegradable aromatic–aliphatic poly(ester–amides) from monolignol-based ester dimers. Acs Sustainable Chemistry & Engineering, 6(3), 3659-3668. https://doi.org/10.1021/acssuschemeng.7b03784
53. Vazquez-Martel, C., Becker, L., Liebig, W., Elsner, P., & Blasco, E. (2021). Vegetable oils as sustainable inks for additive manufacturing: a comparative study. Acs Sustainable Chemistry & Engineering, 9(49), 16840-16848. https://doi.org/10.1021/acssuschemeng.1c06784
54. Villa, A. (2024). Sustainable approaches for the additive manufacturing of ceramic materials. Ceramics, 7(1), 291-309. https://doi.org/10.3390/ceramics7010019
55. Viretto, A. and Galy, J. (2018). Development of biobased epoxy matrices for the preparation of green composite materials for civil engineering applications. Macromolecular Materials and Engineering, 303(5). https://doi.org/10.1002/mame.201700521
56. Voet, V., Strating, T., Schnelting, G., Dijkstra, P., Tietema, M., Xu, J., … & Folkersma, R. (2018). Biobased acrylate photocurable resin formulation for stereolithography 3d printing. Acs Omega, 3(2), 1403-1408. https://doi.org/10.1021/acsomega.7b01648
57. Vyavahare, S., Teraiya, S., Panghal, D., & Kumar, S. (2020). Fused deposition modelling: a review. Rapid Prototyping Journal, 26(1), 176-201. https://doi.org/10.1108/rpj-04-2019-0106
58. Wan, "Recent advances in lignin-based 3D printing materials: A mini-review." International Journal of Biological Macromolecules (2023). doi:10.1016/j.ijbiomac.2023.126660.
59. Weiss, M., Haufe, J., Carus, M., Brandão, M., Bringezu, S., Hermann, B., … & Patel, M. (2012). A review of the environmental impacts of biobased materials. Journal of Industrial Ecology, 16(s1). https://doi.org/10.1111/j.1530-9290.2012.00468.x
60. WouldWood. (2018). Retrieved 07/06/2022 from https://www.wouldwood.se
61. Yang, J., An, X., Liu, L., Tang, S., Cao, H., Xu, Q., & Liu, H. (2020). Cellulose, hemicellulose, lignin, and their derivatives as multi-components of bio-based feedstocks for 3D printing. 250, 116881. https://doi.org/10.1016/j.carbpol.2020.116881
62. Yang, Y., Song, X., Li, X., Chen, Z., Zhou, C., Zhou, Q., … & Chen, Y. (2018). Recent progress in biomimetic additive manufacturing technology: from materials to functional structures. Advanced Materials, 30(36). https://doi.org/10.1002/adma.201706539

63. Yefremova, S., Zharmenov, A., Sukharnikov, Y., Bunchuk, L., Kablanbekov, A., Anarbekov, K., ... & Palianytsia, B. (2019). Rice husk hydrolytic lignin transformation in carbonization process. Molecules, 24(17), 3075. https://doi.org/10.3390/molecules24173075
64. Yin, D. (2024). Multifunctional biobased polyurethane/tannic acid composites with controllable damping, flame-retardant, and ultraviolet-shielding performances. Acs Applied Polymer Materials, 6(14), 8409-8418. https://doi.org/10.1021/acsapm.4c01289
65. Zadeh, E., O'Keefe, S., & Kim, Y. (2018). Utilization of lignin in biopolymeric packaging films. Acs Omega, 3(7), 7388-7398. https://doi.org/10.1021/acsomega.7b01341
66. Zboinska, M. A., Larsson, K., & Holmgren, C. (2021). *WouldWood: Biocomposite Design-to-Fabrication Strategies*. Chalmers University of Technology Technical Report.
67. Zhang, P. and Pei, Z. (2010). Effects of ultrasonic treatments on cellulose in cellulosic biofuel manufacturing: a literature review.. https://doi.org/10.1115/msec2010-34180
68. Zhao, W., Simmons, B., Singh, S., Ragauskas, A., & Cheng, G. (2016). From lignin association to nano-/micro-particle preparation: extracting higher value of lignin. Green Chemistry, 18(21), 5693-5700. https://doi.org/10.1039/c6gc01813k
69. Ahmad, M. N. et al. (2023). *A Review of Natural Fiber-Based Filaments for 3D Printing*. Materials, 16(11), 4052. https://doi.org/10.3390/ma16114052
70. Li, Y. (2025). *Direct Ink Writing of Polymer-Based Materials: A Review*. Polymer Engineering & Science. https://doi.org/10.1002/pen.27038
71. Dananjaya, S. A. V., Chevali, V. S., Dear, J. P., Potluri, P., & Abeykoon, C. (2024). 3D printing of biodegradable polymers and their composites – Current state-of-the-art, properties, applications, and machine learning for potential future applications. *Progress in Materials Science*, 146, 101336. https://doi.org/10.1016/j.pmatsci.2024.101336
72. Ford, S., & Despeisse, M. (2016). Additive manufacturing and sustainability: An exploratory study of the advantages and challenges. *Journal of Cleaner Production*, 137, 1573–1587. https://doi.org/10.1016/j.jclepro.2016.04.150
73. Aharoni, L., Bachelet, I., & Carstensen, J. V. (2021). Topology optimization of rigid interlocking assemblies. *Computers & Structures*, 250, 106521. https://doi.org/10.1016/j.compstruc.2021.106521

10. APPENDIX

	F_{max}	dL at F_{max}	a_0	b_0	S_0	
	N	mm	mm	mm	mm²	
Specimen 21	16,14102	0,905856		4	10	40
Specimen 22	58,72425	3,923144		4	10	40
Specimen 23	39,60574	1,414915		4	10	40
Specimen 24	39,00386	5,031499		4	10	40
Specimen 25	54,14184	5,039812		4	10	40
Specimen 26	55,01193	2,163989		4	10	40
Specimen 27	49,86696	0,818825		4	10	40
Specimen 28	37,38844	0,567295		4	10	40
Specimen 29	80,74603	7,044846		4	10	40
Specimen 30	43,44646	2,601341		4	10	40
Specimen 31	64,43394	2,157415		4	10	40
Specimen 32	44,57671	1,624586		4	10	40
Specimen 33	46,99934	0,401492		4	10	40
Specimen 34	51,3117	3,605718		4	10	40
Specimen 35	38,22548	1,642271		4	10	40
Specimen 36	63,84178	3,948161		4	10	40
Specimen 37	67,58797	3,944875		4	10	40
Specimen 38	66,13749	2,823887		4	10	40
Specimen 39	62,45379	4,163128		4	10	40
Specimen 40	40,57715	1,629693		4	10	40
Specimen 41	54,9906	5,938065		4	10	40

Series	F_{max}	dL at F_{max}	a_0	b_0	S_0	
n = 21	N	mm	mm	mm	mm²	
x	51,20059	2,923372	4	10	40	
s	14,19172	1,858208	0	0	0	
ν [%]	27,71788	63,56387	0	0	0	

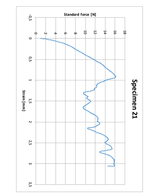
Standard Time (S)
Specimen Z2
Load (lbs)

1,609105 10,03493
1,611391 9,98014
1,615733 9,9078
1,619183 9,794643
1,622496 9,739934
1,625756 9,687023
1,629125 9,678518
1,632602 9,643181
1,635724 9,606249
1,639039 9,662801
1,642325 9,661267
1,64564 9,654658
1,649089 9,63173
1,652375 9,570739
1,655677 9,566161
1,659139 9,543718
1,662427 9,573392
1,665793 9,573824
1,669135 9,55465
1,673313 9,564654
1,675736 9,591771
1,679996 9,674491
1,682356 9,679496
1,685712 9,687441
1,689072 9,724955
1,692468 9,773344
1,695809 9,826512
1,699151 9,875123
1,702464 9,925437
1,70575 9,961684
1,709124 10,00169
1,712454 10,05115
1,715773 10,09206
1,719169 10,14326
1,72251 10,21169
1,725825 10,27242
1,729247 10,33197
1,732647 10,39101
1,736047 10,43964
1,739242 10,5239
1,742357 10,59494
1,745844 10,63239
1,749239 10,69012
1,752416 10,72378
1,755824 10,78139
1,7591 10,79839
1,762449 10,83307
1,765863 10,85948
1,769285 10,90422
1,772491 10,95416
1,775858 10,98409
1,779143 11,03773
1,782432 11,07093
1,785745 11,10368
1,789005 11,13508
1,792429 11,2265
1,795851 11,294
1,799083 11,34003
1,802479 11,41039
1,8059 11,44383
1,809202 11,47583
1,812502 11,56062
1,815843 11,64556
1,819156 11,68818
1,822469 11,74155
1,825676 11,81438
1,829044 11,86312
1,832435 11,91683
1,835699 11,93791
1,839067 11,98207
1,842544 12,02656
1,845804 12,04179
1,849144 12,07855
1,852459 12,11799
1,855824 12,1577
1,859031 12,17983
1,862345 12,21675
1,865633 12,25173
1,869055 12,30235
1,872341 12,32702
1,875765 12,35627
1,879099 12,38938
1,882419 12,39128
1,885759 12,40901
1,889183 12,44498
1,892442 12,47241
1,895729 12,49412
1,899015 12,53376
1,902393 12,53477
1,905752 12,53787
1,909179 12,54393
1,912553 12,60096
1,915857 12,59769
1,919116 12,60416
1,922429 12,58923
1,925798 12,57655
1,929113 12,558
1,932502 12,5557
1,935712 12,522
1,939107 12,49765
1,942449 12,5259
1,945817 12,54056
1,949186 12,51517
1,952581 12,5331
1,955898 12,53993
1,959162 12,53998
1,962577 12,54239
1,96589 12,53678
1,96915 12,54548
1,972492 12,5361
1,975723 12,51229
1,979107 12,5008
1,982459 12,49057
1,985801 12,49624
1,989169 12,47069
1,992538 12,49507
1,995824 12,52288
1,999219 12,60993
2,002744 12,67502
2,006098 12,7532
2,009107 12,72002
2,012367 12,76275
2,015762 12,81269
2,019157 12,84935
2,022416 12,87791
2,025785 12,88104
2,02918 12,88068
2,032497 12,88004
2,035863 12,89722
2,03915 12,87694
2,042409 12,87585
2,045749 12,88632
2,049082 12,88588
2,052324 12,86038
2,055699 12,83449
2,05906 12,83449
2,062509 12,79316
2,065876 12,73132
2,069083 12,65885
2,073478 12,60699
2,077791 12,54037
2,081092 12,49313
2,084393 12,47412
2,087507 12,35515
2,088994 12,30034
2,092389 12,21627
2,095702 12,239
2,099017 12,22416
2,101465 12,2016
2,105753 12,04497
2,109093 12,11426
2,112412 11,98701
2,115721 11,98701
2,119008 11,90875
2,122349 11,83786
2,125662 11,71634
2,129139 11,64941
2,133346 11,44859
2,136589 11,43841
2,139589 10,83641
2,142504 10,54361
2,145737 10,42274
2,149132 10,41755
2,152445 10,49176
2,155732 10,43381
2,159139 9,99004
2,162468 10,00004
2,165837 10,04711
2,169178 10,62153
2,172492 10,67251
2,175995 10,78189
2,179255 10,85244
2,182541 10,92104
2,18591 11,02821
2,189249 11,09021
2,192439 11,17327
2,195744 11,23041
2,199057 11,28597
2,202479 11,38746
2,205821 11,4534
2,209162 11,53155
2,212499 11,60958
2,215899 11,64958
2,219159 11,73933
2,222554 11,81873
2,22584 11,91367
2,2291 11,95964
2,232387 12,00715
2,235691 12,08205
2,23913 12,1222
2,242463 12,16367
2,245778 12,22153
2,2492 12,26163
2,252515 12,3008
2,255719 12,38133
2,259049 12,40979
2,262429 12,49719
2,265769 12,70974
2,269029 12,82361
2,27227 12,88001
2,275739 12,97548
2,279107 13,05622
2,282393 13,14431
2,285762 13,19758
2,289198 13,25048
2,29239 13,30687
2,29573 13,37646
2,299125 13,41083
2,302384 13,49004
2,305699 13,54487
2,309012 13,63082
2,312396 13,69746
2,315696 13,75746
2,319036 13,75158
2,322431 13,80705
2,325772 13,85802
2,329114 13,87955
2,332427 13,92133
2,335824 13,96474
2,339002 14,01475
2,342341 14,05944
2,345656 14,07798
2,348996 14,13806
2,352338 14,16778
2,355624 14,19571
2,358947 14,2387
2,36247 14,29807
2,365703 14,34413
2,369042 14,38249
2,372437 14,40022
2,375726 14,39841
2,379066 14,44618
2,382376 14,46469
2,385693 13,93791
2,389197 14,51939
2,392457 14,53782
2,395881 14,57419
2,399249 14,58771
2,402535 14,59928
2,405903 14,62164
2,409245 14,64569
2,412614 14,65946
2,415858 14,66346
2,419131 14,6383
2,422446 14,62329
2,425814 14,62002
2,429127 14,5838
2,432496 14,58228
2,435824 14,56943
2,439232 14,53943
2,442519 14,49705
2,445854 14,48603
2,44912 14,42912
2,452433 14,40159
2,455748 14,38127
2,459107 14,34993
2,462512 14,31752
2,465788 14,25923
2,469058 14,22053
2,472561 14,20687
2,475794 14,13912
2,479107 14,05449
2,482417 13,98699
2,485817 13,9699
2,489104 13,93871
2,492417 13,91643
2,495677 13,91691
2,4991 13,91063
2,502387 13,87885
2,5057 14,01782
2,50915 14,08048
2,512993 14,11369
2,515733 14,11003
2,519146 14,15751
2,522406 14,19168
2,525637 14,25307
2,529006 14,31437
2,532292 14,35484
2,535604 14,40179
2,539084 14,47179
2,54237 14,5378
2,545792 14,60231
2,549078 14,6452
2,552338 14,71865
2,555762 14,76176
2,559139 14,8097
2,56239 14,85997
2,565677 14,91336
2,568963 14,96173
2,572385 15,03867
2,575727 15,05457
2,579066 15,06894
2,582403 15,11969
2,585803 15,13369
2,589036 15,1916
2,592431 15,21461
2,595773 15,29938
2,599113 15,23365
2,602319 15,25107
2,605687 15,25455
2,609136 15,29369
2,612497 15,28972
2,615792 15,29972
2,619214 15,31417
2,622582 15,33802
2,625869 15,34666
2,629221 15,35978
2,632524 15,39684
2,635852 15,39394
2,639152 15,39194
2,642356 15,40658
2,645753 15,38877
2,649175 15,35871
2,652461 15,34913
2,655776 15,29688
2,659102 15,25982
2,662511 15,21582
2,665826 15,07619
2,669168 14,94478
2,672507 14,83589
2,675767 14,5912
2,679027 14,32338
2,682417 14,09777
2,685817 14,00777
2,68905 13,86955
2,692472 13,69335
2,695868 13,49913
2,699 13,27452
2,702468 13,11405
2,705918 13,03703
2,709096 13,01867
2,713382 12,96936
2,716733 12,93614
2,72001 12,85795
2,723461 12,91666
2,726747 12,94663
2,72906 12,96772
2,732511 12,97918
2,735798 13,02917
2,739191 13,08284
2,742433 13,10784
2,745713 13,30496
2,749026 13,42233
2,752367 13,56287
2,755627 13,68053
2,759049 13,77203
2,762309 13,84665
2,765677 13,95167
2,769139 14,02427
2,77244 14,11742
2,775753 14,21338
2,779095 14,28123
2,782408 14,36506
2,785614 14,45841
2,788983 14,52423
2,792364 14,60146
2,795684 14,71496
2,799088 14,75395
2,802374 14,81393
2,805851 14,88377
2,809164 14,96462
2,812424 15,0116
2,815824 15,0501
2,819079 15,09773
2,822447 15,11973
2,825707 15,13725
2,829048 15,17907
2,832443 15,19801
2,835865 15,27049
2,839224 15,31749
2,842549 15,35499
2,845915 15,397
2,849148 15,41864
2,852543 15,4484
2,855858 15,49984
2,859144 15,49782
2,862417 15,5417
2,865737 15,54517
2,869112 15,60329
2,872509 15,61905
2,87574 15,62812
2,879164 15,64861
2,882586 15,66793
2,885845 15,68644
2,889187 15,72292
2,892554 15,7468
2,895842 15,74489
2,899046 15,76502
2,902442 15,79115
2,905729 15,81517
2,90915 15,81501
2,91241 15,80183
2,915994 15,81004
2,919255 15,81511
2,921462 15,80295
2,924857 15,79947
2,92917 15,82302
2,932456 15,85123
2,935771 15,84149
2,939099 15,83892
2,942399 15,83892
2,945768 15,82894
2,949081 15,80757
2,95234 15,81391
2,955871 15,82724
2,959104 15,85476
2,962417 15,89169
2,965732 15,91522
2,969018 15,93808
2,972331 15,84195
2,975591 15,83738
2,979015 15,84173
2,982356 15,82138
2,985696 15,79294
2,989064 15,79139
2,992369 15,74239
2,995719 15,72618
2,999196 15,73083
3,002429 15,71031
3,005689 15,71567
3,009002 15,7178
3,012344 15,74109
3,015697 15,80596
3,019107 15,80596
3,022311 15,83189
3,025762 15,88468
3,029157 15,88986
3,032443 15,91465
3,03573 15,93879
3,039124 15,94178
3,042495 15,95439
3,045808 15,95115
3,049094 15,9499
3,052409 15,97185
3,055831 15,97103
3,059091 15,94046
3,062417 15,9499
3,06265 15,9372
3,062285 15,5285
3,062596 15,41091
3,062569 15,30981
3,062569 15,23375
3,062541 15,13772
3,062568 15,07497
3,062569 14,99307
3,062569 14,93935
3,062569 14,93123
3,062569 14,87305
3,062569 14,83924
3,062569 14,79923
3,062569 14,7594
3,062541 14,70087
3,062569 14,63968
3,062569 14,61068
3,062569 14,59254
3,062569 14,57122
3,062569 14,54875

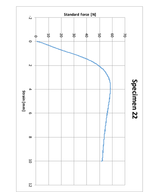
Standard Temp 296
Specimen Z2
Load (kN)
Extension (mm)

4,022994 58,53049
4,031634 58,53165
4,039862 58,49346
4,047984 58,3293
4,054216 58,60842
4,064772 58,63551
4,071111 58,62193
4,080462 58,58719
4,089461 58,58719
4,097884 58,60271
4,106493 58,63841
4,114779 58,59147
4,122847 58,56471
4,131213 58,60294
4,139481 58,64153
4,148081 58,64453
4,15431 58,58613
4,164568 58,49351
4,173071 58,47055
4,181654 58,45533
4,189936 58,45456
4,198007 58,45312
4,206457 58,45137
4,214703 58,45137
4,223212 58,43375
4,23136 58,43212
4,239565 58,42012
4,248038 58,38605
4,256625 58,37409
4,264716 58,39108
4,273284 58,40987
4,281367 58,47783
4,289763 58,50612
4,298129 58,47401
4,306304 58,45923
4,314563 58,45471
4,323009 58,46481
4,331284 58,47112
4,33974 58,42212
4,347808 58,40515
4,356231 58,39969
4,364841 58,45675
4,373179 58,47075
4,381301 58,37021
4,389884 58,36264
4,398143 58,26756
4,406508 58,28588
4,414874 58,29359
4,422942 58,28382
4,431415 58,23729
4,439971 58,22771
4,448423 58,22771
4,456271 58,24017
4,464717 58,2151
4,473056 58,19847
4,481421 58,18303
4,489707 58,18537
4,497886 58,24673
4,506305 58,25809
4,514861 58,29049
4,523215 58,29049
4,531251 58,2812
4,539554 58,22372
4,548079 58,23999
4,556392 58,22412
4,564597 58,15948
4,572883 58,1613
4,581264 58,09999
4,589747 58,24406
4,59817 58,23999
4,606238 58,10756
4,614795 58,05059
4,623294 58,02263
4,631606 58,04685
4,640124 58,06299
4,647906 58,006
4,656436 58,00379
4,664802 57,99649
4,673167 58,00464
4,681235 57,97371
4,689765 57,95353
4,698284 57,95353
4,706443 57,89937
4,714698 57,87709
4,723903 57,87586
4,731322 58,00872
4,739709 57,99052
4,748084 57,96412
4,756148 57,91971
4,764566 57,91971
4,771554 57,95458
4,781466 57,91457
4,789641 57,87337
4,797954 57,80129
4,806238 57,83992
4,814742 57,95839
4,82297 57,90469
4,831284 57,90469
4,839786 57,78172
4,848395 57,78469
4,856654 57,77964
4,864749 57,75119
4,873057 57,73343
4,881454 57,74122
4,889825 57,74122
4,898105 57,71595
4,906142 57,68242
4,914499 57,6809
4,923202 57,62289
4,931514 57,63341
4,939635 57,59984
4,947999 57,59984
4,956367 57,75171
4,964816 57,73081
4,973911 57,69126
4,981223 57,65711
4,989663 57,66502
4,998008 57,70926
5,006418 57,69126
5,014912 57,64438
5,023051 57,64972
5,031474 57,68398
5,039733 57,68753
5,047961 57,57983
5,0563 57,502
5,064719 57,49404
5,073195 57,46316
5,081564 57,46316
5,089576 57,43766
5,097995 57,45607
5,106688 57,4157
5,114944 57,42951
5,123586 57,4063
5,131241 57,38362
5,139883 57,3363
5,148083 57,32363
5,156369 57,35078
5,164544 57,39128
5,172993 57,45134
5,181576 57,45052
5,189888 57,41146
5,198241 57,39128
5,206213 57,367
5,214661 57,39191
5,23168 57,36367
5,231366 57,31275
5,239514 57,29848
5,247853 57,30322
5,25652 57,30432
5,264512 57,37913
5,27298 57,23994
5,281284 57,18241
5,289902 57,18241
5,298188 57,18125
5,306449 57,21071
5,314591 57,11168
5,32304 57,10879
5,331517 57,11386
5,339884 57,15976
5,348031 57,1976
5,356369 57,06243
5,364815 57,03714
5,373238 56,98013
5,381333 57,01674
5,389508 57,07093
5,397911 57,09164
5,406114 57,09164
5,414769 57,03954
5,423863 57,03113
5,431286 57,05484
5,439785 57,0567
5,448098 57,0262
5,456276 56,99955
5,464585 56,98472
5,472911 56,96413
5,48148 57,04172
5,489766 56,98008
5,497914 56,88452
5,50647 56,81351
5,515057 56,8221
5,523285 56,78952
5,531664 56,75206
5,539694 56,75206
5,548059 56,76767
5,556532 56,74398
5,564844 56,74649
5,573859 56,74591
5,581388 56,70259
5,589773 56,66106
5,598173 56,61106
5,606268 56,6907
5,614771 56,77481
5,623303 56,7951
5,631649 56,76674
5,639708 56,72214
5,648275 56,72214
5,656273 56,72007
5,664751 56,69036
5,673107 56,65145
5,681265 56,63347
5,689577 56,6259
5,698107 56,66521
5,706066 56,63194
5,714921 56,57359
5,723469 56,57359
5,731408 56,44941
5,739882 56,46045
5,748331 56,47191
5,756399 56,41401
5,764765 56,41384
5,773291 56,39677
5,781644 56,39677
5,789644 56,39315
5,797903 56,34457
5,806295 56,3224
5,814745 56,25703
5,823111 56,31142
5,831179 56,36914
5,839644 56,40992
5,848201 56,41892
5,856577 56,38034
5,864588 56,33068
5,8729 56,31822
5,881319 56,31855
5,889715 56,3254
5,898178 56,29299
5,906376 56,25309
5,914541 56,30353
5,923204 56,35843
5,931543 56,34101
5,939695 56,23474
5,948034 56,16068
5,956492 56,14301
5,964759 56,12522
5,973144 56,12522
5,98117 56,06769
5,989757 56,05814
5,99834 56,05677
6,006595 56,06306
6,01469 56,0477
6,023029 56,00708
6,031484 56,00708
6,039817 55,98986
6,047966 55,94899
6,056167 56,01913
6,064617 56,02006
6,073173 56,03706
6,081459 56,01428
6,089824 56,01428
6,097999 55,98786
6,106338 55,99979
6,114704 55,95695
6,122909 55,9278
6,131137 55,92843
6,139587 55,94781
6,147966 55,94443
6,156456 55,95443
6,164604 55,84443
6,173107 55,83392
6,18169 55,77512
6,189891 55,7731
6,198123 55,75212
6,206437 55,7408
6,214627 55,7408
6,223167 55,72377
6,231479 55,74277
6,239463 55,7061
6,247955 55,69836
6,256576 55,64963
6,264724 55,63159
6,273583 55,65063
6,281454 55,65063
6,289714 55,72027
6,298084 55,72853
6,306449 55,68892
6,31446 55,68119
6,32291 55,64501
6,33152 55,68898
6,339884 55,68898
6,347873 55,63152
6,356319 55,63612
6,364769 55,68842
6,373051 55,68492
6,381417 55,614
6,389622 55,53918
6,398064 55,49918
6,406651 55,47644
6,415017 55,49371
6,423058 55,48176
6,431424 55,46978
6,439847 55,45744
6,448159 55,45681
6,456484 55,41374
6,464682 55,41374
6,473038 55,40785
6,481514 55,3616
6,489796 55,37551
6,497891 55,44125
6,506367 55,40877
6,514897 55,40118
6,523182 55,45078
6,531666 55,45078
6,539505 55,4186
6,547928 55,42952
6,556427 55,43118
6,564766 55,37589
6,573834 55,35981
6,581311 55,3876
6,589884 55,36264
6,598153 55,41126
6,606354 55,33759
6,614613 55,27369
6,623112 55,2461
6,631508 55,25661
6,63979 55,23187
6,648284 55,22157
6,656388 55,22157
6,665024 55,25102
6,67331 55,2026
6,681324 55,19571
6,68961 55,15402
6,698109 55,12771
6,706488 55,12771
6,71468 55,23411
6,722775 55,17593
6,731331 55,1739
6,739914 55,19595
6,748063 55,16855
6,756268 55,51464
6,764687 55,13781
6,773099 55,159
6,781365 55,11643
6,789753 55,09941
6,797853 55,09941
6,806192 55,09577
6,814029 55,1296
6,823114 55,23587
6,831316 55,01418
6,839903 54,93046
6,848284 54,9278
6,856581 54,9203
6,864756 54,91768
6,873591 54,89506
6,881353 54,89012
6,889853 54,85959
6,898165 54,8754
6,906206 54,84157
6,914552 54,80876
6,923058 54,77629
6,93615 54,81767
6,947937 54,87666
6,956293 54,92024
6,964786 54,89618
6,973062 54,8802
6,981499 54,86989
6,989595 54,85489
6,998178 54,87416
7,006411 54,83172
7,014532 54,77956
7,023044 54,80506
7,031317 54,8172
7,039884 54,80506
7,047998 54,80791
7,05628 54,71073
7,064756 54,68705
7,073286 54,65516
7,081678 54,65938
7,089668 54,64785
7,098044 54,64785
7,106398 54,63193
7,114817 54,6241
7,123129 54,62141
7,131144 54,58912
7,139663 54,56996
7,148146 54,53354
7,156698 54,53354
7,164958 54,50647
7,173029 54,62908
7,181475 54,67109
7,189787 54,65259
7,197962 54,63357
7,206138 54,60995
7,214507 54,60345
7,223053 54,63418
7,231259 54,64218
7,239577 54,54538
7,24797 54,5695
7,256473 54,59829
7,264785 54,61578
7,27207 54,55958
7,281299 54,67721
7,289641 54,62257
7,298247 54,62257
7,306533 54,61941
7,314681 54,57491
7,323077 54,57946
7,331576 54,5664
7,339946 54,57935
7,348284 54,57935
7,356406 54,52175
7,364608 54,50259
7,373027 54,26137
7,381396 54,28628
7,389401 54,57469
7,398017 54,59046
7,406284 54,57192
7,414632 54,57192
7,422927 54,55183
7,431293 54,56385
7,439631 54,55846
7,44797 54,55909
7,456363 54,57729
7,464568 54,51057
7,472927 54,50765
7,481307 54,50765
7,489828 54,51309
7,497977 54,25367
7,506427 54,21312
7,514846 54,16301
7,523158 54,18569
7,531417 54,1778
7,539884 54,1778
7,548041 54,15869
7,55654 54,17311
7,564906 54,16421
7,573894 54,12428
7,581313 54,09875
7,589789 54,06138
7,598189 54,06138
7,606637 54,09892
7,614589 54,16023
7,623956 54,19504
7,631513 54,18362
7,639794 54,13352
7,647862 54,14106
7,656284 54,14106
7,664784 54,1474
7,673017 54,13281
7,681275 54,07421
7,689584 54,07491
7,697953 54,11134
7,706346 54,14862
7,714718 54,19504
7,723058 54,19504
7,731969 53,95537
7,739965 53,93524
7,748258 53,93685
7,756406 53,93768
7,764638 53,90782
7,77111 53,91445
7,781423 53,90578
7,789653 53,87843
7,797856 53,87843
7,806359 53,86654
7,814862 53,85886
7,823091 53,84138
7,831296 53,80507
7,839662 53,93548
7,847999 53,93548
7,85642 53,94249
7,864705 53,91215
7,873771 53,88421
7,881166 53,88813
7,889722 53,91372
7,898198 53,85328
7,906499 53,84718
7,914605 53,84718
7,923997 53,90523
7,93139 53,91455
7,939755 53,83839
7,947934 53,76753
7,956326 53,72943
7,964679 53,71107
7,973173 53,71107
7,981317 53,70601
7,989788 53,7054
7,998168 53,68921
8,006577 53,70426
8,014726 53,83764
8,023051 53,6864
8,031297 53,66175
8,039884 53,64183
8,048084 53,64183
8,056259 53,6778
8,064705 53,71864
8,073261 53,72963
8,081467 53,70763
8,089842 53,67144
8,098239 53,63792
8,106239 53,63792
8,114632 53,67882
8,123135 53,63179
8,131092 53,64926
8,139622 53,67959

8,148205	53,71256
8,156437	53,68991
8,164639	53,60854
8,172977	53,53386
8,181454	53,53095
8,189846	53,52144
8,198158	53,53113
8,20628	53,51299
8,214725	53,51226
8,223282	53,50587
8,231541	53,5176
8,239689	53,49647
8,248028	53,4856
8,256477	53,44426
8,264816	53,41798
8,273018	53,4511
8,281223	53,51489
8,289589	53,53135
8,298225	53,54101
8,306511	53,53374
8,314579	53,48811
8,322918	53,48838
8,331421	53,49637
8,339787	53,47874
8,347988	53,43628
8,356136	53,4454
8,364613	53,47316
8,373142	53,49772
8,381481	53,47653
8,389576	53,38481
8,398079	53,3523
8,406578	53,33788
8,415028	53,33897
8,423012	53,33803
8,431271	53,31401
8,43969	53,31541
8,448166	53,32113
8,456477	53,3247
8,464488	53,3101
8,472991	53,29514
8,481521	53,23328
8,489913	53,21201
8,498008	53,28674
8,50624	53,32107
8,514686	53,35387
8,523108	53,36187
8,531447	53,31628
8,539458	53,31054
8,547935	53,32749
8,556491	53,33774
8,564857	53,30979
8,572871	53,27208
8,58137	53,28994
8,589683	53,30255
8,598022	53,33104
8,606387	53,27249
8,614593	53,18896
8,623122	53,15406
8,631595	53,15115
8,639907	53,17919
8,648028	53,13831
8,656478	53,11529
8,664817	53,11158
8,673156	53,11525
8,681415	53,12172
8,689479	53,09305
8,697928	53,07307
8,706458	53,04561
8,714744	53,0445
8,722865	53,11227
8,731395	53,14725
8,739867	53,16919
8,748015	53,14312
8,756248	53,11813
8,764533	53,11929
8,772899	53,13421
8,781428	53,13092
8,789794	53,07578
8,797751	53,06632
8,806361	53,06845
8,814837	53,14201
8,823123	53,13747
8,831351	53,07255
8,839637	52,97099
8,848166	52,97181
8,856586	52,96796
8,864871	52,9934
8,872969	52,9341
8,881388	52,93918
8,889997	52,94114
8,898283	52,9621
8,906324	52,94358
8,914663	52,93826
8,923109	52,88702
8,931368	52,85749
8,93976	52,87506
8,947855	52,91955
8,956305	52,99186
8,964941	53,02336
8,973116	52,97274
8,981237	52,9574
8,989603	52,9565
8,997999	52,97617
9,006445	52,95385
9,014593	52,95984
9,022772	52,91861
9,031328	52,94039
9,039747	52,98021
9,048113	52,94805
9,056261	52,86892
9,064764	52,7984
9,073214	52,78526
9,081606	52,79482
9,089727	52,78164
9,097956	52,76126
9,106432	52,76845
9,114851	52,76619
9,123163	52,76057
9,131178	52,74096
9,139708	52,71527
9,148211	52,69769
9,156492	52,66572
9,164671	52,68775
9,172899	52,77655
9,181292	52,82342
9,189795	52,82105
9,198107	52,78674
9,206121	52,77057
9,214651	52,7679
9,22315	52,81481
9,231516	52,77821
9,239611	52,72426
9,247869	52,7434
9,256235	52,76553
9,264685	52,81176
9,273157	52,7688
9,281309	52,65985
9,289755	52,62471
9,298391	52,64287
9,30665	52,62555
9,314692	52,63923
9,323057	52,62577
9,33145	52,59264
9,339815	52,61628
9,348127	52,64538
9,356115	52,61084
9,364588	52,59853
9,373228	52,56292
9,381567	52,55725
9,389605	52,61596
9,398027	52,66338
9,406393	52,6632
9,414785	52,6479
9,422964	52,62732
9,431166	52,63646
9,439531	52,65005
9,448034	52,64497
9,456617	52,63705
9,464575	52,60506
9,472971	52,65196
9,481527	52,69783
9,489702	52,71807
9,498014	52,63866
9,5063	52,53328
9,514746	52,49205
9,523195	52,51111
9,531561	52,50766
9,539629	52,53035
9,548075	52,51212
9,556578	52,50128
9,564863	52,51929
9,572985	52,51405
9,581266	52,48042
9,589743	52,4526
9,598162	52,42759
9,606447	52,43301
9,614569	52,51616
9,622992	52,54726
9,631521	52,58538
9,63975	52,56036
9,647924	52,51893
9,656183	52,52201
9,664602	52,53928
9,673025	52,51443
9,681391	52,48465
9,689459	52,46836
9,697931	52,47817
9,706461	52,55751
9,714773	52,56121
9,722975	52,44277
9,731424	52,38791
9,739843	52,35675
9,748266	52,34906
9,756521	52,3679
9,764563	52,33439
9,773039	52,33403
9,781622	52,3264
9,789934	52,34518
9,797972	52,31673
9,806341	52,30623
9,814814	52,28024
9,823099	52,22927
9,831465	52,27573
9,839613	52,35512
9,847925	52,38578
9,856535	52,41413
9,864767	52,36285
9,872889	52,30663
9,881308	52,32797
9,889837	52,36398
9,898016	52,31463
9,906298	52,28593
9,914503	52,30419
9,922976	52,34197
9,931398	52,40044
9,939791	52,33134
9,947939	52,26067
9,956415	52,19866
9,964998	52,17927
9,97331	52,18484
9,981459	52,20262
9,989771	52,17612
9,998137	52,16765
10,00007	52,0407
10,00018	51,52336
10,00018	51,31706
10,00018	51,27654

Specimen 2 Strain mm	Specimen 23 Standard force N
0	1,098674
-2,7E-05	1,105494
-5,4E-05	1,105441
-8,1E-05	1,105458
2,7E-05	1,105441
5,43E-05	1,134851
0,001303	1,319451
0,003233	1,609805
0,005894	1,96433
0,009506	2,413572
0,013906	2,958715
0,019139	3,599284
0,024433	4,153381
0,031967	4,787572
0,039955	5,491674
0,048241	6,15769
0,056309	6,795141
0,06419	7,449926
0,075013	8,240334
0,081446	8,92634
0,089896	9,636544
0,097866	9,450658
0,106258	9,914037
0,114841	10,27781
0,123211	10,55613
0,131248	10,87541
0,139645	11,03004
0,147796	11,20573
0,156349	11,39173
0,164795	11,56186
0,173863	11,80143
0,181446	11,88183
0,190058	12,13416
0,198287	12,36903
0,206435	12,54564
0,21472	12,95618
0,223113	13,28321
0,231509	13,60572
0,239794	13,93604
0,247822	14,20704
0,256255	14,4126
0,264468	14,63766
0,271004	14,83765
0,281325	15,23902
0,289744	15,63563
0,298083	15,99183
0,306449	16,32764
0,314654	16,57252
0,321979	16,8511
0,331931	17,24763
0,339835	17,6762
0,3448063	17,865
0,3542955	18,17811
0,3646888	18,53087
0,373217	18,80784
0,38153	19,29091
0,389704	19,55103
0,398153	19,82162
0,406493	20,18362
0,414992	20,53053
0,423304	20,89405
0,431266	21,23145
0,439738	21,60206
0,448268	21,96314
0,456469	22,30144
0,464675	22,65145
0,473014	22,93372
0,481433	23,24398
0,489745	23,54945
0,498084	23,90577
0,506205	24,27686
0,514599	24,61124
0,523291	24,98231
0,53155	25,27833
0,539565	25,55006
0,54793	25,9148
0,556376	26,23462
0,564688	26,49085
0,573107	26,85914
0,581122	27,20953
0,589652	27,54339
0,598071	27,8165
0,606602	27,93734
0,616613	28,11478
0,623116	28,3483
0,631845	28,59417
0,640196	28,89847
0,649104	29,09232
0,656311	29,35147
0,664677	29,6005
0,673149	29,86637
0,681461	30,14798
0,68961	30,3732
0,698056	30,59195
0,706499	30,8407
0,714844	31,00296
0,722996	31,29129
0,731197	31,57354
0,739647	31,83683
0,748203	32,05344
0,756378	32,2529
0,764819	32,4966
0,77376	32,66019
0,781532	32,84464
0,789787	33,03509
0,797882	33,2565
0,806248	33,49856
0,814724	33,71357
0,823107	33,93004
0,831402	34,14368
0,83955	34,23415
0,84816	34,37844
0,854743	34,52913
0,864968	34,6747
0,873097	34,80068
0,881284	34,93478
0,889494	35,10478
0,89814	35,20367
0,906479	35,41888
0,91452	35,57599
0,922997	35,6888
0,931633	35,82149
0,939865	35,94965
0,948013	36,13416
0,956599	36,24001
0,964718	36,40047
0,97311	36,5752
0,981369	36,6668
0,989491	36,7535
0,997936	36,89717
1,006439	37,04027
1,014783	37,16284
1,023901	37,29047
1,031347	37,34565
1,039823	37,46967
1,048189	37,6095
1,056394	37,6
1,064676	37,64111
1,073107	37,76522
1,081403	37,79432
1,089941	37,90436
1,098115	37,97197
1,106481	38,05497
1,1149	38,1322
1,123186	38,23605
1,131361	38,3031
1,139593	38,3564
1,147958	38,42149
1,156284	38,49167
1,164773	38,53867
1,172868	38,63337
1,181261	38,7516
1,18987	38,88871
1,198209	38,90377
1,206251	38,93384
1,214669	39,00167
1,223065	39,07354
1,231378	39,14401
1,239744	39,12976
1,247838	39,18775
1,256204	39,2426
1,264921	39,26748
1,273103	39,3154
1,281533	39,31354
1,289724	39,3089
1,29817	39,33317
1,306509	39,37217
1,314821	39,38968
1,322942	39,39062
1,331361	39,41488
1,339891	39,44159
1,348284	39,46255
1,356298	39,47913
1,364748	39,48976
1,373193	39,45945
1,381452	39,43063
1,389738	39,47741
1,397886	39,50444
1,406284	39,52006
1,414915	39,60574
1,4232	39,53908
1,431268	39,52296
1,439688	39,54033
1,448111	39,53649
1,456366	39,53496
1,464884	39,54757
1,47188	39,46705
1,481223	39,46189
1,489913	39,50164
1,498145	39,49644
1,50624	39,53331
1,514823	39,27512
1,523107	39,28393
1,531407	39,28353
1,539702	39,35926
1,548014	39,08534
1,556433	39,04096
1,564883	39,03107
1,573169	39,00939
1,581296	38,91514
1,589756	38,85714
1,598151	38,77403
1,606551	38,79408
1,614699	38,83137
1,623038	38,83979
1,631297	38,8259
1,6398	38,79178
1,648053	38,72388
1,656452	38,68014
1,664542	38,61814
1,673156	38,66659
1,681548	38,59026
1,689563	38,514
1,697901	38,53207
1,706427	38,53377
1,714825	38,47153
1,723025	38,41158
1,731284	38,82969
1,739787	38,2459
1,748259	38,21108
1,756572	38,20802
1,76472	38,22371
1,773107	38,23984
1,781508	38,25894
1,789874	38,00075
1,798022	37,97462
1,806227	37,91498
1,81462	37,89431
1,823066	37,81189
1,831542	37,80271
1,839887	37,80113
1,848025	37,82388
1,856615	37,84087
1,864897	37,77742
1,873938	37,71843
1,881224	37,67616
1,889643	37,67265
1,898092	37,61671
1,906457	37,58265
1,914499	37,52115
1,922972	37,53111
1,931528	37,53125
1,93992	37,51609
1,947988	37,3816
1,956411	37,2725
1,964893	37,2725
1,973196	37,19185
1,981568	37,12312
1,989603	37,06057
1,998106	37,04184
2,006552	36,98746
2,015001	36,96174
2,023403	36,91107
2,031931	36,85934
2,039774	36,78808
2,048059	36,70962
2,056368	36,70927
2,064489	36,72368
2,073046	36,72874
2,081284	36,69163
2,089781	36,61364
2,097929	36,53204
2,106295	36,49131
2,11466	36,4826
2,123083	36,41956
2,131365	36,36108
2,139517	36,29832
2,147989	36,23309
2,156458	36,18168
2,164858	36,13818
2,172979	35,97147
2,181536	35,83887
2,190012	35,74613
2,198187	35,6533
2,206392	35,52229
2,214907	35,41888
2,23307	35,29166
2,231569	35,19542
2,239882	35,04121
2,247843	34,8927
2,256399	34,75163
2,264925	34,59403
2,273284	34,44669
2,28136	34,34669
2,289646	34,2677
2,298012	34,16339
2,306457	34,03491
2,314743	33,81387
2,322838	33,57801
2,331284	33,41888
2,33987	33,23437
2,348236	32,85535
2,35622	32,60034
2,364443	32,43195
2,373035	32,25982
2,381454	32,07312
2,389824	31,75439
2,397945	31,57622
2,406374	31,39161
2,414974	30,67993
2,423366	30,40137
2,431454	30,03869
2,439747	29,70715
2,448112	29,40015
2,456508	29,07996
2,464911	28,74151
2,473351	28,43811
2,481308	28,33196
2,489864	27,81368
2,49823	27,50513
2,506271	27,20394
2,51469	27,03979
2,523107	26,8125
2,531505	26,41349
2,539707	26,11877
2,547882	25,89404
2,556247	25,68134
2,564697	25,47329
2,573116	25,17432
2,581403	24,89047
2,589607	24,69047
2,598217	24,67081
2,606445	24,33427
2,614731	24,01577
2,623063	24,10069
2,631382	23,92099
2,639911	23,80194
2,64825	23,65125
2,656345	23,49078
2,664774	23,34996
2,673204	23,15995
2,681633	23,04773
2,689647	22,87124
2,698042	22,71707
2,70635	22,56122
2,7148	22,28256
2,723177	21,9824
2,731107	21,96043
2,739652	21,81411
2,748319	21,67431
2,756468	21,46087
2,764642	21,30615
2,772928	21,1394
2,78132	21,01686
2,789653	20,84405
2,797998	20,69403
2,80612	20,60246
2,814623	20,45634
2,823179	20,33357
2,831465	20,19868
2,839613	20,05959
2,848142	19,81789
2,856451	19,68403
2,864931	19,62141
2,873079	19,51235
2,881281	19,47874
2,89073	19,39341
2,898287	19,3143
2,906568	19,26357
2,914889	19,20151
2,923033	19,02531
2,931505	18,89026
2,939817	18,79346
2,948049	18,77443
2,956304	18,79088
2,9647	18,76278
2,973107	18,74107
2,981458	18,59391
2,989527	18,52171
2,997972	18,49784
3,006449	18,44084
3,014868	18,37406
3,022962	18,31347
3,031421	18,2764
3,039868	18,25594
3,048316	18,25748
3,056455	18,15312
3,064604	18,02734
3,073053	17,93017
3,08169	17,86798
3,089918	17,80543
3,098097	17,70356
3,106394	17,63447
3,114851	17,51407
3,123114	17,43148
3,13148	17,358
3,139548	17,2443
3,147887	17,15941
3,156443	17,01388
3,164774	16,90849
3,17301	16,88449
3,181242	16,79451
3,189799	16,62673
3,198111	16,20974
3,206286	15,7709
3,214461	15,613
3,22277	15,5487
3,231467	15,4987
3,239832	15,36156
3,247874	15,25208
3,256293	15,18455
3,264742	15,11823
3,273133	15,03581
3,281599	14,96243
3,289739	14,54147
3,298071	14,4273
3,306628	14,28962
3,314993	14,18803
3,323378	13,9968
3,331481	13,82792
3,339873	13,618
3,348212	13,54419
3,356599	13,43078
3,364419	13,29191
3,373038	13,05433
3,381514	12,72401
3,3898	12,60542
3,397974	12,50751
3,40634	12,54532
3,414757	12,49886
3,423155	12,33426
3,43133	12,28385
3,439642	12,18611
3,447981	12,11725
3,456347	12,0506
3,464823	11,99359
3,473264	11,9377
3,481337	11,87487
3,48992	11,86602
3,498206	11,78698
3,506381	11,53737
3,514719	11,44993
3,523142	11,38246
3,531554	11,32977
3,539821	11,27187
3,547969	11,21375
3,556415	11,16011
3,564971	11,097
3,57323	11,08443
3,581298	11,04248
3,589851	10,98789
3,598091	10,94772
3,606479	10,90255
3,614734	10,9452
3,62294	11,01324
3,631152	11,03568
3,639915	11,04835
3,648201	10,97137
3,656242	10,93375
3,664599	10,90172
3,67308	10,90572
3,681503	10,85841
3,689598	10,80851
3,697826	10,74851
3,706275	10,76174
3,714748	10,79322
3,723139	10,59531
3,731239	10,59531
3,739849	10,55857
3,748352	10,50191
3,75666	10,48632
3,764728	10,44938
3,77304	10,375
3,781429	10,32188
3,78635	10,32188
3,786434	10,15783
3,78638	10,15606
3,786325	10,07948
3,786325	10,02182
3,786352	10,01834
3,786325	9,983769
3,786353	9,983769
3,786325	9,963741
3,786325	9,939767
3,786325	9,938168
3,786325	9,941268
3,786353	9,918395
3,786353	9,896302
3,786353	9,873844
3,786325	9,893126
3,786325	9,895126
3,786325	9,893708

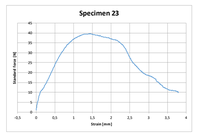

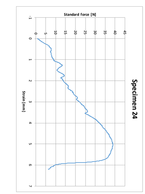
Standard Time (ft)
Specimen #4
Load (lbf)

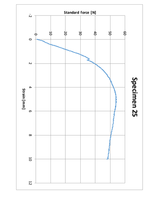
Standard Time (S)
Specimen 23
Load (kN)

4,02294	52,323597
4,031322	52,319413
4,039808	52,31629
4,04812	52,309827
4,056189	52,48914
4,064634	52,57938
4,073244	52,61483
4,080624	52,629867
4,089624	52,62967
4,09791	52,64869
4,106329	52,73356
4,114725	52,7584
4,123091	52,72355
4,131268	52,76934
4,139553	52,80964
4,148153	52,89663
4,156473	52,88954
4,164621	52,83379
4,173151	52,81399
4,181627	52,82864
4,189854	52,85447
4,198188	52,88751
4,206739	52,90177
4,214739	52,96177
4,223319	52,99451
4,231651	53,0021
4,239593	53,0329
4,248038	53,06791
4,256115	53,06506
4,264743	53,09943
4,272884	53,13662
4,281214	53,17178
4,28968	53,24284
4,298263	53,27412
4,306468	53,2576
4,314506	53,29152
4,322982	53,31182
4,331284	53,32996
4,339904	53,32296
4,347919	53,30685
4,356257	53,34861
4,364757	53,39894
4,373099	53,47169
4,381465	53,43692
4,389884	53,44107
4,39817	53,50194
4,406642	53,50541
4,415011	53,49935
4,423106	53,4096
4,431388	53,41708
4,439727	53,42447
4,448153	53,4369
4,456113	53,51588
4,464557	53,48941
4,473029	53,50897
4,481586	53,47979
4,489818	53,46898
4,498046	53,56426
4,506385	53,63417
4,51475	53,70714
4,523171	53,68762
4,531375	53,68762
4,539416	53,67693
4,547999	53,70622
4,556556	53,73309
4,564841	53,74175
4,572909	53,72905
4,581284	53,73114
4,589805	53,81281
4,598117	53,88973
4,606509	53,83179
4,614657	53,75222
4,623134	53,75414
4,631633	53,77582
4,639984	53,78107
4,648043	53,78505
4,656488	53,78536
4,664938	53,83621
4,67322	53,83178
4,681372	53,85532
4,689547	53,82671
4,697888	53,80189
4,706442	53,80169
4,714808	53,84704
4,723982	53,93006
4,731432	53,99004
4,739988	54,01247
4,748217	53,98934
4,756369	54,00568
4,764911	54,0209
4,773969	54,0308
4,781412	54,04806
4,789831	54,00357
4,797846	54,01464
4,806318	54,02769
4,814959	54,07751
4,823187	54,10991
4,831662	54,12707
4,839785	53,96138
4,84823	53,97381
4,856627	53,9896
4,864882	53,97286
4,873976	53,96753
4,881372	53,98415
4,889866	53,96008
4,898321	53,99607
4,906305	53,98399
4,914644	54,00113
4,923227	53,97653
4,931433	53,93102
4,939772	53,96935
4,948284	54,00179
4,956398	54,06123
4,964815	54,0914
4,973181	54,07011
4,981249	54,06211
4,989668	54,08239
4,998091	54,08413
5,006469	54,09107
5,014742	54,01097
5,023297	54,05796
5,031336	54,04872
5,039812	54,14184
5,048231	54,21022
5,056325	54,22036
5,064828	53,98699
5,073358	53,97148
5,081446	53,9707
5,089818	54,02151
5,098077	53,99443
5,106496	53,98666
5,114889	53,98336
5,123174	54,01267
5,131242	53,97741
5,139699	53,97989
5,148202	53,93089
5,15653	53,92889
5,164762	53,99974
5,17299	54,04126
5,181329	54,04862
5,189859	54,08941
5,198284	54,09106
5,206513	54,01696
5,214551	54,04779
5,223161	54,07966
5,2315	54,0867
5,239595	54,03705
5,248044	54,04164
5,256357	54,09317
5,264722	54,13925
5,273195	54,05255
5,281693	53,96966
5,289703	53,97511
5,298402	53,95226
5,306715	53,93536
5,314703	53,9418
5,323148	53,95633
5,331487	53,93665
5,339884	53,94122
5,348138	53,96122
5,356206	53,93101
5,364599	53,93109
5,373182	53,88111
5,381494	53,88408
5,389589	53,89801
5,398011	53,93944
5,406511	53,97749
5,414823	53,94117
5,423028	53,93106
5,431283	53,92786
5,439543	53,93439
5,448045	53,93166
5,456491	53,90155
5,464559	53,89169
5,473008	53,90177
5,481592	53,85763
5,48982	53,95173
5,498025	53,86342
5,506364	53,8171
5,514894	53,77813
5,523186	53,7858
5,531552	53,76954
5,539636	53,73934
5,548032	53,74214
5,556442	53,71989
5,564844	53,72946
5,573049	53,72667
5,581335	53,68958
5,589824	53,64169
5,59823	53,61433
5,606405	53,65577
5,614526	53,70958
5,623056	53,73322
5,631528	53,78461
5,639843	53,73
5,648284	53,69554
5,656501	53,7123
5,664724	53,7324
5,67309	53,69466
5,681428	53,63191
5,689523	53,64736
5,698053	53,63917
5,706472	53,6946
5,714864	53,66139
5,723059	53,63499
5,731488	53,51493
5,739965	53,49118
5,748304	53,53169
5,756452	53,48864
5,764654	53,49339
5,773077	53,46454
5,781469	53,44697
5,789892	53,46087
5,797876	53,43775
5,806379	53,41195
5,814878	53,38402
5,823221	53,33351
5,831369	53,3776
5,839884	53,41127
5,84802	53,45022
5,85663	53,4667
5,864805	53,41971
5,873873	53,36937
5,881319	53,37534
5,889878	53,31627
5,898284	53,28987
5,906216	53,28987
5,914568	53,25328
5,923987	53,28223
5,93141	53,30952
5,939803	53,25397
5,947951	53,24331
5,956144	53,21967
5,964564	53,21916
5,973296	53,23916
5,98139	53,22355
5,989729	53,07779
5,998095	53,06594
6,006514	53,06644
6,014773	53,05162
6,023068	53,03859
6,031468	53,02009
6,039937	52,97147
6,048235	52,92997
6,056277	52,88365
6,064669	53,02156
6,073145	53,03336
6,081458	53,00159
6,089838	52,99438
6,097838	52,99438
6,10651	52,9611
6,114893	52,97135
6,123206	52,94195
6,131274	52,92627
6,13975	52,94299
6,148183	52,93187
6,156481	53,02187
6,16474	52,91102
6,173022	52,81667
6,181525	52,78791
6,190001	52,7873
6,198313	52,80085
6,206884	52,77492
6,215403	52,75937
6,223503	52,74727
6,231662	52,77401
6,239653	52,73688
6,247965	52,7283
6,256468	52,70927
6,264807	52,66526
6,273173	52,6897
6,281599	52,71284
6,289744	52,82606
6,298216	52,82343
6,306476	52,79058
6,314651	52,78335
6,323063	52,76828
6,331175	52,78262
6,339599	52,77447
6,348007	52,75041
6,356212	52,71859
6,364604	52,75587
6,373214	52,7835
6,38158	52,79507
6,389648	52,70311
6,398107	52,66993
6,40657	52,59591
6,414962	52,60122
6,423168	52,60619
6,431289	52,59319
6,439765	52,59254
6,448322	52,56156
6,456469	52,54468
6,464665	52,54468
6,473064	52,54317
6,481514	52,5211
6,489879	52,48925
6,498027	52,53377
6,50634	52,57758
6,514652	52,62141
6,523358	52,63345
6,531911	52,62141
6,539535	52,5494
6,547927	52,56563
6,55651	52,58312
6,564823	52,5611
6,573517	52,50146
6,581146	52,48373
6,589658	52,46098
6,598068	52,56098
6,606517	52,51997
6,614692	52,42874
6,623168	52,37526
6,631725	52,35403
6,639873	52,38015
6,648284	52,36966
6,656533	52,33741
6,664752	52,33317
6,673122	52,35112
6,681541	52,33926
6,689525	52,3379
6,698028	52,29932
6,706437	52,29932
6,714933	52,25919
6,723992	52,3188
6,731305	52,27172
6,739808	52,39944
6,748147	52,37936
6,756348	52,34892
6,764523	52,34317
6,773519	52,34426
6,781582	52,34685
6,789989	52,32966
6,79788	52,27727
6,806382	52,31387
6,814774	52,3326
6,823143	52,36398
6,831318	52,28705
6,839631	52,35238
6,847988	52,33967
6,856659	52,31867
6,864945	52,18721
6,873986	52,19817
6,881543	52,16556
6,889828	52,14308
6,898247	52,53058
6,906395	52,17989
6,914928	52,1193
6,923399	52,12599
6,931439	52,07959
6,939835	52,0677
6,947983	52,13438
6,956429	52,18218
6,964852	52,19562
6,973191	52,53643
6,981599	52,54468
6,989541	52,14029
6,997937	52,1381
7,006493	52,2121
7,014748	52,07733
7,02287	52,06561
7,031346	52,0848
7,039695	52,0848
7,048295	52,11355
7,056363	52,03593
7,064675	51,96706
7,073178	51,94917
7,081507	51,94524
7,089909	51,96587
7,098324	51,97731
7,106423	51,93731
7,115006	51,91934
7,123318	51,93023
7,131333	51,91666
7,139808	51,88397
7,14812	51,83819
7,156776	51,79557
7,165192	51,8059
7,17292	51,85554
7,181339	51,89668
7,189922	51,92307
7,198207	51,89856
7,206249	51,87828
7,214694	51,87398
7,223367	51,86952
7,231504	51,85112
7,239685	51,81114
7,247943	51,81612
7,256202	51,8411
7,264812	51,89583
7,273231	51,85868
7,281272	51,75745
7,289668	51,69424
7,298358	51,69424
7,30664	51,79606
7,314708	51,79517
7,32294	51,66479
7,331413	51,6615
7,339862	51,66063
7,348284	51,64744
7,356218	51,64744
7,364742	51,6214
7,373298	51,58935
7,381504	51,53059
7,389678	51,60167
7,397937	51,66237
7,406284	51,64988
7,414779	51,61406
7,423145	51,60064
7,43134	51,60916
7,439685	51,60925
7,448135	51,59454
7,456527	51,56668
7,464569	51,53788
7,472934	51,5332
7,481284	51,52614
7,489746	51,56115
7,498115	51,49808
7,506263	51,39356
7,514793	51,35432
7,523456	51,33489
7,531715	51,33745
7,540095	51,29098
7,548091	51,29098
7,556516	51,27573
7,564882	51,25313
7,573194	51,24086
7,581285	51,21371
7,589654	51,17038
7,598023	51,13399
7,606623	51,13399
7,614645	51,16995
7,623037	51,20824
7,631429	51,21179
7,639768	51,20891
7,648027	51,18171
7,656414	51,18412
7,664514	51,18412
7,673234	51,16512
7,681409	51,11301
7,689604	51,10587
7,69795	51,09689
7,706537	51,13012
7,715003	51,12743
7,723092	51,0771
7,731363	50,85945
7,739835	50,90666
7,748258	50,9151
7,756544	50,91363
7,764638	50,85925
7,773138	50,88326
7,781667	50,86119
7,790021	50,86119
7,798021	50,86963
7,806333	50,83024
7,814779	50,83111
7,823038	50,73519
7,831514	50,79369
7,839978	50,84215
7,848337	50,86129
7,856657	50,86129
7,864896	50,83084
7,873934	50,80662
7,881303	50,79432
7,889669	50,81376
7,898115	50,79381
7,906484	50,77115
7,914495	50,79715
7,923025	50,72123
7,931328	50,79803
7,93992	50,76793
7,948015	50,83385
7,956518	50,50447
7,964988	50,53408
7,97379	50,54408
7,98145	50,51323
7,989545	50,49309
7,998101	50,48088
8,006551	50,47213
8,01489	50,49464
8,023985	50,45812
8,03135	50,45629
8,039833	50,43365
8,048165	50,33365
8,05634	50,39763
8,064569	50,45867
8,073018	50,47178
8,081464	50,46994
8,089749	50,45025
8,098197	50,43153
8,10652	50,43153
8,114766	50,4039
8,123162	50,35868
8,131337	50,348
8,139552	50,33577

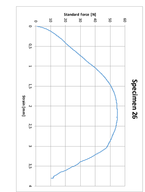
Standard Temp (°F)
Specimen 2d
Strain (mm)

Specimen :	Specimen 27
Strain	Standard force
mm	N
0	1,155015
-2,7E-05	1,150584
-8,1E-05	1,148697
-0,00011	1,162441
-0,00011	1,15356
-8,1E-05	1,180595
0,000842	1,402885
0,002688	1,997856
0,005188	2,802543
0,008556	3,733696
0,012438	4,749809
0,017219	5,799126
0,022299	6,849604
0,02822	7,907221
0,035609	8,993647
0,043757	9,849604
0,052069	10,4934
0,060137	10,92211
0,068614	11,34252
0,077166	11,76293
0,085398	12,07873
0,09363	12,21722
0,101832	12,27982
0,110224	12,41641
0,11862	12,60098
0,127013	12,92325
0,135134	13,43326
0,14358	14,08658
0,15222	14,81119
0,160502	15,49991
0,168597	16,15909
0,176993	16,89395
0,185439	17,61002
0,193831	18,44742
0,202063	19,21793
0,210211	19,91178
0,218661	20,70279
0,227244	21,42252
0,235583	22,19449
0,243624	22,88761
0,251963	23,6005
0,260409	24,34171
0,268801	25,03116
0,27698	25,76749
0,285155	26,58927
0,293631	27,3671
0,302188	28,09464
0,310389	28,77188
0,318537	29,42789
0,32685	30,12955
0,335353	30,90347
0,343798	31,57315
0,35195	32,20694
0,360179	32,89542
0,368598	33,57999
0,376994	34,29972
0,385493	34,94107
0,393534	35,43888
0,402011	36,05729
0,410674	36,6669
0,418906	37,26432
0,427001	37,77091
0,435284	38,37125
0,443733	38,93619
0,452099	39,49601
0,460464	40,03946
0,468532	40,4921
0,477005	41,02506
0,485481	41,49137
0,493931	41,93424
0,501915	42,4816
0,5102	43,04142
0,518593	43,52262
0,527069	43,90519
0,535381	44,28299
0,543446	44,6464
0,551895	45,05777
0,560398	45,4733
0,568897	45,74662
0,576912	46,02225
0,585304	46,40189
0,59367	46,77933
0,601982	47,11869
0,610458	47,35294
0,618607	47,52054
0,626999	47,75992
0,635612	47,98178
0,643951	48,23069
0,651962	48,40073
0,660385	48,6251
0,668858	48,80631
0,67717	48,98252
0,685375	49,13584
0,69347	49,23401
0,701942	49,35099
0,710472	49,4274
0,718864	49,50984
0,726826	49,6125
0,735355	49,71324
0,743774	49,78926
0,752113	49,75142
0,760315	49,70328
0,768574	49,72774
0,776833	49,74742
0,785305	49,76996
0,793781	49,75657
0,801823	49,71661
0,810379	49,80398
0,818825	49,86696
0,827137	49,85192
0,835232	49,7675
0,843651	49,7087
0,852126	49,71334
0,860522	49,717
0,868804	49,70675
0,876845	49,68764
0,885348	49,73385
0,893905	49,72568
0,902217	49,75233
0,910281	49,72949
0,91862	49,72836
0,92699	49,71629
0,935329	49,65878
0,943721	49,66653
0,951896	49,7155
0,960319	49,74142
0,968844	49,74287
0,97713	49,67187
0,985225	49,6072
0,993537	49,57401
1,001987	49,56175
1,010432	49,45686
1,018607	49,3575
1,026729	49,27318
1,035258	49,25278
1,043761	49,2203
1,052127	49,08463
1,060248	48,9058
1,068698	48,8184
1,077281	48,75091
1,085593	48,69106
1,093688	48,61529
1,101974	48,547
1,110366	48,49357
1,118785	48,44829
1,127208	48,40118
1,135303	48,28567
1,143668	48,25393
1,152198	48,16658
1,160453	48,05253
1,168658	48,02501
1,17686	48,02207
1,185363	47,94631
1,193809	47,86669
1,202067	47,72326
1,210082	47,59722
1,218608	47,52517
1,227111	47,48993
1,235476	47,35482
1,243491	47,20684
1,251967	47,16353
1,260249	47,08812
1,268619	47,07028
1,277038	46,88846
1,285186	46,70206
1,293689	46,60785
1,302299	46,53186
1,310557	46,43733
1,318706	46,30458
1,327018	46,24037
1,335437	46,16139
1,343802	46,05074
1,352115	45,94563
1,360076	45,82362
1,368632	45,73064
1,377242	45,60747
1,385444	45,47841
1,393622	45,38785
1,401988	45,31314
1,410434	45,25977
1,418693	45,08163
1,426951	44,91403
1,4351	44,74033
1,443492	44,64679
1,452022	44,54059
1,460441	44,35687
1,468535	44,10272
1,476901	43,95251
1,485541	43,84602
1,49377	43,64564
1,501918	43,34962
1,510287	43,00721
1,518786	42,63892
1,527183	42,26978
1,535491	41,82764
1,543616	41,48731
1,552035	41,04176
1,560538	40,57349
1,568904	40,07252
1,576972	39,60865
1,585254	39,20045
1,59365	38,71827
1,602096	38,13331
1,610381	37,62452
1,618449	37,19117
1,626979	36,72022
1,635535	36,2981
1,643737	35,75953
1,651938	35,31715
1,660171	34,92335
1,668563	34,46168
1,677093	33,90601
1,685241	33,34888
1,693471	32,78876
1,702027	32,17133
1,710503	31,60663
1,718762	31,06195
1,726884	30,45453
1,735413	29,89789
1,743859	29,39814
1,752118	28,91376
1,760484	28,40668
1,768578	27,83808
1,776971	27,28266
1,785474	26,69916
1,793839	26,12568
1,801854	25,54364
1,8103	25,03095
1,818803	24,40717
1,827115	23,74311
1,83537	23,21918
1,843438	22,74823
1,851941	22,29511
1,860524	21,76825
1,868756	21,32611
1,876794	20,9411
1,885216	20,61591
1,893853	20,35663
1,902085	20,00678
1,910233	19,6623
1,918572	19,42853
1,926858	19,19281
1,935303	19,01099
1,943726	18,60547
1,951874	18,07178
1,960431	17,68567
1,969041	17,4187
1,977273	17,14612
1,985364	16,8866
1,993676	16,66889
2,002072	16,45173
2,010411	16,18207
2,01875	15,87214
2,026761	15,59577
2,035264	15,43305
2,0439	15,24933
2,052239	15,06269
2,060227	15,00621
2,068619	14,97071
2,077149	14,85806
2,085351	14,7254
2,093636	14,51995
2,101731	14,30804
2,11018	14,20795
2,118736	14,10847
2,127129	13,97156
2,13517	13,8487
2,143642	13,79716
2,152035	13,6468
2,160267	13,36189
2,168659	13,2374
2,176891	13,09361
2,185368	12,98969
2,193897	12,91021
2,202206	12,89765
2,210274	12,79592
2,21867	12,7109
2,227169	12,65582
2,235508	12,62824
2,243687	12,59772
2,251862	12,55624
2,260307	12,52661
2,26873	12,47169
2,277096	12,46791
2,285271	12,53172
2,293636	12,55658
2,302113	12,57955
2,310425	12,55034
2,318626	12,52038
2,326832	12,51976
2,335224	12,53459
2,343674	12,51693
2,351982	12,47202
2,360134	12,44757
2,3685	12,43517
2,369533	12,26251
2,36956	12,14977
2,36956	12,09351
2,369506	12,02303
2,369506	11,98493
2,369452	11,92325
2,369452	11,8989
2,369452	11,88602
2,369452	11,8392
2,369452	11,80572
2,369479	11,80775
2,369479	11,77014
2,369479	11,75021
2,369479	11,75215
2,369479	11,74816

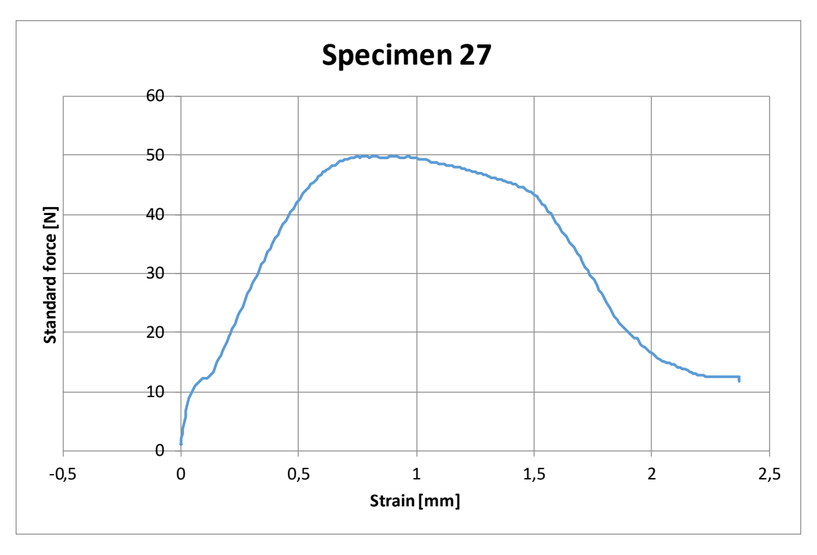

Specimen :	Specimen 28
Strain mm	Standard force N
0	0,850543
2,72E-05	0,886309
2,72E-05	0,901472
2,72E-05	0,920151
5,42E-05	0,928098
8,14E-05	0,938951
0,000679	1,077798
0,002308	1,560586
0,004779	2,421915
0,008012	3,380411
0,012113	4,489786
0,016486	5,540567
0,021375	6,613809
0,027108	7,666055
0,03436	8,469277
0,042562	8,603749
0,050847	8,680425
0,058942	8,849858
0,067144	9,090947
0,075593	9,306462
0,084039	9,581853
0,092378	10,01557
0,10053	10,5727
0,108896	11,14765
0,117479	11,78119
0,125764	12,39106
0,133859	12,97748
0,142251	13,63349
0,150644	14,26362
0,159009	14,78437
0,167321	15,14557
0,175496	15,58246
0,183999	16,15961
0,192582	16,72236
0,200921	17,30634
0,208989	17,83246
0,217302	18,51435
0,225694	19,0644
0,23406	19,62787
0,242345	20,22138
0,250413	20,81562
0,258943	21,39033
0,267473	22,00141
0,275811	22,63178
0,28388	23,28608
0,292325	23,97407
0,300718	24,60175
0,309057	25,15644
0,317262	25,68842
0,3254	26,32245
0,33386	26,98945
0,342386	27,54096
0,350698	28,08295
0,358819	28,59907
0,367296	29,19257
0,375744	29,7792
0,384056	30,32437
0,392258	30,7604
0,40057	31,22183
0,409046	31,66177
0,417492	32,1586
0,425858	32,57998
0,433873	32,98404
0,442345	33,3793
0,450821	33,78164
0,459187	34,18667
0,467282	34,58731
0,475567	34,93057
0,483933	35,25857
0,492325	35,49069
0,500664	35,79831
0,508843	36,14816
0,517315	36,46579
0,525872	36,7474
0,534157	36,93606
0,542198	37,05557
0,550484	37,22641
0,55893	37,36627
0,567295	37,38844
0,575661	37,32498
0,583702	37,04941
0,592232	36,58261
0,600762	35,87411
0,609074	35,07578
0,617249	34,3436
0,625698	34,0643
0,634198	33,70773
0,64243	33,36093
0,650742	33,1257
0,658837	32,98518
0,667282	32,90884
0,675839	32,77245
0,684124	32,67535
0,692246	32,55657
0,700665	32,48725
0,709061	32,39351
0,717373	32,22905
0,725548	32,20409
0,73375	32,20969
0,742279	32,1714
0,750809	32,06305
0,759011	31,87018
0,767136	31,6955
0,775582	31,58442
0,784085	31,41901
0,792396	31,1867
0,800598	30,9135
0,808857	30,76635
0,817196	30,58934
0,825725	30,4507
0,834038	30,13747
0,842133	29,83632
0,850716	29,61977
0,859325	29,37355
0,867584	29,12185
0,875648	28,81752
0,883881	28,57442
0,8923	28,35714
0,900749	28,09932
0,909115	27,86251
0,917156	27,58956
0,925739	27,39498
0,934132	27,13131
0,942524	26,84493
0,950592	26,63729
0,958904	26,47292
0,967327	26,31075
0,975666	26,00704
0,983974	25,7192
0,992126	25,4952
1,000492	25,28896
1,009048	25,08028
1,017467	24,80306
1,025616	24,54201
1,033928	24,36007
1,04232	24,15779
1,050743	23,93373
1,059002	23,61916
1,067284	23,37484
1,07568	23,23
1,084316	22,9894
1,092602	22,79079
1,100639	22,54866
1,109089	22,39321
1,117565	22,22158
1,125873	22,05056
1,134025	21,87996
1,1422	21,70601
1,150619	21,50588
1,159069	21,31948
1,167488	21,20902
1,175503	21,11794
1,183948	21,00751
1,192589	20,85577
1,200901	20,62726
1,208911	20,45237
1,21717	20,32325
1,225616	20,20774
1,234039	20,06346
1,242378	19,86466
1,250446	19,67753
1,258865	19,57325
1,267421	19,48011
1,275787	19,35429
1,283908	19,13334
1,292384	18,99058
1,300803	18,85227
1,309226	18,70689
1,317428	18,54771
1,325549	18,43052
1,333999	18,37743
1,342582	18,26177
1,350894	18,1677
1,358932	18,05411
1,367328	17,95587
1,37572	17,82818
1,384197	17,68939
1,392371	17,62099
1,40044	17,60646
1,408912	17,59446
1,417468	17,52354
1,425781	17,36162
1,433902	17,29381
1,442268	17,25547
1,450771	17,2017
1,459083	17,1405
1,467288	17,04043
1,47549	16,95649
1,483909	16,88904
1,492412	16,82369
1,500751	16,72606
1,508872	16,5443
1,517375	16,42383
1,525985	16,34165
1,534271	16,24346
1,542365	16,18189
1,550594	16,11617
1,55907	15,98998
1,567489	15,83288
1,575721	15,75413
1,583816	15,65101
1,592399	15,5215
1,600765	15,4091
1,609187	15,31975
1,617309	15,29482
1,625593	15,25229
1,633959	15,1924
1,642405	15,12974
1,650744	15,02372
1,658785	14,88749
1,667261	14,76707
1,675844	14,70442
1,684183	14,55064
1,692194	14,37822
1,700644	14,32285
1,709009	14,23666
1,717375	14,18196
1,725687	13,94893
1,733973	13,73329
1,742365	13,61512
1,750921	13,45131
1,759153	13,34691
1,767302	13,25578
1,775721	13,21075
1,78417	13,17335
1,792399	13,13306
1,800657	13,10587
1,80889	13,0557
1,817309	13,01705
1,825754	12,93184
1,834093	12,87786
1,842245	12,89287
1,850638	12,82857
1,859194	12,67439
1,867506	12,54073
1,875517	12,42159
1,883803	12,31325
1,889862	12,09537
1,890025	11,85404
1,890025	11,74661
1,890025	11,65581
1,889998	11,61173
1,889971	11,56969
1,889944	11,49608
1,889944	11,48081
1,889944	11,45773
1,889944	11,44037
1,889944	11,4267
1,889944	11,3896
1,889944	11,39235
1,889944	11,38869
1,889944	11,38302

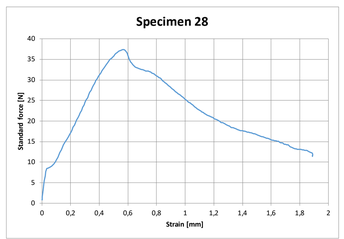

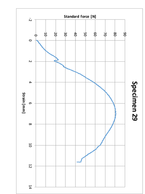
Standard Time (%)
Specimen #2
Load (lbs)

4,019709 58,77344
4,020048 58,84492
4,036604 58,94493
4,044806 59,03913
4,052954 59,93163
4,061457 59,49476
4,069983 59,66884
4,078484 59,83591
4,086339 59,98285
4,094651 60,99482
4,103936 60,15338
4,111435 60,29118
4,119721 60,35951
4,127896 60,46342
4,136209 60,57053
4,143609 60,71953
4,151241 60,88469
4,161335 60,90105
4,169781 60,98104
4,176504 61,08712
4,18617 61,18525
4,194879 61,36384
4,203422 61,5464
4,211927 61,70042
4,220089 61,66894
4,228375 61,80516
4,236435 61,9813
4,244725 62,01601
4,253117 62,13708
4,261456 62,22124
4,269884 62,34549
4,277574 62,54436
4,286339 62,70147
4,294949 62,82103
4,303208 62,90485
4,311329 63,01919
4,319615 63,13262
4,328004 63,29442
4,336483 63,39462
4,344658 63,45504
4,35286 63,57462
4,361363 63,75209
4,369839 63,94014
4,378232 64,02126
4,386554 64,09999
4,394829 64,14105
4,403328 64,18264
4,411698 64,34921
4,419735 64,47363
4,428074 64,57795
4,436497 64,66016
4,444778 64,76004
4,453128 64,9249
4,46127 64,98382
4,469796 65,0755
4,478245 65,16882
4,486611 65,24857
4,494705 65,4259
4,50299 65,59465
4,511413 65,74059
4,519658 65,85997
4,528118 65,93842
4,536155 66,00282
4,544658 66,13072
4,553241 66,28044
4,561607 66,35506
4,569622 66,39547
4,577966 66,50737
4,58641 66,67565
4,594829 66,83819
4,603141 66,89951
4,611236 66,9093
4,619792 66,97873
4,628349 67,10358
4,636824 67,23564
4,644783 67,27851
4,653228 67,40385
4,661567 67,49439
4,669853 67,61845
4,678112 67,71992
4,686206 67,79351
4,694554 67,90124
4,702233 67,94785
4,711601 68,05753
4,719615 68,22366
4,728145 68,37979
4,736537 68,50079
4,74485 68,55467
4,753082 68,67244
4,761558 68,7274
4,769899 68,83779
4,778125 68,93899
4,786598 69,01083
4,794559 69,0658
4,803115 69,21711
4,811588 69,35401
4,81982 69,45408
4,828236 69,54053
4,836644 69,69053
4,84489 69,76235
4,853256 69,83875
4,861541 69,75073
4,869689 69,81016
4,878086 69,92149
4,886498 70,00301
4,894697 70,11497
4,902992 70,18881
4,91133 70,25853
4,91978 70,32129
4,928199 70,39355
4,936511 70,53396
4,944958 70,66103
4,953082 70,78369
4,961412 70,88742
4,96984 70,95182
4,978045 71,01305
4,986354 71,14185
4,99475 71,21934
5,003218 71,29763
5,011391 71,35761
5,019749 71,45491
5,027968 71,51956
5,036525 71,69713
5,04481 71,77172
5,053012 71,73209
5,061435 71,78485
5,069991 71,85486
5,078405 71,94007
5,086505 72,05053
5,09468 72,06976
5,103156 72,23439
5,111632 72,26063
5,119971 72,30953
5,128609 72,41708
5,136944 72,5207
5,144961 72,53579
5,153163 72,60764
5,161448 72,71358
5,16965 72,8419
5,178073 72,95105
5,186572 73,06396
5,194888 73,16992
5,203052 73,24133
5,211318 73,23868
5,219922 73,34793
5,22824 73,38764
5,236335 73,4321
5,244514 73,52062
5,253097 73,62338
5,261462 73,73117
5,269908 73,73855
5,278284 73,77655
5,286426 73,77935
5,295142 73,85097
5,303374 73,92542
5,311469 74,00701
5,319835 74,0488
5,328149 74,03381
5,336497 74,12564
5,344853 74,2568
5,352891 74,30788
5,361421 74,37935
5,369924 74,41457
5,378236 74,47751
5,386357 74,60059
5,394683 74,69124
5,403162 74,78104
5,411454 74,82188
5,419774 74,87884
5,427972 74,94002
5,436257 75,02305
5,44484 75,10889
5,453258 75,13353
5,461328 75,17161
5,469496 75,24892
5,478233 75,34892
5,486451 75,40869
5,49471 75,2705
5,502969 75,34282
5,511498 75,39405
5,519998 75,48042
5,528284 75,57896
5,536405 75,57896
5,544827 75,64741
5,55333 75,72718
5,561666 75,78744
5,569707 75,87162
5,577993 75,86762
5,586284 75,94007
5,594668 76,0417
5,603227 76,06957
5,611375 76,16198
5,619767 76,27187
5,628297 76,3122
5,636502 76,39165
5,645004 76,45499
5,653704 76,46144
5,661382 76,54623
5,669831 76,63976
5,67806 76,63474
5,686234 76,67319
5,694684 76,75175
5,703321 76,81513
5,711579 76,89456
5,719988 76,97435
5,72812 76,8715
5,736569 76,87543
5,744935 76,94613
5,753166 77,00922
5,761287 77,04984
5,769763 77,09883
5,778104 77,16403
5,786632 77,19743
5,794696 77,24092
5,803092 77,28117
5,811649 77,30038
5,81985 77,30997
5,828136 77,40912
5,836477 77,50403
5,844707 77,58401
5,853233 77,66288
5,861518 77,69077
5,869613 77,70087
5,877979 77,78048
5,886562 77,85806
5,894888 77,90004
5,903023 77,80114
5,911254 77,91982
5,919673 78,01662
5,92807 78,11533
5,936489 78,13634
5,94469 78,26596
5,953166 78,29737
5,961696 78,3755
5,970004 78,42364
5,97833 78,51352
5,986415 78,23998
5,994806 78,27967
6,003173 78,3053
6,011566 78,36153
6,019527 78,39326
6,027994 78,40357
6,036693 78,43957
6,044895 78,43865
6,053989 78,50418
6,061386 78,64827
6,069778 78,72849
6,07817 78,7463
6,086624 78,77744
6,094604 78,79754
6,103023 78,84839
6,111153 78,90535
6,119949 78,93953
6,127986 78,94755
6,136436 78,97971
6,144859 79,01998
6,153114 79,1338
6,161399 79,23498
6,169737 79,35952
6,178213 79,55438
6,186686 79,59918
6,194998 79,74248
6,203423 79,8417
6,211458 79,91472
6,219824 79,2398
6,228273 79,25525
6,236448 79,30045
6,244654 79,30991
6,253073 79,3312
6,261629 79,27501
6,269804 79,35891
6,278255 79,4107
6,286451 79,57183
6,294905 79,61696
6,303186 79,63063
6,311365 79,62595
6,319651 79,64109
6,328043 79,70614
6,336499 79,74387
6,344748 79,74387
6,352869 79,72432
6,361272 79,78839
6,369928 79,8605
6,378294 79,88665
6,386469 79,83149
6,394883 79,83415
6,403284 79,83415
6,411623 79,87456
6,419962 79,88531
6,428003 79,89569
6,436422 79,93805
6,444952 79,95786
6,453299 79,95438
6,461339 79,95438
6,469725 79,98872
6,47809 79,99298
6,486456 79,99186
6,494848 80,06501
6,502916 80,13111
6,511366 80,20115
6,519976 80,24153
6,528284 80,27554
6,536299 80,2186
6,544668 80,23752
6,553114 80,29389
6,561426 80,28629
6,569712 80,29336
6,577987 80,29126
6,586284 80,40766
6,594784 80,40766
6,603203 80,40659
6,611324 80,33357
6,619881 80,33332
6,628384 80,32782
6,636696 80,34167
6,645139 80,37153
6,653019 80,37153
6,661469 80,37209
6,669861 80,38627
6,6782 80,42799
6,686295 80,43458
6,694744 80,41763
6,703191 80,39027
6,711555 80,39027
6,719704 80,48746
6,727989 80,54401
6,736439 80,59548
6,744778 80,59515
6,75309 80,56303
6,761265 80,56965
6,769657 80,56999
6,778214 80,62195
6,786693 80,58525
6,794701 80,58525
6,803013 80,60252
6,811489 80,65872
6,819775 80,67638
6,828056 80,65483
6,836315 80,56628
6,844696 80,56139
6,853403 80,56139
6,861687 80,56522
6,869781 80,54369
6,878094 80,53488
6,886486 80,54729
6,894932 80,57546
6,903137 80,54369
6,911512 80,57055
6,919836 80,57552
6,928288 80,54499
6,936573 80,53706
6,944641 80,5383
6,953171 80,67027
6,961536 80,71556
6,969849 80,701
6,978256 80,68369
6,986256 80,68369
6,994758 80,8974
7,003232 80,89492
7,011517 80,66882
7,019612 80,64732
7,028058 80,6663
7,036484 80,74403
7,044846 80,74403
7,053102 80,8646
7,061444 80,81133
7,069809 80,59004
7,078255 80,6125
7,086651 80,611
7,095098 80,56828
7,103138 80,58528
7,111748 80,56382
7,120007 80,56976
7,128102 80,53731
7,136441 80,52505
7,144833 80,52147
7,153092 80,52102
7,161511 80,51769
7,169858 80,51769
7,178025 80,61696
7,186635 80,60363
7,194947 80,58585
7,203015 80,54134
7,211327 80,55185
7,21975 80,58219
7,228241 80,58219
7,236481 80,50595
7,244523 80,49805
7,252968 80,51786
7,261498 80,55787
7,26989 80,53165
7,278065 80,39932
7,286483 80,39932
7,294991 80,36649
7,30333 80,32155
7,311451 80,33307
7,31968 80,27402
7,328072 80,25811
7,336575 80,2498
7,345026 80,2498
7,353662 80,22797
7,361512 80,19608
7,369957 80,13773
7,37827 80,0756
7,386422 80,11483
7,394113 80,16736
7,402519 80,19608
7,411119 80,18847
7,419885 80,1131
7,427927 80,08719
7,436292 80,05475
7,444902 80,0838
7,45313 80,03955
7,461396 80,0014
7,469968 79,96338
7,478564 79,96009
7,486516 80,01472
7,494771 79,96635
7,503977 79,81004
7,511533 79,75938
7,520063 79,77353
7,528291 79,73344
7,536699 79,69562
7,544805 79,65462
7,553117 79,8301
7,561567 79,80447
7,569932 79,93087
7,57792 79,93263
7,586446 79,91369
7,594879 79,90554
7,603261 79,86429
7,611463 79,91096
7,619749 79,84424
7,628145 79,40264
7,636564 79,4304
7,644739 79,37103
7,653114 79,3304
7,661383 79,30997
7,669919 79,30648
7,678232 79,2123
7,686353 79,18352
7,694719 79,17769
7,703195 79,18204
7,711749 79,20367
7,72019 79,26947
7,727994 79,93987
7,736467 79,81142
7,745023 79,85576
7,753155 79,85812
7,76135 79,79138
7,76988 79,75761
7,778272 79,69893
7,786758 79,73355
7,794759 79,67955
7,802991 79,61592
7,81141 79,56987
7,819913 79,50578
7,828199 79,4616
7,836292 79,49559
7,844758 79,52169
7,853325 79,52169
7,861607 78,467
7,869648 78,38628
7,87796 78,35166
7,886299 78,3507
7,894802 78,30328
7,903189 78,2557
7,911182 78,21433
7,919655 78,16231
7,928211 78,17677
7,936634 78,14634
7,944756 78,03057
7,953175 77,91271
7,961662 77,85163
7,969952 77,81163
7,978191 77,78315
7,986233 77,73109
7,994789 77,68601
8,003292 77,64471
8,011684 77,62277
8,019753 77,57963
8,028065 77,51722
8,036484 77,4889
8,044876 77,38985
8,053108 77,39848
8,06123 77,40164
8,069649 77,39928
8,078259 77,34875
8,086491 77,29082
8,094987 77,24161
8,103031 77,18503
8,111507 77,17696
8,11962 77,15501
8,128105 77,0445
8,1362 76,99516

8,144672 76,99934
8,151229 76,99979
8,161541 76,9341
8,169609 76,79806
8,178276 76,69791
8,186749 76,66895
8,195054 76,61628
8,203189 76,55903
8,211188 76,52955
8,219753 76,49054
8,228226 76,46313
8,236675 76,44397
8,244579 76,33847
8,253052 76,28748
8,260967 76,25553
8,269807 76,21552
8,277988 76,20326
8,286354 76,19912
8,29475 76,18592
8,303143 76,13315
8,311453 76,05664
8,319492 76,01606
8,327999 75,9614
8,336417 75,90147
8,344937 75,84422
8,352932 75,78548
8,361408 75,74473
8,369747 75,74008
8,378193 75,71444
8,386341 75,59419
8,394889 75,54015
8,40313 75,41405
8,411686 75,35027
8,420025 75,33352
8,428066 75,24856
8,436459 75,23582
8,444931 75,14852
8,453284 75,0911
8,461475 75,00155
8,469734 74,98328
8,478016 74,925
8,486546 74,82478
8,494804 74,78963
8,503979 74,81358
8,512409 74,83114
8,519428 74,8011
8,528297 74,71316
8,536355 74,64648
8,544621 74,55069
8,552986 74,53288
8,561489 74,48435
8,569886 74,4393
8,578704 74,32953
8,586315 74,2886
8,594872 74,28791
8,603264 74,26086
8,611416 74,20963
8,619835 73,98695
8,628147 73,88394
8,636566 73,84287
8,644988 73,82817
8,65292 73,72817
8,661503 73,67907
8,670006 73,60896
8,678234 73,59386
8,686413 73,49428
8,694752 73,41471
8,703099 73,40446
8,711483 73,24448
8,719795 73,23733
8,727917 73,23367
8,736362 73,21915
8,744976 73,17077
8,753204 73,09051
8,761659 73,06532
8,769691 73,06202
8,778061 72,92434
8,786437 72,84415
8,794739 72,75298
8,80286 72,70916
8,811359 72,66168
8,819664 72,64858
8,828148 72,56938
8,836349 72,42711
8,844906 72,33952
8,853355 72,25772
8,861668 72,20674
8,869816 72,12849
8,877937 72,05025
8,886353 71,92446
8,894913 71,92446
8,903156 71,89413
8,91124 71,8017
8,919769 71,7261
8,928299 71,61894
8,936501 71,57054
8,944759 71,53088
8,953284 71,51511
8,961411 71,51511
8,969883 71,41221
8,978142 71,34721
8,986237 71,26526
8,994713 71,23575
9,003185 71,20062
9,011453 71,09446
9,019619 71,0179
9,027958 70,96546
9,036407 70,95066
9,044773 70,94059
9,053022 70,84706
9,061314 70,85106
9,069753 70,8401
9,078452 70,59993
9,086765 70,57122
9,09478 70,49087
9,103146 70,45233
9,111565 70,39121
9,11985 70,33812
9,128167 70,27389
9,136511 70,21934
9,144733 70,15088
9,153263 70,0191
9,161629 69,98963
9,169724 70,03001
9,178036 69,98826
9,186619 70,00158
9,194901 69,94328
9,203269 69,9401
9,211201 69,881
9,219646 69,77579
9,228123 69,75492
9,236488 69,65437
9,244583 69,5487
9,253113 69,54772
9,261469 69,50158
9,269897 69,53178
9,278049 69,39017
9,286415 69,27164
9,294861 69,1912
9,303531 69,15344
9,311596 69,10442
9,319949 69,07388
9,32811 68,97388
9,336746 68,90911
9,344978 68,86935
9,353073 68,81307
9,361439 68,74975
9,369831 68,69585
9,378197 68,61159
9,386562 68,59864
9,394124 68,61899
9,402716 68,58767
9,411716 68,58767
9,419891 68,5127
9,428043 68,41685
9,436356 68,40638
9,444721 68,38107
9,453114 68,32112
9,461566 68,2854
9,469627 68,1854
9,477966 68,18201
9,486633 68,18739
9,494919 68,13459
9,503014 68,00628
9,511566 67,92344
9,520019 67,79634
9,528318 67,79634
9,53653 67,7651
9,544682 67,69643
9,553101 67,64407
9,561657 67,59572
9,570049 67,59979
9,578007 67,49679
9,586456 67,44435
9,594888 67,28197
9,603188 67,28197
9,611366 67,20251
9,619705 67,20047
9,628017 67,12668
9,636654 67,29129
9,644802 67,21457
9,653284 67,12668
9,661346 67,07768
9,669872 67,06958
9,678131 66,98935
9,686279 66,90048
9,694565 66,85434
9,703121 66,83962
9,711569 66,7945
9,719826 66,7945
9,727974 66,64909
9,736504 66,56451
9,745087 66,49117
9,753426 66,45726
9,761494 66,38683
9,769889 66,27445
9,778172 66,2467
9,78651 66,23346
9,794849 66,21485
9,802864 66,14446
9,81131 66,09765
9,819977 66,00776
9,828236 65,93167
9,836711 65,9305
9,844972 65,89706
9,853142 65,86345
9,861481 65,89788
9,869713 65,82173
9,877808 65,77021
9,886227 65,75487
9,894836 65,71201
9,903109 65,6794
9,911354 65,57954
9,919693 65,55769
9,928191 65,53724
9,93645 65,52245
9,944762 65,37779
9,953048 65,21339
9,961399 65,19619
9,969996 65,06121
9,978335 64,98053
9,986401 64,8953
9,994876 64,83668
10,00333 64,75419
10,01164 64,69279
10,02009 64,6407
10,02799 64,44498
10,03644 64,33412
10,04489 64,20197
10,05323 64,09666
10,06135 64,05054
10,06979 64,01936
10,07831 64,00119
10,08665 63,80122
10,09495 63,68238
10,10298 63,52277
10,11133 63,45363
10,11975 63,37603
10,12822 63,24266
10,13618 63,13349
10,14471 63,09866
10,15299 62,99855
10,1616 62,99855
10,16964 62,82343
10,17815 62,69956
10,18662 62,58274
10,19499 62,52181
10,20325 62,43403
10,21166 62,3127
10,21973 62,2737
10,22842 62,10795
10,23666 62,01623
10,24461 62,0512
10,25304 61,97087
10,26148 61,87629
10,26996 61,7787
10,27813 61,72857
10,28634 61,70539
10,29473 61,64637
10,30323 61,61243
10,31151 61,49918
10,31969 61,36802
10,32809 61,32644
10,33665 61,29939
10,34492 61,27607
10,35305 60,94167
10,36125 60,83471
10,36967 60,7508
10,37826 60,71316
10,38657 60,59426
10,39461 60,36697
10,40299 60,2938
10,41169 60,20826
10,42003 60,02708
10,42816 59,89717
10,43641 59,79696
10,44489 59,69112
10,45323 59,56491
10,46166 59,51984
10,46966 59,31994
10,47808 59,19336
10,48658 59,04914
10,49487 58,921
10,50307 58,83174
10,51133 58,73597
10,52004 58,63193
10,52814 58,53193
10,53654 58,42133
10,54449 58,27141
10,55297 58,17576
10,56153 58,1005
10,56994 57,97123
10,57829 57,7944
10,58622 57,72456
10,59477 57,643
10,60319 57,53005
10,61148 57,29311
10,61965 57,20458
10,62813 56,88717
10,63668 56,73159
10,64499 56,63525
10,65354 56,54487
10,66154 56,34667
10,66988 56,20959
10,67824 56,11653
10,68648 55,97875
10,69465 55,80597
10,70302 55,64111
10,71154 55,56478
10,71986 55,3047
10,7279 55,20183
10,73648 55,24597
10,74496 55,17693
10,75321 55,01083
10,76133 54,82697
10,76973 54,7755
10,77793 54,57755
10,78649 54,45694
10,79488 54,28763
10,80289 54,13338
10,81142 53,96964
10,81998 53,82855
10,82824 53,69451
10,83633 53,44851
10,8447 53,2135
10,85323 53,03589
10,86154 52,88574
10,86991 52,73602
10,87806 52,59863
10,88645 52,47418
10,895 52,33191
10,90317 52,23056
10,91162 52,09913
10,9197 51,9913
10,92814 51,87221
10,93648 51,71474
10,94487 51,65543
10,95297 51,63871
10,96147 51,5612
10,96984 51,48257
10,97818 51,33452
10,98627 51,17447
10,99464 51,04059
11,00303 50,93234
11,01153 50,79648
11,01968 50,61502
11,02789 50,52463
11,03664 50,40045
11,04498 50,31685
11,05317 50,17467
11,06135 49,91909
11,06988 49,78093
11,07841 49,69868
11,08664 49,60704
11,09484 49,50444
11,10329 49,40168
11,11149 49,25121
11,11994 49,16736
11,12833 49,05733
11,13626 48,93836
11,14479 48,80168
11,15332 48,65117
11,16164 48,54478
11,1697 48,46578
11,17799 48,40525
11,18641 48,28859
11,19488 48,13219
11,20317 47,8412
11,21123 47,62257
11,21967 47,46679
11,22829 47,36079
11,23655 47,19862
11,24462 47,0486
11,25296 46,92347
11,26138 46,87223
11,26977 46,81414
11,27824 46,7447
11,28631 46,54457
11,29484 46,49805
11,30334 46,45089
11,31166 46,39425
11,31978 46,35825
11,32817 46,30622
11,33646 46,27485
11,34493 46,24159
11,35323 46,2407
11,36133 46,19465
11,36978 46,1552
11,37826 46,07875
11,38663 46,04543
11,39461 46,01984
11,40306 46,0095
11,41153 46,00951
11,41984 46,01542
11,42808 45,99926
11,43625 45,96001
11,44467 45,94785
11,45315 45,92934
11,4616 45,86855
11,46978 45,8611
11,478 45,811
11,48659 45,84292
11,49479 45,81548
11,50307 45,73792
11,51141 45,64981
11,51989 45,60556
11,52824 45,58439
11,53662 45,59434
11,54474 45,55281
11,55313 45,53574
11,56166 45,49332
11,57 45,5026
11,5781 45,4734
11,58641 45,41164
11,59479 45,36968
11,60324 45,32668
11,61154 45,29362
11,61966 45,3261
11,62811 45,30008
11,62998 44,8118
11,63004 44,33743
11,63001 43,90506
11,62998 43,6889
11,62998 43,2731
11,62995 43,00931
11,62995 42,71414
11,62993 42,52805
11,62993 42,34372
11,62993 42,17429
11,62993 41,99249
11,62993 41,81418
11,62995 41,68527
11,62995 41,57953
11,62995 41,5643
11,62995 41,55106

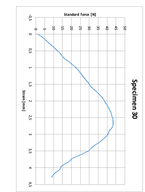
Standard Temp 298
Specimen 80
Load (kN)
0
5
10
15
20
25
30
35
40
45
50
55
60
65
70
75
80
85
90
95
100

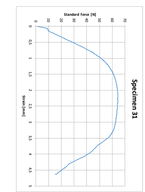
Standard Temp 150
Specimen 33
Load (lbs)

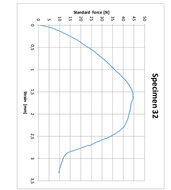
Specimen #2
Standard Force [N]
Strain [mm]

Specimer	Specimen 33
Strain	Standard force
mm	N
0	1,109992
-1E-07	1,077815
-1E-07	1,057074
2,71E-05	1,042937
2,71E-05	1,033717
5,42E-05	1,069861
0,001167	1,402136
0,00296	1,980017
0,005567	2,747596
0,009127	3,620154
0,013416	4,574744
0,018471	5,635779
0,024364	6,738318
0,030529	7,790076
0,03743	8,89701
0,044819	9,963904
0,052204	11,01664
0,059513	12,04935
0,067985	13,10551
0,076626	14,05912
0,084881	14,88969
0,092975	15,82426
0,101372	16,87552
0,109627	17,9766
0,118076	19,0264
0,126415	20,0142
0,134483	21,02689
0,142929	22,08939
0,151596	23,15092
0,159851	24,17533
0,167999	25,12113
0,176502	26,14457
0,184894	27,14506
0,193207	28,17289
0,201492	29,15726
0,209587	30,13285
0,218063	31,18802
0,22662	32,17142
0,234985	33,1973
0,242969	34,12943
0,251366	35,10502
0,259838	36,04398
0,268123	36,92484
0,276462	37,91361
0,284583	38,881
0,292976	39,84438
0,301452	40,76821
0,309818	41,61196
0,317912	42,34487
0,326225	43,19302
0,334861	43,96108
0,3432	44,5956
0,351241	45,16274
0,359554	45,71474
0,368057	46,23769
0,376449	46,60256
0,384788	46,82388
0,392963	46,93627
0,401492	46,99934
0,410049	46,83717
0,418308	46,5785
0,426402	46,20069
0,434688	45,35108
0,440608	44,19971
0,446613	43,16846
0,454868	42,09522
0,463073	41,28663
0,471328	40,81519
0,479698	40,56702
0,48817	40,33582
0,496429	40,17731
0,504577	40,1158
0,512996	40,10229
0,521636	40,06404
0,529891	39,92268
0,537933	39,769
0,546272	39,70338
0,554695	39,68982
0,563033	39,5665
0,571342	39,4057
0,579494	39,28832
0,587993	39,23603
0,596523	39,21191
0,604972	39,08242
0,613094	38,78201
0,621459	38,62399
0,629936	38,44793
0,638217	38,28027
0,646476	38,10571
0,654598	37,87304
0,663047	37,67572
0,671604	37,46246
0,679885	37,24749
0,687953	37,01934
0,696456	36,77984
0,704903	36,51887
0,713135	36,253
0,72131	36,08479
0,729542	35,92152
0,737988	35,73286
0,746571	35,46015
0,754803	35,18586
0,762871	34,91804
0,771263	34,72944
0,779846	34,50397
0,788212	34,27216
0,796227	34,0373
0,804539	33,87855
0,812958	33,70496
0,821434	33,47334
0,829773	33,14912
0,837948	32,74165
0,846424	32,47871
0,855061	32,22114
0,863293	31,99067
0,871414	31,67622
0,879643	31,3819
0,888199	31,15058
0,896511	30,90229
0,904823	30,58662
0,912892	30,29243
0,921364	30,076
0,92992	29,74397
0,938259	29,38874
0,946354	29,18159
0,95472	29,00336
0,963059	28,69123
0,971481	28,31623
0,979767	27,98945
0,987831	27,75178
0,996281	27,51777
1,00481	27,27076
1,013203	26,91737
1,021244	26,57996
1,02969	26,36878
1,038113	26,19416
1,046398	25,98124
1,054817	25,64518
1,062939	25,27518
1,071442	24,98197
1,079998	24,67619
1,088417	24,42301
1,096321	24,17411
1,104744	23,95634
1,1133	23,69315
1,121557	23,44912
1,129732	23,19167
1,137881	22,96645
1,14633	22,78103
1,154776	22,4977
1,163225	22,32723
1,17132	22,2213
1,179632	22,0783
1,188296	21,84771
1,196554	21,48467
1,204592	21,17498
1,212931	20,95354
1,221327	20,7033
1,229666	20,47576
1,238085	20,29717
1,24626	20,16338
1,254545	20,09917
1,263186	19,97204
1,271578	19,7979
1,279726	19,54387
1,288092	19,26189
1,296458	19,01641
1,304907	18,81127
1,313162	18,60265
1,321257	18,43084
1,329733	18,27428
1,338316	18,09472
1,346655	17,88793
1,35475	17,73614
1,363035	17,61422
1,371454	17,45901
1,37974	17,25576
1,388079	17,14486
1,396227	17,06
1,404677	16,92689
1,41326	16,80329
1,421545	16,61176
1,429667	16,4517
1,437948	16,3776
1,446398	16,24198
1,45471	16,10617
1,463076	16,01349
1,471171	15,93987
1,47962	15,89187
1,488093	15,85559
1,496405	15,6676
1,50458	15,41516
1,513193	15,29877
1,521719	15,1854
1,529925	15,09458
1,538129	15,04952
1,546357	15,00688
1,55475	14,97854
1,563253	14,92532
1,571618	14,85232
1,579606	14,80504
1,588079	14,74327
1,596635	14,65741
1,604894	14,53605
1,613015	14,59531
1,621328	14,60374
1,629693	14,60214
1,638196	14,56912
1,646371	14,49174
1,654466	14,44862
1,662969	14,40645
1,671498	14,37322
1,679891	14,32619
1,687932	14,28189
1,696351	14,29558
1,704717	14,30909
1,713082	14,33123
1,721395	14,24905
1,729573	14,15521
1,738073	14,08123
1,746686	14,0683
1,755052	14,0691
1,763036	14,06033
1,771402	14,00984
1,779824	13,99617
1,78819	13,94699
1,796418	13,89429
1,80454	13,85623
1,813043	13,79897
1,821572	13,71662
1,829747	13,66369
1,838006	13,73011
1,846372	13,76341
1,854901	13,73727
1,863187	13,65282
1,871335	13,59959
1,879567	13,56763
1,88796	13,50453
1,896379	13,4663
1,904801	13,36718
1,912839	13,31649
1,921342	13,28931
1,929925	13,26577
1,9381	13,22121
1,946386	13,07921
1,954725	12,94564
1,963144	12,82119
1,971621	12,70739
1,979853	12,6231
1,987948	12,52056
1,996447	12,4469
2,005003	12,37845
2,013288	12,33727
2,021357	12,27286
2,029722	12,22321
2,038034	12,14544
2,04648	12,05446
2,054712	12,07314
2,06286	12,06603
2,071363	12,05428
2,079893	11,99997
2,088232	11,91767
2,096273	11,83251
2,104582	11,80676
2,113005	11,76919
2,12137	11,69848
2,129656	11,59838
2,137857	11,51007
2,146334	11,44445
2,15489	11,40812
2,163118	11,32388
2,171324	11,17813
2,17988	11,09551
2,188272	11,03182
2,193137	10,94264
2,193273	10,80958
2,193218	10,70916
2,193191	10,64738
2,193164	10,59664
2,193164	10,53563
2,193164	10,51155
2,193164	10,4831
2,193191	10,47058
2,193191	10,46413
2,193191	10,44083
2,193191	10,39864
2,193164	10,37709
2,193164	10,3781
2,193164	10,37785

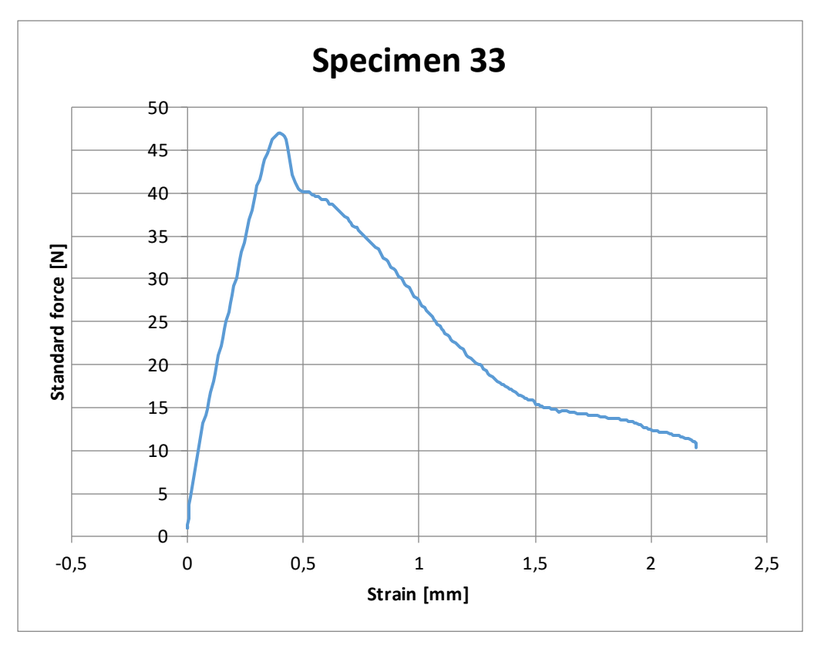

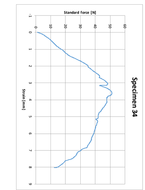
Standard Temp [°F]
Spectrum [nm]
Spectrum 34

4,005829 47,63904
4,014111 47,73151
4,022369 47,74691
4,030518 47,78911
4,036883 47,80931
4,047319 47,84
4,055752 47,87569
4,063998 47,89113
4,071339 47,90773
4,080769 47,93176
4,089054 47,93572
4,09726 47,97753
4,105408 47,99118
4,113907 47,9602
4,122169 47,98194
4,130589 47,98194
4,13871 47,92696
4,147259 47,90738
4,155739 47,83908
4,164051 47,7267
4,172146 47,63664
4,180459 47,56203
4,188677 47,50112
4,197273 47,57718
4,205585 47,49388
4,21384 47,3744
4,2234 47,31117
4,230926 47,27891
4,239211 47,25511
4,247359 47,23878
4,255584 47,22849
4,263984 47,22849
4,272467 46,98179
4,280688 46,90398
4,28873 46,82263
4,297206 46,79058
4,305842 46,69896
4,314207 46,6
4,322165 46,64477
4,330615 46,63493
4,339007 46,59204
4,34732 46,50525
4,355578 46,41323
4,363673 46,3659
4,372004 46,32033
4,380649 46,25153
4,389098 46,14266
4,397082 46,0425
4,405501 45,99038
4,414004 45,93898
4,422454 45,81463
4,430914 45,74198
4,439514 45,6788
4,447103 45,47232
4,455783 45,38706
4,464095 45,34641
4,473109 45,23321
4,480582 45,20277
4,489139 45,11002
4,497478 45,06778
4,505984 44,99779
4,514938 44,91512
4,52233 44,85627
4,530643 44,74677
4,539065 44,69281
4,547076 44,70317
4,555179 44,66801
4,563599 44,61774
4,571951 44,49371
4,580543 44,40346
4,588771 44,34418
4,597247 44,32529
4,605693 44,26763
4,613925 44,19672
4,622369 44,1375
4,630492 44,13791
4,639106 44,14384
4,647497 44,08681
4,655458 43,93891
4,664014 43,80996
4,672487 43,70464
4,680974 43,61909
4,689074 43,51499
4,697126 43,43787
4,7053 43,3501
4,714075 43,23784
4,721414 43,1073
4,730508 42,96793
4,738901 42,85168
4,747284 42,7
4,755632 42,59283
4,763891 42,57394
4,771323 42,58817
4,780515 42,6012
4,789098 42,52916
4,79741 42,40106
4,805452 42,30797
4,813774 42,2637
4,822374 42,30942
4,830602 42,29462
4,838861 42,24669
4,847089 42,22228
4,855485 42,23512
4,863958 42,24582
4,872284 42,25
4,880529 42,07767
4,889112 42,03999
4,897642 42,01658
4,905843 42,00251
4,913965 41,97264
4,922277 41,95562
4,930699 41,94007
4,939092 41,93908
4,947351 41,99731
4,955389 42,00245
4,963865 41,99738
4,972475 41,99984
4,980707 41,99407
4,989169 42,00124
4,997167 42,12354
5,00564 42,16754
5,013978 42,16898
5,022264 42,20349
5,030332 42,25128
5,038751 42,22289
5,047391 41,99459
5,05581 41,95417
5,063999 41,90124
5,072109 41,84628
5,080692 41,83438
5,088951 41,82161
5,097226 41,69715
5,105518 41,57334
5,113968 41,45588
5,122369 41,36124
5,13081 40,46162
5,138847 40,39053
5,147297 40,37054
5,155827 40,53946
5,164082 40,63312
5,172367 40,78727
5,180881 41,00271
5,188881 41,20171
5,197411 41,05141
5,205643 41,1702
5,213791 41,353
5,22224 41,46386
5,230077 41,56704
5,239052 41,58471
5,247231 41,57478
5,255432 41,57567
5,263977 41,6
5,27219 41,61139
5,28056 41,58776
5,288788 41,60917
5,297153 41,60153
5,305763 41,66861
5,314133 41,64159
5,322497 41,59929
5,3307 41,59929
5,339092 41,36819
5,347431 41,34652
5,355637 41,30083
5,363785 41,25326
5,372261 41,25402
5,380774 41,25947
5,389099 41,25947
5,397251 41,16858
5,405643 41,10509
5,413956 41,07482
5,422401 40,98119
5,430607 41,02741
5,438702 41,08509
5,447174 41,07549
5,455644 41,03318
5,464043 41,03318
5,472137 40,99152
5,480168 40,97575
5,489035 40,94706
5,497316 40,92168
5,505495 40,81036
5,513826 40,75799
5,522226 40,75799
5,530645 40,72374
5,539031 40,64468
5,54711 40,51199
5,555853 40,40712
5,564219 40,4064
5,572609 40,3811
5,580599 40,36178
5,588831 40,33663
5,597303 40,33447
5,605726 40,28572
5,614119 40,25563
5,622379 40,24036
5,630882 40,22148
5,639082 40,22148
5,647341 40,03786
5,655596 40,12277
5,663801 40,12764
5,6723 40,17206
5,680639 40,1615
5,688009 40,08757
5,696946 40,03628
5,705284 40,03628
5,714079 40,02378
5,722445 39,96697
5,730459 39,91861
5,738852 39,90686
5,747197 39,9225
5,755556 39,9634
5,763994 39,8988
5,772154 39,75857
5,780626 39,7346
5,789209 39,68868
5,797548 39,74908
5,80539 39,67789
5,813902 39,66711
5,822284 39,66711
5,830744 39,64112
5,839003 39,59137
5,84704 39,53915
5,855597 39,51495
5,8641 39,44501
5,872358 39,40989
5,880824 39,41026
5,888473 39,45326
5,897401 39,45093
5,905714 39,4088
5,913862 39,33154
5,922063 39,2973
5,930113 39,27411
5,938905 39,25963
5,947145 39,19053
5,955558 39,20517
5,963869 39,1943
5,972452 39,20032
5,980764 39,17498
5,988859 39,24982
5,997304 38,93447
6,005617 38,85563
6,014119 38,81102
6,022378 38,81102
6,0305 38,80003
6,038946 38,77964
6,047422 38,71503
6,055734 38,72006
6,063936 38,67883
6,072284 38,6255
6,08004 38,57293
6,08901 38,45943
6,097265 38,46315
6,105386 38,43822
6,113863 38,42347
6,122448 38,39707
6,130849 38,32947
6,138742 38,21947
6,147165 38,18579
6,155584 38,14424
6,163923 38,119
6,171182 38,09427
6,180383 37,97177
6,188743 37,96386
6,197403 37,96386
6,205728 37,91352
6,213823 37,77515
6,222379 37,68771
6,230772 37,64498
6,23911 37,63811
6,247343 37,62349
6,255517 37,61198
6,263958 37,6125
6,271386 37,58139
6,280832 37,57273
6,288766 37,50274
6,297292 37,4747
6,305688 37,47024
6,314027 37,3863
6,322466 37,36755
6,330461 37,40765
6,338933 37,47223
6,347383 37,49321
6,355611 37,42025
6,363679 37,40125
6,372155 37,3927
6,380622 37,35326
6,388977 37,35326
6,397092 37,28254
6,405538 37,23467
6,413877 37,27337
6,422406 37,29314
6,430608 37,20536
6,438999 37,17214
6,447189 37,21421
6,455926 36,97991
6,464292 36,95426
6,472278 36,89897
6,480588 36,83551
6,489011 36,78994
6,49743 36,73873
6,505662 36,63455
6,513999 36,57404
6,522178 36,41456
6,530679 36,31714
6,539098 36,23479
6,547246 36,2192
6,555385 36,19463
6,564088 36,19753
6,572407 36,16455
6,580522 36,03675
6,588727 35,96457
6,597066 35,93085
6,605649 35,9132
6,614041 35,89919
6,622109 35,76392
6,630605 35,73976
6,639005 35,67876
6,647397 35,64329
6,655399 35,46752
6,663911 35,33561
6,67225 35,25112
6,680753 35,23231
6,689086 35,20732
6,697186 35,09731
6,705636 35,0397
6,714162 34,98918
6,722421 34,95555
6,730571 34,90147
6,7388 34,85132
6,747278 34,79111
6,755615 34,71806
6,76398 34,71605
6,772284 34,72441
6,780578 34,72441
6,788161 34,68984
6,797363 34,59062
6,805511 34,4957
6,813823 34,42964
6,822162 34,38246
6,830599 34,3219
6,838871 34,27919
6,847019 33,98637
6,855464 33,60752
6,864078 33,07774
6,872386 32,75567
6,880508 32,33409
6,889058 32,09213
6,897299 31,92589
6,905799 31,75299
6,913974 31,54979
6,922149 31,41868
6,930572 31,29197
6,939102 31,17055
6,947521 31,07734
6,955535 30,95015
6,963999 30,87553
6,971431 30,83763
6,980606 30,57782
6,988945 30,51603
6,997203 30,45265
7,005512 30,34772
7,014041 30,20374
7,022399 29,99569
7,030448 29,81586
7,038787 29,82586
7,047344 29,49852
7,055656 29,32639
7,063777 29,20483
7,072063 28,87809
7,080412 28,6747
7,088613 28,5417
7,097101 28,43723
7,105472 28,29191
7,113948 28,18925
7,122585 28,03817
7,13087 28,08033
7,139091 28,0722
7,147514 27,97122
7,155669 27,87737
7,164065 27,88376
7,172377 27,84714
7,180415 27,77695
7,188864 27,70391
7,197194 27,64682
7,205706 27,54856
7,213991 27,49102
7,222193 27,37973
7,230559 27,34507
7,238978 27,4779
7,247237 27,3905
7,255385 27,31596
7,263724 27,29435
7,272049 27,24151
7,280783 27,18166
7,288851 27,0812
7,297244 27,04962
7,305583 27,02099
7,314002 26,98901
7,322314 26,82705
7,330685 26,68992
7,338885 26,55292
7,347495 26,43112
7,35578 26,37192
7,363902 26,27732
7,372294 26,17478
7,380744 26,07545
7,389124 25,97547
7,397504 25,87547
7,405516 25,77904
7,413882 25,61543
7,422358 25,45634
7,43064 25,31874
7,438735 25,24066
7,447264 25,17939
7,455821 25,07393
7,464178 24,97169
7,472274 24,75186
7,48046 24,57339
7,488741 24,4526
7,497244 24,26266
7,50561 24,03572
7,513751 23,83712
7,522099 23,64784
7,530618 23,44784
7,539076 23,24826
7,547118 22,79818
7,555644 22,35141
7,564091 22,11089
7,572487 21,84014
7,580911 21,67183
7,58881 20,67183
7,597313 20,30474
7,60587 20,09862
7,614155 20,00002
7,622193 19,9073
7,630158 19,82086
7,638599 19,7757
7,64734 19,57783
7,655606 19,54718
7,663754 19,50695
7,672226 19,47891
7,680703 19,3914
7,689013 19,26689
7,697344 19,20124
7,705469 19,09434
7,713925 19,01639
7,722344 18,93819
7,730465 18,75978
7,738754 18,63718
7,747223 18,57023
7,755726 18,51429
7,764065 18,37417
7,772284 18,2753
7,780636 18,2783
7,789193 17,97515
7,797585 17,85104
7,805626 17,77802
7,813855 17,67054
7,822331 17,56181
7,830849 17,50414
7,839062 17,3414
7,84713 17,35615
7,855607 16,97152
7,864136 16,70712
7,872365 16,52067
7,88065 16,40289
7,889148 16,24125
7,897749 16,24125
7,90572 16,13297
7,913952 16,01655
7,92199 15,88987
7,93052 15,80131
7,939076 15,74123
7,947411 15,64859
7,955931 15,44859
7,963822 15,32976
7,972134 15,23995
7,98061 15,10743
7,988922 14,85131
7,997097 14,19086
8,00056 13,96163
8,014736 13,82328
8,022999 13,69169
8,031307 13,2828
8,039259 13,26145
8,047259 13,14005
8,055232 12,98716
8,063205 12,87026
8,071205 12,75045
8,079205 12,63054
8,087205 12,53354
8,095205 12,47196
8,103205 12,40158
8,111205 12,40143

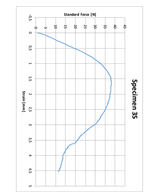
Standard Temp (°F)
Specimen 55
Elevation (feet)

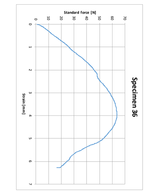
Standard Temp 100
Specimen 96
Strain [mm]

Specimen 27
Standard Temp (°C)
Specimen 27
Standard Temp (°C)

4,21398 67,48154
4,220048 67,4763
4,036414 67,47387
4,044753 67,45595
4,051372 67,4108
4,061511 67,44991
4,069716 67,49958
4,080665 67,49958
4,086665 67,53716
4,094973 67,50802
4,103045 67,45533
4,1113 67,45473
4,11975 67,44035
4,128115 67,41402
4,136408 67,39167
4,144574 67,36167
4,152995 67,26034
4,161688 67,26789
4,16989 67,21573
4,178149 67,25545
4,186172 66,93027
4,195017 66,94478
4,203159 66,97031
4,211719 66,97031
4,21971 66,54744
4,228129 66,46109
4,236739 66,34604
4,244998 66,26289
4,253012 66,14561
4,261485 66,04154
4,269998 65,96115
4,278246 65,79115
4,286501 65,68955
4,294596 65,61132
4,303099 65,54787
4,311602 65,44653
4,31983 65,29183
4,328228 65,20547
4,336428 65,09147
4,344904 65,01025
4,353159 64,88793
4,361308 64,72845
4,369647 64,59154
4,37815 64,52695
4,386151 64,40787
4,394481 64,30722
4,403033 64,05759
4,411479 63,79636
4,420062 63,61403
4,428454 62,62106
4,430926 61,60544
4,438997 59,61108
4,444497 59,61108
4,444756 59,39748
4,453228 59,03166
4,46162 58,90969
4,469933 60,17825
4,477974 60,37142
4,486393 60,5953
4,49506 60,72556
4,503147 60,89153
4,51141 61,07119
4,519722 61,29714
4,528225 61,49422
4,536564 61,63345
4,544796 61,73606
4,552834 61,83433
4,561099 61,99254
4,569093 62,05187
4,578316 62,15646
4,586353 62,24682
4,594749 62,39935
4,603105 62,54499
4,611561 62,721
4,619997 62,8455
4,628105 63,0495
4,636471 63,3629
4,644974 63,57866
4,653366 63,19523
4,661377 63,29328
4,669907 63,3666
4,678405 63,58949
4,686695 63,68949
4,694763 63,69823
4,703045 63,79913
4,711468 63,85421
4,719987 63,93109
4,728172 64,02806
4,73632 64,22118
4,744707 64,40358
4,753057 64,4655
4,761581 64,49394
4,76973 64,55083
4,778015 64,65144
4,786438 64,73083
4,79475 64,77435
4,803196 64,80686
4,811737 64,85947
4,820736 64,9547
4,828377 65,05981
4,836662 65,09221
4,844727 65,05879
4,853202 65,07984
4,861625 65,13356
4,870048 65,1787
4,879219 65,20156
4,886397 65,25125
4,894816 65,27423
4,903199 65,29712
4,911658 65,36131
4,919753 65,37953
4,928154 65,40429
4,936111 65,45429
4,944877 65,39522
4,953109 65,41762
4,96131 65,55959
4,969649 65,63045
4,978343 65,65282
4,986693 65,64419
4,994993 65,61419
5,003005 65,62835
5,011535 65,61926
5,019954 65,68808
5,027942 65,64075
5,036334 65,65642
5,044473 65,68775
5,053267 65,7295
5,061599 65,69255
5,06972 65,51955
5,078219 65,50927
5,086696 65,45173
5,095115 65,44349
5,103536 65,45503
5,111468 65,35223
5,120016 65,29379
5,128226 65,26376
5,136649 65,22732
5,14466 65,21941
5,153136 65,04915
5,161639 64,94726
5,169894 64,84086
5,178284 64,76323
5,186439 64,7623
5,194858 64,67635
5,20325 64,63313
5,211562 64,28899
5,219523 64,06753
5,227996 63,8825
5,236636 63,77782
5,245002 63,63499
5,253043 63,3342
5,261477 63,0958
5,269803 63,05958
5,278222 63,7035
5,286534 63,80122
5,294629 63,83118
5,303122 63,62307
5,311822 63,63153
5,320179 63,63981
5,328578 63,62882
5,336595 63,63999
5,34496 63,59013
5,353383 63,58071
5,361505 63,54947
5,369626 63,47168
5,378109 63,3977
5,386321 63,30179
5,394914 63,24749
5,403282 63,23057
5,411454 63,18524
5,419984 63,10843
5,428243 62,98642
5,436364 62,83798
5,444876 62,7456
5,453109 62,6331
5,461545 62,531
5,469964 62,38458
5,477952 62,24865
5,486344 62,13736
5,494981 62,05175
5,503266 61,93806
5,511719 61,8187
5,51978 61,6684
5,528256 61,28315
5,536649 61,13455
5,544881 61,0052
5,553056 60,85194
5,561505 60,74946
5,569824 60,6187
5,578427 60,54908
5,586385 60,45572
5,59475 60,28676
5,603173 60,16656
5,611428 60,03002
5,619824 59,98044
5,628228 59,90744
5,636418 59,80194
5,645001 59,85876
5,653207 59,72369
5,661382 59,8263
5,669641 59,54276
5,678086 59,47215
5,686163 59,49119
5,694565 59,27987
5,702994 59,17787
5,711416 59,14117
5,719945 59,15153
5,728204 59,03357
5,736352 58,86747
5,744936 58,77152
5,753381 58,69804
5,761844 58,5777
5,769845 58,57744
5,77802 58,5122
5,786493 58,47938
5,794942 58,41178
5,803281 58,36819
5,811349 58,2817
5,819757 58,23146
5,828325 58,13421
5,836557 58,03341
5,844896 58,04882
5,853017 58,04939
5,86141 58,03137
5,869968 58,03693
5,878284 57,96175
5,886238 57,84175
5,894685 57,83322
5,903295 57,80917
5,911527 57,75758
5,919622 57,69558
5,928068 57,6671
5,936417 57,67166
5,944744 57,6566
5,953195 57,56964
5,961343 57,40509
5,969816 57,33412
5,978456 57,3184
5,986731 57,28082
5,994779 57,19479
6,003202 57,13266
6,011599 57,05826
6,019823 57,03926
6,028219 57,0405
6,036514 56,94807
6,044759 56,89544
6,053316 56,82132
6,061548 56,77286
6,070023 56,69614
6,078172 56,64514
6,086538 56,63051
6,094877 56,77016
6,103105 56,70134
6,111336 56,67414
6,119648 56,63668
6,128004 56,57142
6,136424 56,55742
6,144692 56,53372
6,153141 56,52306
6,161614 56,54137
6,169873 56,51866
6,178101 56,43549
6,186483 56,29918
6,194863 56,29458
6,203339 56,27343
6,211631 56,26312
6,219773 56,19915
6,228165 56,20655
6,236695 56,15457
6,244923 56,11518
6,253071 56,07145
6,261496 56,04883
6,269861 53,94983
6,278252 53,91625
6,286564 53,88388
6,294659 53,91076
6,303078 53,91823
6,311665 53,96244
6,320008 53,89502
6,328068 53,89502
6,336327 53,86208
6,344777 53,86125
6,353142 53,82724
6,361454 55,75942
6,369629 55,73518
6,378109 55,7326
6,386662 55,7744
6,394864 55,7609
6,403065 55,64196
6,411488 55,56935
6,41986 55,54456
6,428299 55,56081
6,436649 55,5703
6,44468 55,5703
6,453103 55,46167
6,461602 55,45152
6,470025 55,45671
6,478035 55,39852
6,486512 55,37778
6,494957 55,33808
6,503343 55,29785
6,511858 55,34124
6,520017 55,38308
6,528426 55,38314
6,536858 55,34841
6,545069 55,29793
6,553499 55,29776
6,561858 55,25147
6,570157 55,24876
6,578562 55,18853
6,586951 55,20064
6,595387 55,23753
6,603758 55,29193
6,612179 55,25519
6,620582 55,2187
6,62956 55,03863
6,637596 55,00792
6,646045 54,99176
6,654523 54,92775
6,662889 54,92587
6,671255 54,89805
6,679702 54,86127
6,688122 54,86127
6,70589 54,81263
6,713446 54,79063
6,720003 54,713
6,728515 54,69868
6,736383 54,71629
6,744775 54,80159
6,753171 54,82958
6,761564 54,79169
6,769973 54,75163
6,77971 54,70163
6,78631 54,59679
6,794946 54,71302
6,803258 54,65556
6,811353 54,60281
6,819719 54,62233
6,828107 54,6219
6,836561 54,62194
6,844846 54,54306
6,853185 54,44764
6,861604 54,42888
6,870023 54,38041
6,878362 54,36726
6,886494 54,31973
6,894953 54,25746
6,903299 54,23986
6,911691 54,23938
6,91987 54,21228
6,927965 54,12589
6,93641 54,07974
6,94486 53,99016
6,953179 53,97318
6,961622 53,93922
6,96981 53,89879
6,978269 53,87725
6,986554 53,89756
6,994676 53,80963
7,003088 53,74939
7,011464 53,68739
7,019858 53,64007
7,028085 53,60079
7,036237 53,39563
7,044709 53,31491
7,053185 53,27481
7,061688 53,13462
7,069699 52,90805
7,078104 52,80194
7,086695 52,57108
7,094907 52,44266
7,103356 52,33669
7,111394 52,18819
7,11979 52,07781
7,128343 51,93236
7,136773 51,81756
7,144933 51,66194
7,153146 51,49094
7,161592 51,37125
7,169797 51,1998
7,178216 51,11408
7,186311 51,0576
7,194757 50,96145
7,203206 50,87879
7,211394 50,7757
7,219613 50,59892
7,228005 50,48594
7,236535 50,41373
7,244847 50,28504
7,253049 50,15591
7,261334 49,98052
7,269699 49,89744
7,27676 49,82568
7,286569 49,64798
7,294637 49,4343
7,303246 49,26517
7,311776 49,13353
7,320055 49,04134
7,328403 48,9176
7,336385 48,78705
7,344834 48,65689
7,353227 48,55411
7,361675 48,44447
7,369019 48,34492
7,377635 48,25106
7,385966 48,16121
7,394491 47,92167
7,403045 47,80911
7,411327 47,69658
7,419803 47,72338
7,428195 47,57324
7,436561 47,4154
7,444576 47,29098
7,452995 47,1515
7,461349 47,00158
7,469917 46,85766
7,478042 46,7035
7,486381 46,58589
7,494853 46,524
7,503192 46,43138
7,511425 46,24162
7,519849 46,0903
7,528209 45,80163
7,536849 45,67009
7,545051 45,50467
7,553146 45,31389
7,561512 45,09984
7,569934 44,89171
7,578284 44,70163
7,586628 44,53352
7,594707 44,36009
7,603126 44,19963
7,611656 44,03843
7,619884 43,92627
7,628032 43,80505
7,636401 43,69349
7,644902 43,63049
7,65327 43,69286
7,661445 43,59168
7,669673 43,49316
7,678012 43,43286
7,686342 43,36993
7,694678 43,29868
7,703004 43,23868
7,711372 43,10249
7,720008 43,08179
7,728183 42,98864
7,736389 42,79845
7,744808 42,63146
7,753227 42,55486
7,761623 42,46854
7,769999 42,34411
7,777999 42,33411
7,786529 42,27353
7,794978 42,22782
7,803317 42,18347
7,811412 42,15322
7,819804 42,07207
7,828232 41,98705
7,836569 41,85703
7,844958 41,85695
7,853942 41,84477
7,861419 41,80511
7,869975 41,74969
7,878314 41,66972
7,886664 41,62135
7,894664 41,51355
7,903167 41,26639
7,911479 41,10502
7,919684 41,04425
7,927886 40,97372
7,936389 40,88833
7,944758 40,8469
7,953284 40,749
7,961322 40,53055
7,969962 40,40071
7,978408 40,28395
7,98664 40,10777
7,994842 40,09668
8,00202 39,97452
8,011519 39,90062
8,019861 39,83898
8,028361 39,61898
8,036319 39,51649
8,044822 39,37413
8,053378 39,16246
8,061637 38,94926
8,069732 38,84173
8,078284 38,7163
8,08641 38,62892
8,094882 38,5298
8,103251 38,39897
8,111262 38,29301
8,119739 38,23775

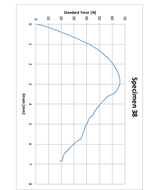
Standard Temp 150
Specimen 88
Load (lbs)

4,023781 50,22153
4,053204 50,13181
4,040813 49,97127
4,049015 49,84952
4,057137 49,79204
4,065422 49,78341
4,073898 49,75547
4,082463 49,69452
4,09063 49,64652
4,098698 49,3134
4,107063 49,24772
4,115704 49,21681
4,124563 49,0012
4,13208 48,86979
4,139683 48,7977
4,148665 48,71978
4,157341 48,66265
4,165546 48,47082
4,173748 48,26299
4,182251 48,16189
4,190807 48,06313
4,1992 47,98008
4,207653 47,89452
4,215553 47,87042
4,223099 47,74244
4,232395 47,62959
4,240707 47,53469
4,248665 47,39339
4,257168 47,29409
4,265578 47,16355
4,273884 47,08259
4,282074 47,02199
4,290577 46,96873
4,298943 46,93087
4,307308 46,80734
4,315567 46,65176
4,323662 46,58152
4,331997 46,5447
4,340051 46,47068
4,348896 46,37268
4,357071 46,27491
4,365574 46,25986
4,37402 46,24117
4,382387 46,20657
4,390628 45,96491
4,398928 45,95681
4,40724 45,91062
4,415743 45,84724
4,424055 45,79766
4,432215 45,73035
4,440596 45,65119
4,448937 45,54419
4,457357 45,54419
4,465532 45,45217
4,473845 45,36995
4,482237 45,28001
4,490633 45,18857
4,498945 45,15276
4,507067 45,13574
4,515459 45,13047
4,523881 44,9552
4,532181 44,91179
4,540422 44,82862
4,548788 44,72086
4,55718 44,6589
4,565519 44,52943
4,573885 44,33346
4,582204 44,32127
4,590403 44,09729
4,598928 43,96325
4,607325 43,7958
4,615499 43,44024
4,624029 43,2268
4,632475 43,07495
4,640853 42,9552
4,649093 42,85191
4,657114 42,73445
4,665586 42,63353
4,674116 42,53411
4,682402 42,45565
4,690443 42,32003
4,698884 42,23107
4,707465 42,21497
4,715677 41,97783
4,723825 41,82141
4,732058 41,81575
4,740477 41,67005
4,74898 41,82102
4,757185 41,66898
4,765356 41,52452
4,773564 41,52433
4,781562 41,49666
4,790074 41,40874
4,798822 41,25005
4,807081 41,29179
4,82155 41,29207
4,824303 41,25106
4,832668 41,20673
4,84042 41,20673
4,849047 41,02047
4,857176 40,95129
4,865862 40,90131
4,87703 40,8167
4,882238 40,82347
4,890654 40,77182
4,899054 40,77182
4,907312 40,71019
4,91535 40,63583
4,9238 40,57737
4,932463 40,50558
4,940668 40,44467
4,949228 40,44467
4,957235 40,44434
4,965605 40,45755
4,973917 40,37446
4,982225 40,30352
4,990367 40,23429
4,998796 40,14138
5,007122 40,14089
5,015412 39,84482
5,023733 39,69674
5,032179 39,61452
5,040655 39,54052
5,048967 39,51755
5,057196 39,37003
5,065454 39,23975
5,073984 39,19422
5,082292 39,07771
5,090786 39,07771
5,099837 38,98378
5,107176 38,91082
5,115705 38,90899
5,124098 38,84868
5,132193 38,82072
5,140612 38,70899
5,148617 38,70899
5,157347 38,61144
5,165712 38,59577
5,1737 38,6282
5,182226 38,60777
5,190729 38,64379
5,199048 38,64379
5,207083 38,53768
5,21542 38,47943
5,223896 38,41627
5,232155 38,41803
5,240547 38,33584
5,248669 38,29315
5,257145 38,27881
5,265671 38,27353
5,274167 38,2454
5,282586 38,2454
5,290607 38,0136
5,29903 37,96646
5,307339 37,92472
5,315624 37,87061
5,323803 37,83136
5,332249 37,79472
5,340564 37,68838
5,349004 37,68838
5,357185 37,63754
5,365578 37,57497
5,374081 37,51414
5,382366 37,45417
5,390594 37,37147
5,399049 37,32264
5,407219 37,32264
5,415722 37,23061
5,424004 37,23376
5,432125 37,13335
5,440485 37,14521
5,448994 37,13596
5,457279 37,06007
5,465427 36,98576
5,473884 36,98576
5,482216 36,91952
5,490608 36,87022
5,498958 36,87889
5,507069 36,78978
5,515678 36,71571
5,524155 36,67049
5,532477 36,61786
5,540642 36,51786
5,548901 36,52667
5,557293 36,43658
5,565689 36,37659
5,574081 36,30351
5,582012 36,19557
5,590525 36,19557
5,599125 36,05685
5,607437 35,96328
5,615448 36,00674
5,623817 36,00146
5,631183 35,98999
5,640575 35,94258
5,648982 35,8769
5,656982 35,7969
5,665485 35,72327
5,673984 35,69617
5,682407 35,62004
5,690475 35,53178
5,698814 35,50288
5,707313 35,4475
5,715545 35,4475
5,723994 35,40716
5,732086 35,38952
5,740535 35,0847
5,749145 34,98971
5,757537 34,8806
5,765525 34,83839
5,773891 34,25804
5,782292 34,25804
5,790679 33,85485
5,799034 33,64866
5,807056 33,45512
5,815506 33,28813
5,823951 33,13992
5,832347 33,02227
5,840753 32,9129
5,848921 32,70129
5,857391 32,62428
5,865676 32,45101
5,873798 32,14222
5,881053 31,95253
5,890419 31,81239
5,898658 31,68007
5,90756 31,53409
5,915355 31,01957
5,923938 30,85568
5,932361 30,84015
5,940807 30,74353
5,948848 30,554
5,957241 30,29417
5,965956 30,29417
5,974509 30,27335
5,982368 30,09658
5,990379 29,98169
5,998909 29,91322
6,007465 29,82147
6,015804 29,7128
6,023899 29,53099
6,032284 29,29895
6,040603 29,28895
6,049069 28,80913
6,057254 28,66784
6,065349 28,60838
6,073825 28,53896
6,082435 28,43503
6,090853 28,2121
6,099015 28,2121
6,107164 28,01369
6,11352 27,93118
6,123912 27,75466
6,132144 27,57522
6,140346 27,43886
6,148757 27,29476
6,157321 27,29476
6,165718 27,12619
6,173786 26,89365
6,182342 26,75363
6,190814 26,65038
6,1991 26,57881
6,207454 26,3934
6,215854 26,29704
6,223926 26,2997
6,232456 26,21107
6,240741 26,13167
6,248699 26,03967
6,257228 25,88313
6,265705 25,7722
6,273933 25,63216
6,282284 25,49494
6,290451 25,49494
6,298933 25,25692
6,307346 25,08413
6,315547 24,9514
6,323642 24,80168
6,332088 24,7379
6,340494 24,38384
6,348094 24,38384
6,357078 24,21227
6,365448 24,21014
6,373893 24,04163
6,382232 23,95293
6,390598 23,78355
6,398993 23,64899
6,407302 23,64899
6,415885 23,53915
6,424228 23,24264
6,432319 23,10706
6,440578 22,99068
6,449028 22,87815
6,457349 22,74197
6,465669 22,74197
6,473744 22,6148
6,482247 22,5166
6,490693 22,36206
6,499062 22,241
6,507126 22,19524
6,515549 22,10479
6,524106 22,10479
6,532477 22,03449
6,540513 21,94178
6,548887 21,84189
6,557026 21,80352
6,565583 21,75232
6,573975 21,66205
6,582043 21,62459
6,590549 21,62459
6,599049 21,62309
6,607331 21,60635
6,615616 21,4581
6,623929 21,37695
6,632241 21,31389
6,640744 21,27162
6,649049 21,27162
6,657231 21,23432
6,665596 21,19192
6,67418 21,15143
6,682412 21,10315
6,690587 21,10322
6,698815 21,09288
6,707249 21,0849
6,715605 20,9899
6,723889 20,90552
6,732037 21,04895
6,740513 21,06362
6,74915 21,07052
6,757382 21,04868
6,765446 21,01897
6,773812 21,01685
6,782208 20,99372
6,790684 20,95414
6,798884 20,95414
6,806923 20,96314
6,815453 20,97549
6,824093 21,00615
6,832406 20,94352
6,840661 20,60722
6,849103 20,5666
6,854633 19,29896
6,854633 19,96162
6,854579 19,84077
6,854579 19,72004
6,854525 19,62201
6,854525 19,53364
6,854552 19,47914
6,854552 19,37585
6,854552 19,31585
6,854552 19,24757
6,854552 19,19791
6,854552 19,1532
6,854552 19,09838
6,854552 19,06958
6,854579 19,01905
6,854579 18,94451
6,854579 18,94451
6,854552 18,92388
6,854552 18,80793
6,854552 18,80951
6,854552 18,89157

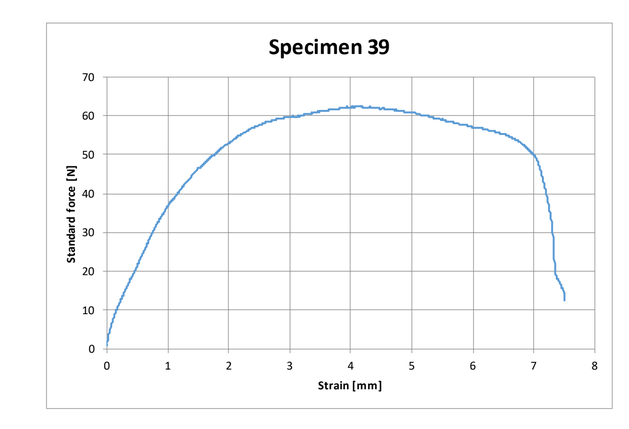

Specimen 3	Specimen 39
Strain	Standard force
mm	N
0	1,061219
0	1,060472
0	1,054862
0	1,092473
0	1,100026
2,72E-05	1,09537
0,000951	1,190222
0,002743	1,36698
0,005295	1,635413
0,008692	2,015296
0,012984	2,446448
0,017981	2,848059
0,023764	3,260657
0,030558	3,719641
0,038271	4,188391
0,046419	4,64469
0,054678	5,147131
0,06288	5,653967
0,071329	6,135657
0,079829	6,575354
0,088141	6,938879
0,096265	7,312256
0,104684	7,71045
0,11313	8,118896
0,121473	8,461426
0,129594	8,825928
0,137933	9,172363
0,146245	9,522705
0,154718	9,956787
0,16311	10,28809
0,171262	10,55762
0,179872	10,86694
0,188375	11,14526
0,196657	11,43579
0,204725	11,7616
0,213037	12,07617
0,221376	12,3866
0,229879	12,72461
0,238164	13,02222
0,246229	13,30615
0,254705	13,56433
0,263234	13,8584
0,271463	14,15332
0,279668	14,50842
0,288007	14,87622
0,296373	15,203
0,304822	15,43982
0,313051	15,70618
0,321172	16,00293
0,329595	16,26965
0,338151	16,53625
0,346517	16,79651
0,354585	17,02557
0,363031	17,30621
0,371423	17,59271
0,379846	17,91583
0,388074	18,11829
0,396333	18,36694
0,404752	18,60254
0,413335	18,89722
0,421731	19,16394
0,429742	19,3783
0,438081	19,63428
0,446557	19,93054
0,45487	20,22864
0,463071	20,4978
0,47125	20,73755
0,479722	21,01318
0,488145	21,22473
0,496538	21,48877
0,504579	21,87646
0,512997	22,22515
0,521607	22,52276
0,529839	22,7719
0,538014	23,03814
0,546162	23,28252
0,554585	23,57049
0,563084	23,87554
0,571427	24,11968
0,579518	24,37554
0,587914	24,66497
0,596497	24,99566
0,604836	25,2691
0,613038	25,44451
0,621461	25,65209
0,629906	25,93383
0,638245	26,23632
0,646584	26,55627
0,654572	26,81994
0,663102	27,11913
0,671574	27,37682
0,679997	27,65002
0,688061	27,92651
0,696431	28,21886
0,70477	28,50072
0,713109	28,70446
0,721448	29,0415
0,729542	29,34814
0,737935	29,62975
0,746625	29,93652
0,754857	30,18566
0,762978	30,41967
0,771371	30,69079
0,779767	30,99877
0,788159	31,22051
0,796307	31,43804
0,804509	31,68157
0,812932	31,96404
0,821488	32,29644
0,829774	32,51635
0,838002	32,66271
0,846478	32,87426
0,854981	33,10314
0,863263	33,33471
0,871411	33,53002
0,87967	33,74523
0,888093	33,99792
0,896538	34,24474
0,904904	34,51757
0,912945	34,71709
0,921422	34,91344
0,929921	35,10677
0,93818	35,27761
0,946408	35,49941
0,954667	35,72383
0,963006	35,99092
0,971482	36,21163
0,979768	36,4048
0,987859	36,58455
0,996308	36,77028
1,004838	37,0038
1,013123	37,17556
1,021325	37,3174
1,029664	37,48336
1,037976	37,70113
1,046452	37,94484
1,054818	38,07921
1,06302	38,18953
1,071442	38,33345
1,079999	38,52608
1,088338	38,70861
1,096402	38,8698
1,104798	39,0454
1,113217	39,19652
1,121449	39,34984
1,129758	39,52446
1,137826	39,65303
1,146302	39,78348
1,154939	39,94107
1,163224	40,13236
1,171265	40,35648
1,179604	40,54172
1,188214	40,76047
1,196526	40,92728
1,204594	41,09629
1,212769	41,26505
1,221188	41,45639
1,229718	41,61386
1,238114	41,75153
1,246125	41,90888
1,254681	42,13752
1,263211	42,36103
1,271523	42,54584
1,279725	42,62413
1,288037	42,71762
1,296513	42,86502
1,304932	43,04144
1,313165	43,2016
1,321233	43,32501
1,329816	43,47589
1,338345	43,59292
1,346547	43,76575
1,354806	43,90961
1,363061	44,02262
1,371483	44,21482
1,379738	44,30087
1,388108	44,49538
1,396145	44,699
1,404729	44,87655
1,413342	45,05172
1,42149	45,1592
1,429665	45,28149
1,437951	45,42025
1,446343	45,58181
1,454682	45,69448
1,463021	45,83257
1,471169	45,9854
1,479645	46,14587
1,488202	46,34362
1,496567	46,45776
1,504635	46,4687
1,513219	46,57698
1,521611	46,70515
1,529896	46,81212
1,538102	46,93318
1,54633	47,08693
1,554696	47,181
1,563145	47,29568
1,571511	47,43887
1,579552	47,49935
1,588109	47,62765
1,596581	47,75567
1,604893	47,83367
1,612961	48,00506
1,621274	48,21203
1,629719	48,36285
1,638169	48,501
1,646397	48,59377
1,654523	48,67159
1,662942	48,80343
1,671551	48,97134
1,679864	49,07964
1,687852	49,15913
1,696217	49,29261
1,70469	49,43195
1,713086	49,5799
1,721425	49,62309
1,729653	49,65914
1,738072	49,7535
1,746712	49,85195
1,754998	49,99373
1,763117	50,14459
1,771349	50,23041
1,779852	50,37115
1,788218	50,48958
1,796473	50,58434
1,804461	50,66276
1,812964	50,79206
1,821463	50,85259
1,829886	50,9504
1,837981	51,14034
1,8464	51,27676
1,854765	51,43002
1,863158	51,53286
1,871417	51,59498
1,879458	51,67732
1,887877	51,77438
1,896433	51,90482
1,904883	52,0137
1,912867	52,05444
1,921397	52,19247
1,929873	52,38101
1,938185	52,50912
1,946414	52,54852
1,954619	52,57413
1,963145	52,67316
1,971621	52,75163
1,979933	52,87937
1,988001	52,94324
1,9965	53,05857
2,004977	53,15401
2,013182	53,26366
2,021357	53,3653
2,029585	53,43442
2,038035	53,50069
2,046591	53,54972
2,054766	53,65184
2,062914	53,79722
2,071471	53,93272
2,080027	54,06651
2,088233	54,16545
2,096301	54,2225
2,10464	54,34317
2,112978	54,45621
2,121397	54,54606
2,129763	54,57376
2,137805	54,66986
2,146334	54,78406
2,154864	54,92038
2,163256	54,99414
2,171351	54,98337
2,179827	55,0446
2,188219	55,09712
2,196585	55,21187
2,204813	55,28217
2,212965	55,34549
2,221384	55,41977
2,230047	55,48907
2,238226	55,5789
2,246264	55,63713
2,254793	55,71566
2,263079	55,75263
2,271418	55,78886
2,279757	55,91236
2,287962	56,0333
2,296381	56,1493
2,304884	56,27042
2,313112	56,29842
2,321234	56,36143
2,329684	56,42768
2,33816	56,56144
2,346499	56,65263
2,35462	56,65555
2,362875	56,75309
2,371378	56,83536
2,379797	56,95827
2,388136	56,98471
2,396342	56,95383
2,404761	56,98243
2,413401	57,05405
2,42174	57,14813
2,429751	57,18259
2,43801	57,23733
2,446512	57,31288
2,454794	57,3519
2,463133	57,41753
2,471228	57,44707
2,479677	57,49841
2,488287	57,55823
2,496573	57,55671
2,504721	57,65519
2,51298	57,74527
2,521399	57,86178
2,529875	57,90109
2,538077	57,92518
2,546118	57,9596
2,554564	58,04143
2,563204	58,13311
2,571596	58,14025
2,579664	58,16812
2,588003	58,22738
2,596449	58,37658
2,604817	58,44978
2,613156	58,3767
2,621251	58,34147
2,629724	58,38065
2,638337	58,41788
2,646649	58,48592
2,654634	58,50383
2,663136	58,54107
2,671636	58,5877
2,679921	58,64442
2,688069	58,6963
2,696275	58,71465
2,704694	58,74402
2,713197	58,72695
2,721482	58,79255
2,729604	58,88831
2,738133	58,98185
2,746606	59,04429
2,754811	59,06836
2,762959	59,07744
2,771298	59,10841
2,779664	59,1996
2,78814	59,23777
2,796479	59,22771
2,80449	59,2494
2,812993	59,33155
2,821576	59,40807
2,829808	59,46256
2,837956	59,39699
2,846375	59,38626
2,854932	59,3939
2,863217	59,41469
2,87153	59,43371
2,879678	59,42592
2,888101	59,4762
2,896684	59,49923
2,904996	59,54387
2,91298	59,56279
2,921399	59,57933
2,929711	59,59332
2,93805	59,58054
2,946473	59,60839
2,954648	59,71643
2,962987	59,80403
2,97157	59,84069
2,979775	59,79805
2,987977	59,79409
2,996209	59,81618
3,004735	59,85693
3,013104	59,85779
3,02128	59,82768
3,029538	59,83894
3,038064	59,9025
3,04646	59,9643
3,054853	59,95021
3,062948	59,8748
3,071477	59,83416
3,080007	59,79457
3,088235	59,79918
3,09641	59,80419
3,104696	59,79424
3,113088	59,82426
3,121484	59,85543
3,129903	59,90667
3,137998	59,9146
3,146337	59,92118
3,15492	59,89008
3,163259	59,88529
3,171407	59,97596
3,179639	60,04551
3,188005	60,10458
3,196561	60,16315
3,204767	60,18328
3,212831	60,19363
3,221227	60,23959
3,229863	60,31381
3,238149	60,31998
3,246351	60,31921
3,254636	60,37746
3,262948	60,4521
3,271451	60,52055
3,279733	60,49703
3,287992	60,45992
3,296468	60,45601
3,305131	60,50375
3,313337	60,54646
3,321374	60,55276
3,32977	60,56534
3,338189	60,6077
3,346555	60,65734
3,354814	60,71677
3,362962	60,69921
3,371301	60,74243
3,379831	60,71267
3,388223	60,72621
3,396264	60,83531
3,404683	60,91166
3,41316	60,97882
3,421445	60,97868
3,429647	60,98052
3,437905	61,01509
3,446324	61,0787
3,4548	61,09756
3,463112	61,10726
3,471207	61,09243
3,479679	61,14742
3,488266	61,21639
3,496441	61,26019
3,504643	61,22524
3,513092	61,14621
3,521485	61,16077
3,529877	61,19144
3,538216	61,25154
3,546284	61,23009
3,55476	61,29813
3,56329	61,32422
3,571572	61,37737
3,57975	61,38713
3,587979	61,37673
3,596428	61,38413
3,60482	61,37099
3,613079	61,40335
3,621254	61,49292
3,629704	61,54673
3,63823	61,61694
3,646488	61,63934
3,65469	61,61663
3,662949	61,6483
3,671372	61,68695
3,679791	61,71964
3,688019	61,69442
3,696171	61,73267
3,704617	61,76274
3,713173	61,84199
3,721596	61,86694
3,72966	61,77685
3,738137	61,76508
3,746613	61,75594
3,754978	61,77119
3,76318	61,81641
3,771275	61,81433
3,779751	61,85527
3,788224	61,87238
3,796646	61,8788
3,804604	61,86345
3,813107	61,88588
3,821553	61,90335
3,829891	61,89682
3,838097	61,97398
3,846218	62,0162
3,854637	62,07111
3,863194	62,10204
3,871506	62,10456
3,87952	62,11948
3,887993	62,17242
3,896523	62,20221
3,904808	62,17734
3,912903	62,16042
3,921322	62,19073
3,929691	62,29067
3,93811	62,3256
3,946423	62,28628
3,954624	62,21386
3,963154	62,1845
3,97171	62,20953
3,979996	62,25818
3,988117	62,23967
3,996456	62,24678
4,004822	62,26846
4,013187	62,29614

4,0215 62,3096
4,029514 62,30185
4,038097 62,27831
4,0466 62,24912
4,054829 62,21902
4,063577 62,27454
4,071396 62,35185
4,080078 62,38177
4,088078 62,38177
4,096416 62,35799
4,104511 62,3741
4,112957 62,37932
4,121513 62,39525
4,129852 62,36628
4,137974 62,3741
4,146313 62,37908
4,154816 62,43009
4,163128 62,45379
4,171387 62,38082
4,179615 62,29372
4,188091 62,2686
4,196701 62,27369
4,205193 62,27557
4,213593 62,27557
4,221447 62,26152
4,22995 60,2466
4,238235 62,25969
4,246437 62,25724
4,254612 62,23391
4,263115 62,19621
4,271499 62,19621
4,279876 62,18319
4,287913 62,2286
4,296236 62,2613
4,304893 62,29193
4,313121 62,25853
4,321353 62,21471
4,329804 62,21348
4,338004 62,25249
4,346503 62,26125
4,354735 62,23921
4,362857 62,17972
4,37126 62,1804
4,379863 62,22642
4,388284 62,25969
4,39635 62,25508
4,404769 62,25501
4,413102 61,99648
4,421584 61,98771
4,43067 61,99396
4,438018 61,96348
4,446913 61,93922
4,454913 61,97222
4,463279 61,92664
4,471236 61,87008
4,479712 61,88731
4,488102 61,86704
4,496444 61,79615
4,504729 61,84437
4,512877 61,90335
4,521283 61,93506
4,529983 61,91904
4,538222 61,89479
4,54618 61,84882
4,554456 61,84351
4,563128 61,87825
4,571467 61,85406
4,579889 61,82966
4,587901 61,77567
4,596213 61,78318
4,604823 61,83125
4,613162 61,7919
4,621314 61,68997
4,629786 61,66012
4,638284 61,63992
4,646655 61,63992
4,654777 61,61436
4,663089 61,58946
4,671454 61,57587
4,67982 61,55685
4,688215 61,54176
4,696633 61,53127
4,704674 61,50827
4,713159 61,46951
4,721571 61,44647
4,729639 61,5046
4,737951 61,52467
4,746344 61,52733
4,754763 61,49464
4,763132 61,44974
4,771511 61,45774
4,779593 61,4302
4,788122 61,42941
4,796621 61,38528
4,804556 61,35909
4,813048 61,3419
4,821341 61,36922
4,829816 61,3419
4,838018 61,29915
4,846277 61,20674
4,854407 61,17935
4,863306 61,11959
4,871665 61,137
4,87974 61,0875
4,888148 61,0875
4,896502 61,03585
4,90484 61,02538
4,913126 61,03908
4,921137 60,97189
4,929064 60,95124
4,938196 60,8709
4,946444 60,86021
4,954474 60,90909
4,963049 60,94464
4,971498 60,94621
4,979753 60,91964
4,987959 60,87998
4,996298 60,84173
5,004668 60,84173
5,013168 60,81444
5,021479 60,77377
5,029543 60,72763
5,037992 60,72291
5,046549 60,75196
5,054888 60,70429
5,063036 60,69905
5,071402 60,51731
5,079888 60,51731
5,088243 60,41551
5,096582 60,44632
5,104677 60,37996
5,113126 60,3792
5,121656 60,34409
5,129911 60,32109
5,138284 60,3107
5,146371 60,22499
5,154821 60,18098
5,163049 60,10311
5,171472 60,1323
5,17934 60,07312
5,187959 60,18694
5,196284 60,18694
5,204983 60,14524
5,213896 60,10254
5,221262 60,07739
5,229791 60,06762
5,238077 60,04351
5,246232 59,98565
5,25448 59,94366
5,262983 59,91617
5,271488 59,96613
5,279824 59,96613
5,28703 59,7814
5,296476 59,72709
5,304895 59,6867
5,313207 59,67072
5,321439 59,62226
5,329614 59,57607
5,337888 59,53419
5,34659 59,53419
5,354848 59,50805
5,362943 59,46005
5,371419 59,42254
5,379976 59,38501
5,388204 59,33311
5,396584 59,29769
5,404984 59,27269
5,41303 59,09379
5,42148 59,07056
5,429819 59,00732
5,43786 59,26165
5,446279 59,24958
5,454889 59,23129
5,463121 59,19457
5,471668 59,1922
5,479608 59,10207
5,488027 59,11519
5,496423 59,11935
5,504762 59,03848
5,513017 58,99603
5,521467 58,84192
5,529983 58,8407
5,538305 58,80164
5,546427 58,7535
5,554739 58,71439
5,563108 58,66349
5,571527 58,64896
5,57984 58,63692
5,588221 58,59853
5,596327 58,52853
5,60491 58,43977
5,613142 58,42163
5,62129 58,45123
5,629736 58,40175
5,638132 58,48901
5,646583 58,47113
5,654783 58,47113
5,662874 58,39932
5,671244 58,376
5,679743 58,3822
5,688062 58,28126
5,696314 58,21128
5,704679 58,22349
5,713182 58,29059
5,721503 58,30319
5,729723 58,31066
5,737928 58,8036
5,746428 57,85262
5,754877 57,85306
5,763269 57,91682
5,771338 57,89094
5,779888 57,85306
5,788206 57,81656
5,796545 57,81708
5,804804 57,76562
5,813032 57,74094
5,821371 57,70943
5,829737 57,63789
5,838004 57,61657
5,846107 57,69157
5,854727 57,71632
5,86331 57,79823
5,871569 57,83191
5,879583 57,58743
5,887949 57,57703
5,896284 57,5511
5,904734 57,55198
5,912992 57,48343
5,921114 57,46662
5,929564 57,48216
5,9382 57,49515
5,946566 57,47005
5,95469 57,29369
5,963151 57,26502
5,971529 57,26761
5,979868 57,21196
5,9881 57,19876
5,996328 57,12343
6,004747 57,12215
6,013234 57,10106
6,021563 57,0757
6,029896 56,99158
6,038076 56,99158
6,046579 56,9493
6,054892 56,90923
6,063013 56,91118
6,071245 56,91541
6,079611 56,96656
6,087966 56,96656
6,096479 56,9914
6,104548 56,87842
6,11302 56,85917
6,12155 56,85299
6,129782 56,7986
6,13801 56,76193
6,146284 56,76193
6,154634 56,76521
6,163054 56,79766
6,17145 56,73126
6,179571 56,61053
6,188128 56,55938
6,196764 56,50602
6,204983 56,47139
6,213206 56,45193
6,221319 56,42339
6,229849 56,42711
6,238188 56,39945
6,246527 56,35912
6,254541 56,325
6,263014 56,29267
6,271197 56,23676
6,279577 56,19863
6,287977 56,19863
6,296316 56,23323
6,304766 56,24864
6,313074 56,22612
6,321413 56,19424
6,329938 56,22669
6,338284 56,24864
8,34654 56,09574
6,354827 56,05696
6,363091 55,95506
6,371314 55,93436
6,379813 55,93438
6,388152 55,93626
6,396584 55,93626
6,404698 55,71996
6,413116 55,67786
6,421672 55,64767
6,430011 55,63564
6,437945 55,58224
6,446443 55,52268
6,454889 55,49199
6,463206 55,46199
6,471354 55,42168
6,47972 55,25067
6,488032 55,29488
6,496451 55,25083
6,504764 55,21793
6,513069 55,21905
6,521361 55,22147
6,529888 55,22148
6,538257 55,21587
6,546298 55,04896
6,554553 54,99657
6,562949 54,96375
6,571395 54,91574
6,579761 54,82057
6,588124 54,7887
6,596505 54,74887
6,604835 54,73378
6,613227 54,70604
6,621322 54,55877
6,629794 54,43572
6,638164 54,3633
6,646609 54,30146
6,654811 54,29146
6,66299 54,17174
6,671435 54,10799
6,680018 54,05407
6,688251 53,96907
6,696219 53,88314
6,704609 53,82014
6,713241 53,71468
6,721469 53,63153
6,729701 53,59899
6,737849 53,58155
6,746299 53,5282
6,754909 53,47226
6,763194 53,33355
6,771205 53,27321
6,779652 53,17984
6,787966 53,09657
8,79636 52,94957
6,804669 52,81395
6,813848 52,71811
6,82124 52,65805
6,829823 52,637
6,838082 52,47453
6,846487 52,37977
6,854887 52,23577
6,863343 52,00766
6,871682 51,90994
6,87975 51,7966
6,888035 51,70971
6,896348 51,60266
6,904847 51,5186
6,913152 51,4391
6,921719 51,36711
6,929673 51,13756
6,938149 51,00607
6,946572 50,87469
6,954747 50,7776
6,963032 50,6768
6,971341 50,56133
6,979888 50,43164
6,988129 50,17882
6,996171 49,99174
7,004636 49,81751
7,013226 49,65965
7,021565 49,45268
7,029606 49,25175
7,038004 49,06433
7,046475 48,83546
7,05476 48,6346
7,063019 48,30208
7,071358 47,88802
7,079777 47,5135
7,088334 47,17207
7,096824 46,8
7,104741 46,25956
7,111106 45,74068
7,121636 45,18819
7,129891 44,61153
7,138123 44,07637
7,146191 43,53855
7,154654 43,09469
7,163014 42,7
7,171479 42,36426
7,179627 41,5201
7,188076 41,03583
7,196497 40,45406
7,204836 39,74363
7,213058 39,13937
7,22137 38,65735
7,229791 38,40776
7,238112 37,51448
7,246451 36,37912
7,254826 35,63084
7,263045 35,02073
7,271441 34,3884
7,279833 33,83082
7,288284 33,29747
7,29632 31,83747
7,304823 30,94528
7,313414 29,87395
7,315768 28,8486
7,310109 27,79267
7,322344 26,57126
7,330836 25,46973
7,331278 24,19826
7,335707 23,10153
7,338938 22,01364
7,342253 20,9238
7,347495 19,84372
7,355807 19,19846
7,363999 18,63952
7,372214 18,53952
7,380606 18,24655
7,388999 17,9862
7,397204 17,77628
7,405422 17,57953
7,413828 17,37937
7,422411 17,14255
7,430697 16,87912
7,438999 16,62123
7,4471 16,0123
7,455576 15,75565
7,463889 15,60117
7,472147 15,43131
7,480376 15,31014
7,488799 15,02095
7,496999 14,86657
7,496703 14,29682
7,496676 14,08173
7,496649 13,83413
7,496622 13,37976
7,496594 13,13782
7,496594 12,99744
7,496567 12,79564
7,496513 12,64969
7,496513 12,61569
7,496513 123424
7,496513 12,47639
7,49654 12,40174
7,49654 12,41948
7,49654 12,40916
7,49654 12,39568
7,49654 12,28459

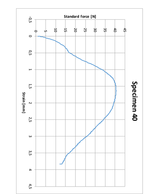
Standard Tone (18)
Spectrum dB
Frequency

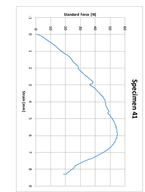
Standard Time (S)
Specimen #3
Load (kN)

3,894299 46,23142
3,854828 46,23282
3,861567 46,32909
3,871315 46,33492
3,879437 46,37781
3,887093 46,45743
3,894259 46,5255
3,900139 46,54012
3,91203 46,54512
3,921269 46,59296
3,929799 46,68268
3,936138 46,74054
3,944423 46,84938
3,954478 46,84544
3,963599 46,91557
3,971573 46,93173
3,979861 46,8773
3,987936 46,84392
3,996455 46,88075
4,004928 46,75565
4,013244 46,76871
4,021308 46,79382
4,029369 46,85542
4,038043 46,83898
4,046382 46,79288
4,054774 46,87217
4,062869 46,94775
4,071345 47,04572
4,079928 47,07663
4,088187 47,07124
4,096458 47,09978
4,104648 47,13678
4,112903 47,14926
4,121352 47,23385
4,129691 47,13334
4,137786 47,10339
4,146258 47,12697
4,154599 47,15008
4,163154 47,21508
4,171248 47,08242
4,179778 47,01955
4,188228 46,97678
4,19654 46,96408
4,204795 46,96171
4,213166 47,00199
4,221366 47,05199
4,229896 47,07518
4,238261 47,19511
4,246245 47,24472
4,254695 47,27376
4,263141 47,33408
4,271552 47,34497
4,279738 47,4487
4,287913 47,55414
4,296216 47,6484
4,304835 47,69696
4,313121 47,73806
4,321216 47,77042
4,329581 47,83899
4,338004 47,86143
4,346273 47,90503
4,354571 47,93669
4,362937 47,98678
4,371387 48,07572
4,379832 48,21881
4,388118 48,25077
4,396297 48,22868
4,404653 48,26776
4,412379 48,31723
4,421691 48,39866
4,429706 48,46577
4,437991 48,48112
4,446437 48,52671
4,45486 48,57294
4,463284 48,62977
4,471156 48,64966
4,479602 48,68501
4,488189 48,70358
4,496528 48,72229
4,504649 48,79389
4,512877 48,85167
4,521098 48,89705
4,529826 48,99595
4,538058 49,04224
4,546073 49,04284
4,554519 49,03778
4,563155 49,08368
4,571467 49,03382
4,579589 48,93
4,588012 48,9574
4,596356 48,93176
4,60469 48,97019
4,613082 48,80512
4,621314 48,61062
4,629733 48,47113
4,638016 48,38532
4,646602 48,37477
4,654884 48,39102
4,663142 48,35502
4,671565 48,44417
4,679851 48,50043
4,688132 48,55784
4,696147 48,60422
4,704703 48,63155
4,713009 48,69276
4,721431 48,76696
4,729556 48,83351
4,738032 49,08952
4,746642 49,21644
4,75479 49,27892
4,762938 49,37157
4,771284 49,47135
4,77959 49,56994
4,787986 49,6717
4,796378 49,71127
4,804553 49,77348
4,81292 49,80115
4,821587 50,01939
4,829964 50,06009
4,838068 50,0974
4,846386 50,15617
4,854685 50,20889
4,863225 50,26229
4,871157 50,31564
4,879632 50,41904
4,888028 50,49738
4,896611 50,56594
4,904999 50,62564
4,913054 50,70708
4,921273 50,77218
4,929776 50,83965
4,938115 50,88781
4,946454 50,99828
4,954495 51,11712
4,962914 51,19102
4,97155 51,25336
4,979783 51,35522
4,987904 51,40952
4,996243 51,50084
5,004693 51,57937
5,013058 51,62578
5,021264 51,68253
5,029426 51,73856
5,038018 51,81034
5,046321 51,93192
5,05478 51,91998
5,062928 51,90916
5,071484 51,94427
5,079934 51,96789
5,088189 52,03732
5,096447 52,09869
5,104886 52,16167
5,113125 52,21657
5,121518 52,27167
5,13 52,35122
5,137898 52,37166
5,146401 52,42965
5,154847 52,46345
5,163284 52,50169
5,171307 52,57932
5,179619 52,70835
5,187985 52,79398
5,196541 52,86143
5,20472 52,88438
5,212758 52,89407
5,221 52,94362
5,229871 53,04362
5,238184 53,03389
5,246195 53,04203
5,254507 53,1291
5,262873 53,18414
5,271402 53,27626
5,279661 53,29335
5,287893 53,33188
5,296284 53,35997
5,305033 53,37068
5,313314 53,33778
5,321383 53,37313
5,329748 53,39156
5,338144 53,44756
5,346426 53,47747
5,354685 53,50127
5,362833 53,53235
5,371283 53,53927
5,379946 53,53363
5,388178 53,58818
5,396189 53,60696
5,404745 53,7298
5,413124 53,76102
5,421453 53,79827
5,429602 53,80467
5,437857 53,85875
5,446196 53,89686
5,454752 53,93586
5,463121 53,92251
5,471284 54,00127
5,479742 54,01509
5,488102 54,08043
5,496331 54,091
5,504652 54,04832
5,513018 54,03425
5,521437 54,02069
5,52986 54,0481
5,538172 54,05008
5,546512 54,09562
5,554796 54,10991
5,563215 54,13879
5,571581 54,18724
5,579649 54,18425
5,587988 54,20021
5,59638 54,20967
5,604911 54,23102
5,613169 54,27499
5,621264 54,37254
5,629629 54,45153
5,638186 54,51767
5,646496 54,49573
5,654701 54,49179
5,663049 54,52102
5,671352 54,53535
5,679771 54,57483
5,687973 54,58634
5,696152 54,55889
5,704624 54,65088
5,713127 54,7042
5,721403 54,6997
5,729725 54,61178
5,738091 54,58952
5,746567 54,59912
5,754906 54,63102
5,763134 54,68172
5,771253 54,669
5,779552 54,6345
5,78804 54,64443
5,79649 54,71857
5,804585 54,71317
5,813007 54,69409
5,821533 54,6873
5,829845 54,63572
5,838051 54,7368
5,846279 54,80532
5,854597 54,85184
5,862232 54,95583
5,871433 54,86778
5,879528 54,84946
5,887974 54,89688
5,896503 54,91955
5,904789 54,88745
5,913107 54,89202
5,921276 54,87205
5,929588 54,91045
5,938065 54,9906
5,94643 54,94432
5,954525 54,81347
5,963028 54,80677
5,971299 54,77126
5,97905 54,76918
5,988045 54,73764
5,9963 54,72739
6,004723 54,69875
6,013115 54,67993
6,021374 54,68958
6,029731 54,67121
6,037941 54,69675
6,046444 54,53321
6,054893 54,53538
6,062824 54,59129
6,071323 54,62518
6,079636 54,66641
6,087975 54,62302
6,09626 54,56945
6,104611 54,53121
6,113031 54,53121
6,121414 54,51885
6,12986 54,44613
6,137875 54,3989
6,146151 54,40761
6,15469 54,42128
6,163004 54,40761
6,171284 54,30168
6,179596 54,19241
6,188099 54,12114
6,196655 54,08655
6,20483 54,03682
6,213872 53,99741
6,221997 53,96478
6,23082 53,94478
6,238186 53,92185
6,246307 53,89111
6,25462 53,82852
6,262985 53,76921
6,271461 53,71126
6,279687 53,66792
6,287922 53,57967
6,296345 53,60793
6,304844 53,70331
6,313049 53,62895
6,321335 53,57327
6,32951 53,53761
6,337902 53,49809
6,346405 53,43553
6,354669 53,40018
6,362755 53,34878
6,371258 53,25908
6,379841 53,2078
6,388153 53,1614
6,396201 53,05608
6,404724 52,87157
6,413009 52,76405
6,421431 52,74305
6,429714 52,72081
6,437889 52,63136
6,446255 52,56877
6,454865 52,47199
6,463177 52,44175
6,471284 52,40923
6,479613 52,29123
6,488085 52,17733
6,496424 52,07119
6,50471 52,0534
6,513751 52,04991
6,521254 53,02
6,529776 53,1
6,538178 51,87196
6,546134 51,803
6,554553 51,72804
6,563082 51,68313
6,571421 51,59857
6,579573 51,44497
6,587828 51,43564
6,596167 51,37893
6,604697 51,34229
6,612963 51,30107
6,621211 51,05952
6,629714 50,92243
6,638054 50,85614
6,646555 50,79605
6,654704 50,69067
6,663962 50,60387
6,672284 50,53911
6,679667 50,39531
6,688086 50,35242
6,696127 50,2117
6,704657 50,11983
6,71316 49,98854
6,721499 49,86696
6,729967 49,80192
6,738375 49,80113
6,746824 49,75235
6,754637 49,63378
6,76303 49,50527
6,771124 49,38771
6,779517 49,2748
6,7881 49,24051
6,796412 49,00356
6,804888 48,87655
6,813266 48,77451
6,821375 48,68735
6,829634 48,58918
6,838 48,3902
6,846201 48,21665
6,854704 47,96491
6,863225 47,82966
6,87116 47,70761
6,879614 47,57035
6,88806 47,44065
6,896456 47,29841
6,904929 47,1786
6,913997 47,04411
6,922284 46,92004
6,929675 46,73429
6,938178 46,57706
6,946379 46,41129
6,954558 46,29148
6,96303 46,1569
6,97148 46,03165
6,979977 45,8907
6,988357 45,67759
6,996162 45,49729
7,004534 45,37894
7,013037 45,20042
7,021269 45,03866
7,029444 44,8621
7,037974 44,74351
7,046417 44,61702
7,054693 44,45593
7,062964 44,29588
7,07141 43,85521
7,079722 43,7411
7,088198 43,56208
7,096564 43,40449
7,104632 43,19477
7,113009 43,04647
7,121581 42,88649
7,129839 42,72141
7,137961 42,53162
7,1463 42,39343
7,154746 42,21569
7,163004 41,96659
7,171429 41,7439
7,179465 41,71139
7,187914 41,57019
7,196524 41,39594
7,204836 41,12933
7,213931 40,90021
7,221217 40,72133
7,229599 40,56477
7,237921 40,41173
7,24626 40,14517
7,254488 39,97924
7,262854 39,85335
7,27141 39,75909
7,27986 39,60132
7,287871 39,35132
7,296464 39,14973
7,304888 38,99775
7,313159 38,7904
7,321418 38,58471
7,329593 38,45967
7,338016 38,23179
7,346462 38,01472
7,354858 37,77941
7,363284 37,59155
7,371518 37,1833
7,379901 36,83051
7,388076 36,53791
7,396251 36,3086
7,40443 36,05103
7,41296 35,83158
7,421284 35,62107
7,429771 35,29759
7,437786 34,97157
7,446231 34,73852
7,454872 34,51124
7,4631 34,26568
7,471279 34,02711
7,479668 33,80483
7,487873 33,67683
7,496349 33,49213
7,504714 33,27797
7,513916 32,92023
7,521419 32,67646
7,530029 32,48713
7,538398 32,27326
7,546758 32,07169
7,554668 31,85011
7,56306 31,70914
7,57151 31,54346
7,579711 31,26933
7,58786 31,16022
7,596263 30,94154
7,604782 30,70704
7,613169 30,5107
7,621273 30,40084
7,629718 30,25922
7,638031 30,07313
7,646396 29,81983
7,654598 29,50965
7,662776 29,19813
7,671284 28,98477
7,679698 28,8177
7,688011 28,63355
7,696159 28,48514
7,704551 28,39222
7,713188 28,26862
7,72142 28,1632
7,729599 27,99813
7,73799 27,79917
7,746382 27,56288
7,754778 27,42961
7,763144 27,23997
7,771266 27,04128
7,779685 26,92353
7,788241 26,77191

Hosea 14:1(1)
Hosea 14:2(2)
Hosea 14:3(3)
Hosea 14:4(4)
Hosea 14:5(5)
Hosea 14:6(6)
Hosea 14:7(7)
Hosea 14:8(8)
Hosea 14:9(9)
Joel 1:1(10)
Joel 1:2(11)
Joel 1:3(12)
Joel 1:4(13)
Joel 1:5(14)
Joel 1:6(15)
Joel 1:7(16)
Joel 1:8(17)
Joel 1:9(18)
Joel 1:10(19)
Joel 1:11(20)
Joel 1:12(21)
Joel 1:13(22)
Joel 1:14(23)
Joel 1:15(24)
Joel 1:16(25)
Joel 1:17(26)
Joel 1:18(27)
Joel 1:19(28)
Joel 1:20(29)
Joel 2:1(30)
Joel 2:2(31)
Joel 2:3(32)
Joel 2:4(33)
Joel 2:5(34)
Joel 2:6(35)
Joel 2:7(36)
Joel 2:8(37)
Joel 2:9(38)
Joel 2:10(39)
Joel 2:11(40)
Joel 2:12(41)
Joel 2:13(42)
Joel 2:14(43)
Joel 2:15(44)
Joel 2:16(45)
Joel 2:17(46)
Joel 2:18(47)
Joel 2:19(48)
Joel 2:20(49)
Joel 2:21(50)
Joel 2:22(51)
Joel 2:23(52)
Joel 2:24(53)
Joel 2:25(54)
Joel 2:26(55)
Joel 2:27(56)
Joel 2:28(57)
Joel 2:29(58)
Joel 2:30(59)
Joel 2:31(60)
Joel 2:32(61)
Joel 3:1(62)
Joel 3:2(63)
Joel 3:3(64)
Joel 3:4(65)
Joel 3:5(66)
Joel 3:6(67)
Joel 3:7(68)
Joel 3:8(69)
Joel 3:9(70)
Joel 3:10(71)
Joel 3:11(72)
Joel 3:12(73)
Joel 3:13(74)
Joel 3:14(75)
Joel 3:15(76)
Joel 3:16(77)
Joel 3:17(78)
Joel 3:18(79)
Joel 3:19(80)
Joel 3:20(81)
Joel 3:21(82)